UNIVERSITY OF THESSALY
POLYTECHNIC SCHOOL

DEPARTMENT OF MECHANICAL ENGINEERING

DIPLOMA THESIS

BAYESIAN LEARNING OF PARAMETERS OF SKELETAL MUSCLE MODELS

by
STAMATINA MORAITI

Thesis Supervisor: **Dr. Costas Papadimitriou**

Submitted in partial fulfillment of the requirements for the Mechanical Engineering Diploma from University of Thessaly.

Volos, June 2019

The approval of the Diploma Thesis by the Department of Mechanical Engineering of the University of Thessaly does not imply acceptance of the author's opinions. (Law 5343/32, article 202, paragraph 2).

Certified by the members of the Thesis Committee:

First Examiner   **Costas Papadimitriou**
(Supervisor)   Professor of Structural Dynamics, Department of Mechanical Engineering, University of Thessaly

Second Examiner   **Leonidas Spyrou**
(Co-Advisor)   Researcher C', Biomechanics Group, CERTH/IBO

Third Examiner   **Michalis Agoras**
Assistant Professor of Nonlinear Composite Materials-Homogenization Theories, Department of Mechanical Engineering, University of Thessaly

Acknowledgements

First and foremost, I would like to express my gratitude to my supervisor Professor Dr. Costas Papadimitriou and my co-advisor Dr. Leonidas Spyrou for their faith and their continuous support and guidance during the development of this thesis. I would like to thank them for giving me the chance to collaborate with them and the knowledge that I acquired through this thesis.

Last but not least, I owe my gratefulness to my family and my friends for giving me always a motivation and encouraging me during the years of my studies.

Abstract

Bayesian learning of parameters of skeletal muscle models

By
Stamatina Moraiti

Thesis Supervisor: **Dr. Costas Papadimitriou**

Computational modeling and experimental investigations have been developed in order to investigate the structural composition of a skeletal muscle and its biological and mechanical properties. However, this goal presents challenges as parameters are not identifiable due to the incomplete experimental data available. As a results the parameter may take values over a low dimensional manifold in the parameter space and a unique set of values is not available. In addition, the parameter values may vary among the different species tested.

The current diploma thesis utilizes complex methods so that we can make a step closer to the identification of the structural internal properties of a muscle. In order to accomplish this task, we use a model that exhibits the mechanical response of the skeletal muscle and we try to approach some experimental data in the most efficient way. Firstly, we implement a simple optimization process, comparing the model with the measured data. As it will be proved, there is a variety of combinations of optimal parameter values such that the model prediction can approach efficiently the realistic experimental response. This multiple solution was our stimulus for developing an elaborate analysis to face this variability, as it is the main factor of the model uncertainty. This method is the Bayesian analysis-approach which is a stochastic analysis leading to the best model inference regarding the realistic data. It is useful set of techniques to deal with the uncertainties which we are confronted with. We have implemented some other applications form Bayesian analysis, too.

We also implement a sensitivity analysis called Sobol analysis, which also contributes to the final results. It is proposed to enhance the performance of the applied methods in terms of the parameter inference in this specific model. Another feature that we will discover is the parameter variability between the species. As the literature offers us a large number of experimental data for each different species, we will be confronted with a great variety in the mechanical behavior of them. So, some steps that are done in this thesis can prove this species variability.

Table of contents

Introduction and literature review

Skeletal muscle is attached with the skeleton and is used to affect skeletal movement, support of the body and other important functions of the living organisms. The movement is achieved by the muscle contraction which is the activation of the tension generating sites of the muscle fibers. Muscle tension is not meant necessarily length change. For instance, human can manage to stand and keep balance without making any movement and shortening his/her skeletal muscles. Seeing this great importance of the muscles in every living organism, every effort of knowing better their internal structure seems useful. Studying skeletal muscles' physiology, their mechanical properties and finally their function is of particular interest as it involves several different physiological aspects.

A variety of extensive research activities in biomechanics have been developed. These are experimental studies, model development and computational analysis. Experimental techniques are fundamental to the research of soft tissues like a muscle as they are done to define the mechanical behavior of biological materials. At the macroscopic level, the experimental measurements are typically stress-strain or force-displacement relationship. A characteristic of the experiments is that they include a large amount of differences among them, such as the species, the kind of the examined muscle, the age and the sex of the animal and the conditions of the experiments. In recent years, mechanical experiments were carried out on a wide variety of species and a large account of specimens from rats [1],[2], rabbits [3] and human [4]. All the mentioned factors influence the final result of the study and the goal of direct properties' determination by the experiments seems to be highly demanding.

Some other researches have been developed, combining the experiments with a model analysis so the barriers of the uncertain factors can be faced [5],[2],[6],[7]. Some of them use a direct comparison of the measured and prediction model data, by developing the weighted least-squares approaches, minimizing the error between them [8]. While this method provides point estimates of the model parameters, it fails to quantify uncertainties in the values of the model parameters or address unidentifiability issues. Instead, the uncertainty quantification is highly recommended. Indeed, this method has gained a lot of attention in the last years [9-12],[13, 14]. So far, only a few publications target the probabilistic identification. In this research, we focus on the most efficient learning of the parameter by implementing not only a direct comparison between model and experimental data but also uncertainty quantification. In this way, we take advantage of each of them, leading to more informed conclusions.

As it is mentioned, model analysis and computational modeling that are based on experimental findings can be used to predict the mechanical response of the muscle and its internal properties. Thus, it is highly recommended to use a greatly

representative model that can approach the muscle's mechanical response. Moreover, this model should combine the microscale with the macroscale as the functioning of skeletal muscles crucially depends on their characteristics and their mechanical properties. In order to achieve the research goal, we chose the model proposed by Spyrou et al. [15] . This model depends on several parameters, some of which represent phenomenological mathematical parameters but some others are not properties only with biological, but also with mechanical meaning. This is a great advantage as other studies have basically used approximate relationships, using parameters without any direct physical meaning. A muscle is a complex mechanical structure while the internal properties and their changes have a crucial impact on the macroscopic mechanical response. Thus, the model parameter estimation of this specific model has great importance. Particularly, it is a three-dimensional constitutive model that takes into account several mechanical and biological characteristics. One of the most important of them is the fiber and the connective tissue volume fraction. The details of the model are also described in the Chapter 1.

Another point that needs to be done is that there is a large diversity and value variability of these biological and mechanical properties, which is caused by the differences in the biological characteristics, muscle structure, sex and age among the species. Thus, reliable characterization of skeletal muscle properties is demanded for efficient predictions of the muscle mechanical loading and behavior. It is the goal of this thesis to estimate representative values of these parameters along with their uncertainties.

Firstly, we introduce an optimization process, presented in Chapter 2. We seek the best set of parameters values that minimizes the discrepancy between the model predicted and the experimental data for the quantity of interest corresponding to the stress-strain relationship. It is noticeable that there is no unique solution for the model parameters. In fact the solution set occupies a lower dimensional manifold in the parameter space, which is indicative of the infinite number of solutions along this manifold. This unidentifiability related to the estimation of the model parameters originates from the fact that the experimental data are not enough to uniquely estimate the model parameters. Consequently, a point-based definition of the parameters seems inaccurate and this is why we investigate more complex methods, such as the Bayesian approach, in order to identify the solution manifold in the parameter space. The same statement is supported in several papers [10] This analysis has been the cornerstone of this research, considering it as an efficient tool for the uncertainty quantification and uncertainty analysis. To reduce the dimensionality of the problem global sensitivity analysis using Sobol indices is performed. Not only can each different result give significant information but the combination of these two analyses can also help us to improve our perception of biological structures.

The used method is a statistical approach named Bayesian inference. Using this, not only can we infer the most probable values of the parameters but we can also quantify the uncertainty that characterize all the model parameters of the muscle. The theory of the Bayes approach is described in [10, 16]and the appropriate software is introduced in [17]. It is a highly qualified method that is used in a variety of mechanical system.

The methodology will be briefly described in chapter 2. More details can be found in the aforementioned paper. It will lead to the whole domain of the optimal parameter set that gives the best model fitting with the realistic response.

The Sobol global sensitivity analysis is applied to identify which parameters are most important in predicting the stress-strain relationship. The most challenging issue in this structure is the typically large amount of the unknown inputs and the internal parameters. The system can be considered as over defined by unknown parameters that are characterized by a large uncertainty. This fact leads also to a large computation cost while implementing complex software. Using this analysis, one can understand which variables are most important, affecting the output quantity of interest. Another great aspect of this method is that one can spot unimportant parameters and reduce the dimension of the problem, leading to the reduction of the computational cost through the analysis. In the first step, this is highly helpful to deal with the uncertainties. Finally, it enhances the performance of the considered methods, helping us to examine and describe each result. Thus, combining the results of all these methods we gain valuable insight on the estimation of the model parameters. The current software is the Global Sensitivity Analysis Toolbox (GSAT), which is a free given software. The theory will be described in chapter 2 but there are also some useful references in [18], as the same analysis is used.

The results delivered by these analyses are described in the Chapter 3. One can find results for six different experiments of the same species and same type of muscle. Particularly, the specimens are taken by six different rats but by the tibialis anterior muscle. The results of each different analysis for every specimens are carefully evaluated and described, so as to make some general conclusions, that will be drawn in the Chapter 4.

CHAPTER 1

Model and parameter description

1.1 Principles of the model-Formulation

Muscle is a complex hierarchical structure, shown in the Fig. 1. Starting from the microscale, each myofibril is surrounded by endomysium. A group of muscle fibers (myofibrils) is bordered to the others by perimysium and a muscle fascicle is formed. In the macroscale, all these fascicles are organized to the entire muscle volume which is wrapped in an epimysial connective tissue layer. In each connective tissue, the collagenous fibrils are surrounded by biofluids and other biological materials. Thus, the model is an analytical model of this type of muscle, the equations of which have been introduced, regarding the structure and its microstructural characteristics. The model is the one proposed by Spyrou, Agoras and Danas [15].
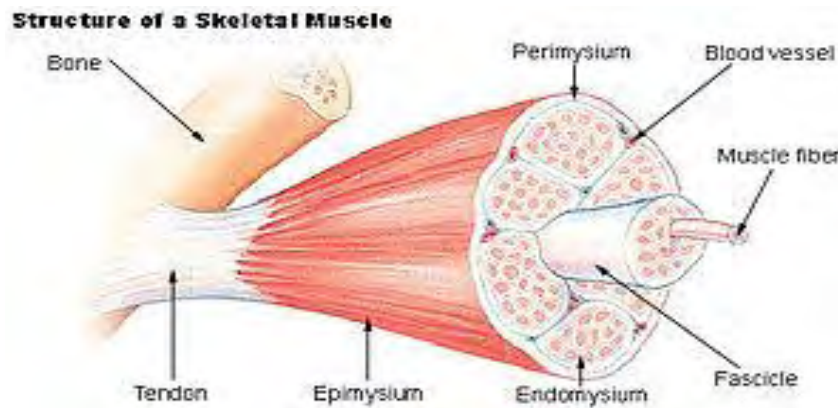
Fig 1.1: Structure of the skeletal muscle

Thus, a muscle can be considered as a fiber reinforced material while it is made from two constituent materials-fibers and biofluid matrix contained in connective tissue. The connective tissue, surrounding the fibers, is the endomysium, perimysium and epimysium. These three types are called collectively extracecullar matrix (ECM). Each component has significantly different physical or chemical properties, <u>nearly incompressible and transversely isotropic solids</u>, characterized by the symmetry axis m_0 . Thus, it has different mechanical behavior contributing to the final mechanical response of the muscle. This contribution depends on the fiber volume fraction c. This property describes the percent of the fibers contained in the muscle. So, it is essential that we should focus on every component's stress-strain relation. It should be remarked that some components are not characterized by a simple linear elastic behavior, but a hyperelastic one, based on nonlinear continuum mechanics [19].

In the reference paper [15], a simple homogenization 3D model is proposed. The macroscopic –homogenized behavior of the muscle is expressed by the Voigt hypothesis that the strain field in the composite is uniform. Moreover, a great advantage of this model is that it can combine the microstructural characteristics with the macroscaled response. The appropriate equations are described below.

Before the formulation about the stress-strain relation is exhibited, it is vital to introduce the vector of the symmetry axis $\mathbf{m}_0$. The fibers are assumed to be aligned along this direction $\mathbf{m}_0$ in the undeformed configuration. It can be supposed that the deformation is applied in the direction of the longitudinal axis, which is the symmetry axis, too. So, considering that the skeletal muscle is subjected to the stretch λ_i, where i=1, 2.., N, the whole information about the deformation in the case of the tension is given by the deformation gradient $\mathbf{F}$. Additionally, the deformation of the volume is given by:

$$dV = \det \mathbf{F} \cdot dV_0 \tag{1.1}$$

Eq. (1.1) The determinant of the $\mathbf{F}$ characterizes the volumetric changes. Skeletal muscle can be considered as an incompressible material. Consequently, the volume does not change under any applied deformation. Under this assumption, it is demanded that:

$$\det \mathbf{F} = 1 \tag{1.2}$$

Thus, it can be proved that the $\mathbf{F}$ is described by:

$$\mathbf{F} = \begin{pmatrix} \dfrac{1}{\sqrt{\lambda_i}} & 0 & 0 \\ 0 & \dfrac{1}{\sqrt{\lambda_i}} & 0 \\ 0 & 0 & \lambda_i \end{pmatrix} \tag{1.3}$$

It is worth to be noted that, the third coordinate represents the considered direction which is the longitudinal axis of muscle.

Now, the vector $\mathbf{m}$, representing the unit vector along the symmetry axis of isotropy in the deformed configuration, is given by:

$$\mathbf{m} = \frac{1}{|\mathbf{F} \cdot \mathbf{m}_0|} \mathbf{F} \cdot \mathbf{m}_0 \tag{1.4}$$

The current total stress tensor $\boldsymbol{\sigma}^{(r)}$ at any given material point in the continuum can be written as the sum of an isotropic part $\boldsymbol{\sigma}_i^{(r)}$ and an anisotropic part $\boldsymbol{\sigma}_a^{(r)}$:

$$\boldsymbol{\sigma}^{(r)} = \boldsymbol{\sigma}_i^{(r)} + \boldsymbol{\sigma}_a^{(r)} \tag{1.5}$$

Where r represents the different phases ($r = 1$ in the fiber phase and $r = 2$ in the ECM phase).

The isotropic response is caused by the matrix of the composite material and it is associated with any response under shearing or transverse loading. The anisotropic part is caused by the fibers and represents the stress response in the preferred direction which is also the symmetry axis and axis of the fibers and in our case it is the third coordinate.

1.1.1 Isotropic part of the muscle

There is an isotropic part σ_i in muscle and connective tissue phase. This stress is produced by a non fibrous matrix and biofluids that surround the fibrils in any phase. These materials behave as hyperelastic, given a current mechanical stress described by the neo-Hookean form, as follows:

$$\boldsymbol{\sigma}_i^{(r)} = \frac{G^{(r)}}{J}\left(\bar{\mathbf{B}} - \frac{1}{3}tr(\bar{\mathbf{B}})\boldsymbol{\delta}\right) + K^{(r)}(J-1)\boldsymbol{\delta} \tag{1.6}$$

where

- $\boldsymbol{\sigma}_i$ is the stress given the stretch λ_i ,i=1,2,..,N
- $G^{(r)}$ is the shear modulus. In particular, $G^{(1)}$ is the fiber shear modulus , $G^{(2)}$ is the ECM matrix shear modulus and c is the fiber volume fraction.
- $J = \det \mathbf{F}$, where $\mathbf{F}$ is the deformation gradient
- $\bar{\mathbf{B}} = J^{-2/3}\mathbf{B}$ with $\mathbf{B} = \mathbf{F}\mathbf{F}^T$ being the left Cauchy-green deformation tensor.

  $tr(\bar{\mathbf{B}})$ is the sum of the diagonal elements of the matrix $\bar{\mathbf{B}}$.
- K is the bulk modulus
- $\boldsymbol{\delta}$ is the identity tensor

Three statements need to be noted:

1. We do not take into consideration the bulking part of the incompressible Neo-Hookean behavior because of the constraint $\det \mathbf{F} = 1$.
2. We are interested in the third coordinate of the tensor.
3. The microstructural properties for estimation are the fiber volume fraction c and the shear modulus, $G^{(1)}$ and $G^{(2)}$.

1.1.2 Anisotropic part of the muscle

As it is mentioned, there are two types of fibrils in the muscle. There are the myofibrils contained in the fascicles and the collagenous fibrils inside the connective tissue. These fibers produce anisotropic current stress. It is $\sigma_{\alpha 1}$ for the myofibrils and $\sigma_{\alpha 2}$ for the collagenous fibrils. The appropriate equations are described in the next

sections. The anisotropic part in each phase can be expressed by the reference stress $\sigma_\alpha^{0(r)}$ as follows:

$$\sigma_\alpha^{(r)} = \sigma_\alpha^{0(r)}\lambda = \sigma_\alpha^{0(r)}(1+\varepsilon) \tag{1.7}$$

It is worth to be noted that we are interested in the third coordinate which is the direction of the loading condition and the symmetry axis. Thus:

$$\boldsymbol{\sigma}_{\alpha,33}^{(r)} = \sigma_\alpha^{(r)}\mathbf{mm} \tag{1.8}$$

where $\mathbf{m}$ is the unit vector along the axis symmetry in the deformed configuration.

After the definition of the $\sigma_{\alpha 1}$ and $\sigma_{\alpha 2}$, we can estimate the total anisotropic stress of the skeletal muscle ,using the equation below:

$$\sigma_\alpha^0 = c\sigma_\alpha^{0(1)} + (1-c)\sigma_\alpha^{0(2)} \tag{1.9}$$

The Eq.(1.9) is a result of the Voigt hypothesis which will be proved in the section 1.3.

Let's concentrate on each anisotropic mechanical behavior.

1.1.2α Anisotropic part of the muscle fibers

Muscle fibers are not as every other material which is subjected to a loading. Not only does it response to this loading giving a "passive" stress, but it also produces an "active" part, caused by the nerves' function. Thus, the nominal anisotropic stress is the sum of the passive and the active part:

$$\sigma_\alpha^{0(1)} = \sigma_{\alpha,pas}^{0(1)} + \sigma_{\alpha,act}^{0(1)} \tag{1.10}$$

In this research we focus on the fiber passive part, which is a linear function of the strain as:

$$\sigma_{a,pas}^{0(1)} = E_p(\varepsilon - \varepsilon_{opt}) \tag{1.11}$$

where

- ε_{opt} is the minimum strain at which it is the first time that we get $\sigma_{\alpha,pas}^{0(1)} > 0$.
- E_P is the fiber passive elastic modulus

Here the properties, which should be inferred from experimental data, are the E_P and ε_{opt} .

1.1.2b Anisotropic part of the ECM

The structure of the ECM's collagenous fibrils (C.F) is helical, wrapped around the fibers with a mean angle with respect of the preferred direction $\mathbf{m}_0$. According to the literature, this mean angle θ between C.F and myofibrils should be about 55-60°. Thus, the direction of collagenous fibrils is different from the myofibrils' one. The latter is also the direction of the stretch λ_m . For this reason, a suitable formula, considered the different direction and the angle, is essential to be used. So, the stretch in the collagenous fibrils' direction is described by:

$$\lambda_H = \sqrt{\cos^2\left(\frac{\theta\pi}{180^o}\right)\lambda_m^2 + \sin^2\left(\frac{\theta\pi}{180^o}\right)\frac{1}{\lambda_m}} \tag{1.12}$$

Where

$$\lambda_m = \sqrt{\mathbf{m}_0 \cdot \mathbf{C} \cdot \mathbf{m}_0} \tag{1.13}$$

Now, we can define the stress strain relation that expresses the C.F response and consequently its influence to the total stress. It can be shown that this relation is an exponential one. So, it can be approximated by:

$$\sigma_\alpha^{0(2)} = T1\exp(T2(\lambda_H - 1)) - T1 \ , \ \lambda_H > 1 \tag{1.14}$$

Otherwise $\sigma_{\alpha 2}^0 = 0$

The parameters $T1$ and $T2$ do not have a specific physical meaning by themselves. They are mathematical parameters that their values give us the information about the ECM's response. So, they need also to be inferred from experimental data as they are consequently related to the total response. Another property, which is introduced in this stage and it should be estimated, is the angle θ .

1.2 Homogenization –Voigt hypothesis

Consider a representative volume element V of the skeletal muscle material .Let's assume $\mathbf{X}$ and $\mathbf{x}(t)$ are the position vector of any point in the undeformed and deformed volume element , respectively. The boundary condition, in microscale, is:

$$\mathbf{x}(t) = \mathbf{F}(\mathbf{X}, t)\mathbf{X} \tag{1.15}$$

where $\mathbf{F}(X,t)$ is the deformation gradient which might be changed with the time.

If we assume that the deformation gradient is depended of the position vector X then it is different all over the volume element. It can be proved that:

$$\frac{1}{V}\int_V \mathbf{F}(\mathbf{X},t)\,d\mathbf{X} = \bar{\mathbf{F}}(t) \tag{1.16}$$

This equation combines the microscale with the macroscale. It is the same equation for the stress, too. Thus, we need to realize that the calculation of every single and local deformation gradient or stress in every different point, leading to the numeric solution of the integral, it is difficult to be solved and it has a great computational cost.

Consequently, the homogenization of heterogeneous materials has gained a lot of attention as it is proved to be a very useful tool. In our case, the Voigt hypothesis is introduced, supporting that the deformation gradient field is uniform in the volume element. Consequently,

$$\mathbf{F}(\mathbf{X},t) = \mathbf{F}(t) \tag{1.17}$$

And thus the stresses of each different component are also uniform. Secondly, it can be shown that the macroscopic stress of the volume element can be expressed by the stresses of each individual component (fibers and connective tissue). Thus,

$$\boldsymbol{\sigma} = c\boldsymbol{\sigma}_1 + (1-c)\boldsymbol{\sigma}_2 \tag{1.18}$$

where:
- $\boldsymbol{\sigma}_1$ denotes the stress in the phase of the fibers
- $\boldsymbol{\sigma}_2$ denotes the stress in the phase of the ECM
- c is the fiber volume fraction

In particular, the isotropic total part is given by Neo-Hookean form where $G = cG^{(1)} + (1-c)G^{(2)}$. In the light of this hypothesis, the anisotropic stress of the skeletal muscle can be estimated by calculating the Eq.(1.9).

1.3 Parameter set

Describing the appropriate formulation that creates a bond between the macro scale muscle's response and the microstructure of it, we are confronted with an unknown parameter set, which is a group of internal microstructural properties. Several experimental studies have been developed so these properties could be estimated or some possible ranges of values could be recommended. However, there is a variety of uncertain factors that would influence the results. Generally, there are some indicative values of the parameters originated from these experiments or other computational analyses, but they cannot represent any animal's response. In this research, Bayesian inference is used as a useful tool for learning the unknown properties from experimental data. In this section we introduce the parameter set and the physical limitations regarding their possible values. (Table 1.1)

Table1.1: Parameter set, the meaning and the range of each parameter

PARAMETERS	MEANING(CODE SYMBOL)	RANGES
c	Fiber volume fraction (VOLF)	[0.5-0.99] [6]
ε_{opt}	Fiber optimal strain (EOPT)	[0-0.2]
E_P	Fiber elastic modulus (P1)	[0.0001-0.5] [20]
$T1$	Mathematical parameter related to the ECM's response (T1)	[0-∞]
$T2$	Mathematical parameter related to the ECM's response (T2)	[0-∞]
θ	Angle between myofibrils and collagenous fibrils (THETA)	[55-60][7]
$G^{(1)}$	Fiber shear modulus (GF)	[0.0001-0.1]
$G^{(2)}$	ECM shear modulus (GM)	[0.0001-0.1]

It is worth to be noted that after assigning values to the aforementioned parameter set, the numerical implementation of the analytical constitutive model can be accomplished. It is also necessary to assign to the maximum strain $\varepsilon_{\max}$ and the increments n. Using these variables, the algorithm calculates the displacement λ_i and the strain ε_i in each different increment and subsequently the stress σ_i in the loading direction. The equations of the algorithm are described in order in the paper [15].

CHAPTER 2

Estimation of model parameters based on the experimental data

2.1 Background and stimulus

As it is mentioned in the previous chapter, some typical values of the internal properties have been proposed in the literature. They recommend that by using these parameter values, we can predict the muscle's response in an indicative way. However this action seems to insert an error since choices of the parameter values may not be supported by the available experimental data. Thus, we developed an optimization process, comparing the model with some experimental data. In this way, we can estimate the optimal parameter values in each different tissue case for which experimental data are available. This analysis is described below.

2.1.1 Optimization problem for estimating model parameters

In order to estimate the model parameters we minimize a measure of the discrepancy between the stress-strain relationship obtained experimentally and the stress strain relationship predicted from the model described in Chapter 1. The optimization problem is:

$$\textbf{Min} \quad Er = \sum_{i=1}^{n} \left(\frac{\sigma_{\text{model}_i}(\mathbf{x}_j, \varepsilon_i) - \sigma_{\text{exp}_i}}{\sigma_e} \right)^2 \tag{1.19}$$

$$\sigma_e = \max \left\{ \frac{\sigma_{\text{exp}}^{\max}}{10}, \sigma_{\text{exp}_i} \right\} \tag{1.20}$$

$$\textbf{Such that } lb \leq x_j \leq ub \tag{1.21}$$

The objective function is similar with the second norm of the error between model and experimental stress matrix and the bounds are determined by physical limitations (Table 1.1) Implementing this procedure, we seek an optimal set of parameter values x such that the error between the model prediction and the set of measured data is globally minimized. However, due to insufficient number of experimental data we do not get a unique solution in this optimization problem. This fact will be analyzed in the Chapter 3. Noticing this multiple solution which is a barrier caused by the experimental data available we use more complex analysis that is capable to give us the whole domain of the optimal parameter values and the optimal relationship among

the parameters. The suitable analysis is carried by the Bayesian method .The theory and the methodology are described in the next section.

2.2 Uncertainty quantification

As we said previously, there are a large number of uncertainties in our model that need to be identified. The uncertainty quantification uses the probability and other stochastic quantities in order to deal with the several types of the uncertainties that we face. Probability models are used to model the incomplete information. For instance, the probability of a statement represents the degree of belief or the plausibility of this statement to be true regarding the incomplete information that we have. Thus, the probability density functions (PDF) assigned on a parameter, are used to quantify how plausible each possible value of this parameter is.

In our model, there are a lot of unknown parameters for estimation .They can get a specific value, but this is inaccurate. Firstly we base on wide information collected from the literature (previous information) in order to improve the accuracy of the parameter estimation. Using the Bayesian statistic, we hope to gain more clues about the appropriate values of the internal muscle properties. Particularly the most important advantage of this method is that we can estimate the possible values of each property across a wide range rather than a point estimation losing a large amount of information, as it happens in the previous method. It is also fundamental that the correlations among these parameters can be investigated through this method. In this section the basic theory and its methodology are described. More information can be found in [21].

2.2.1 Bayesian uncertainty quantification based on the experimental data

Consider the PDF of a parameter x. The interval [a,b] indicates the possible values of x and the PDF indicates how plausible is each possible value of x. A distribution is assigned based in previous information and our perception. This probability is called prior PDF $\pi(\mathrm{x}\,|\,\mathrm{I})$ and it is typically illustrated in the Figure 2.1. As it is shown, there is the most probable value inside the red range with a probability p_1. Using the Bayesian analysis, we will update the prior PDF to an updated (posterior) PDF in an effort to learn the parameters using experimental data available by the system. As it seems in the Figure 2.2, if the experimental data are informative, the spread of the posterior is smaller than that of the prior.
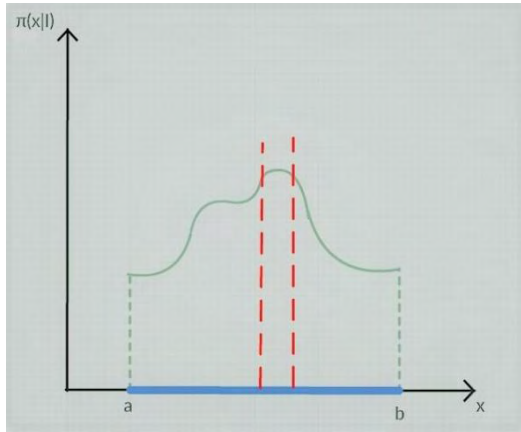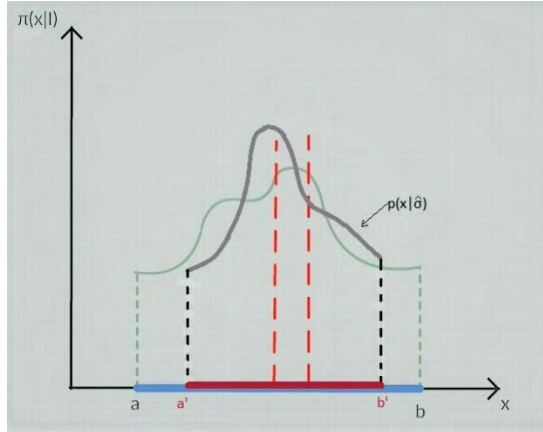
| Figure2.1: Prior PDF | Figure2.2: Posterior- prior PDF |

Let's consider:

- $\hat{\sigma}$ as the experimental data/observation of the muscle stress $\hat{\sigma} = \{\hat{\sigma}_1, \hat{\sigma}_2, ..., \hat{\sigma}_n\}, i = 1, 2, ..., n$

- x as the unknown parameters
- I as the information

BAYES THEOREM:

$$p(\mathrm{x}|\hat{\sigma},\mathrm{I}) = \frac{p(\hat{\sigma}|\mathrm{x},\mathrm{I})\pi(\mathrm{x}|\mathrm{I})}{p(\hat{\sigma}|\mathrm{I})} \tag{1.22}$$

Bayes theorem gives the **posterior** PDF $p(\mathrm{x}|\hat{\sigma},\mathrm{I})$ of the model parameters which quantifies how plausible each possible value of the parameters is in light of the available observations from the system.

The **posterior** is based on two quantities:

1. **Likelihood** $p(\hat{\sigma}|\mathrm{x},\mathrm{I})$ denotes the probability to observe the data from the model given some possible values in the parameter set.
2. **Prior** $\pi(\mathrm{x}|\mathrm{I})$ is the probability of the parameters based on previous information

It should be noted that the **evidence** is a constant term and it does not play any significant role in the probability updating as it is independent from the parameters. However, we use it for the model selection.

2.2.2 Methodology- Software Description

The Bayes theorem is the cornerstone in this analysis. Thus, we need to focus on it in detail so to realize how it is utilized.

The model:

Model

$$\sigma = g(\mathrm{x}, \varepsilon)$$

X ⟶ ⟶ σ
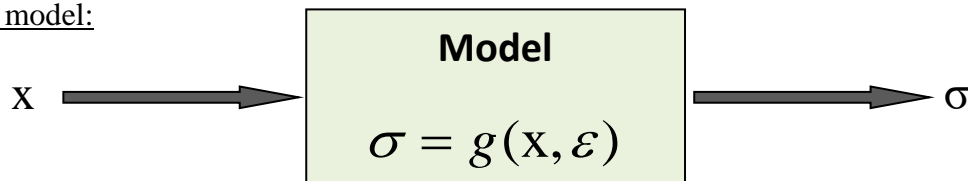
Figure 2.3: Schematic diagram of the model

- σ: output quantity of interest(QoI) given the strain ε.
- x:parameter set x=[x1 x2 x3 x4 x5 x6 x7 x8]. The parameter set is presented in the section 1.3.
- g : mathematical or computational model described in Chapter 1.

Using this model, we can predict the stress of the skeletal muscle which is the output QoI. To calculate this, we need specific values of the parameter set which is the input of the model, while the stresses are finally estimated for each different strain of the experimental data that we have collected. The algorithm is described in the paper [15]

The prediction model (noise model):

Model

$$\hat{\sigma} = g(\mathrm{x}, \varepsilon) + \mathrm{er}$$

x,s ⟶ ⟶ $\hat{\sigma}$

unknown   known
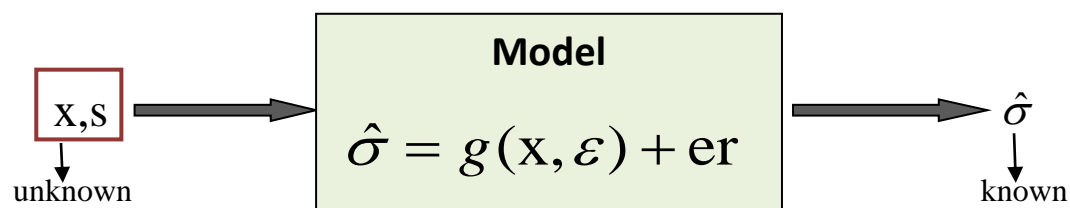
Figure 2.4: Schematic diagram of the prediction model

- $\hat{\sigma}$: the observations/experimental data which are stress-strain sets
- er : prediction error ,assumed to follow Gaussian PDF
    er~N(0,s)

This model represents the discrepancy between the prediction and the experiment. The Gaussian distribution of it expresses that the data are normally distributed around the model output QoI. We will use this expression to develop the Bayes theorem so as to infer the model parameters. Another parameter that we need to quantify is the variances of the prediction error.

We assign a uniform prior PDF to the model parameters with lower and upper bounds defined by the physical limitations and biology knowledge enhanced by previous researchers (Table 1.1). The next quantity which should be defined is the likelihood. The noise model is used to estimate this quantity. Under the assumption that the data

are independent and the prediction error follows a Gaussian distribution, the total form of it is:

$$p(\hat{\sigma} \mid x, s, I) = \frac{1}{(\sqrt{2\pi})^n s^n} \exp\left\{ -\frac{1}{2s^2} \sum_{i=1}^{n} (\hat{\sigma}_i - g(x, \varepsilon_i))^2 \right\} \qquad (1.23)$$

Thus, the posterior can be quantified as it is the product of the likelihood and the prior. The software that it is used in this research has two main components-methods. One is a method for finding the most probable value by minimizing the posterior PDF of the model parameters. We use the Covariance Matrix Adaptation-Evolutionary Stratefy (CMA-ES) [8]. The other one is method for sampling from the posterior distribution. We use the Transitional Markov chain Monte Carlo (TMCMC) method [17]. According to TMCMC, the strategy is to draw samples from the optimal posterior of the model parameter x such that the model $g(x, \varepsilon)$ has a good approximation to the observations. We obtain samples that distributed in the whole support of the posterior, expressing a measure of the variability. It is a repeated process that generates temporary samples from intermediate posterior PDF till finding the samples from the target posterior PDF of the parameters x. In the end, the samples populate the posterior PDF, finding the support of the posterior PDF and thus characterizing the uncertainty in the model parameters. These samples can eventually be used to estimate the mean value and the covariance of the parameters. In addition, it can be used to obtain the marginal distribution of the model parameters. More details are presented in the next chapter.

.

Each component is described in the next paragraphs.

2.2.2.A The CMA-ES software applied in Bayesian analysis

It is used to quantify the most probable values of the parameter set, by optimizing the posterior. Specifically, it minimizes the

$$-\ln(p(x \mid \hat{\sigma}, I)) \qquad (1.24)$$

As we described before, the posterior is the product of the likelihood and the prior. The prior is a uniform distribution and as a consequence it is a constant term in the whole range. Thus the posterior is only dependent on the likelihood and the optimization problem is transformed to optimizing the

$$\ln(p(\hat{\sigma} \mid x, I)) \qquad (1.25)$$

The question that this framework answers is "what are the optimal values of the parameters such that the –ln-likelihood takes the minimum value. In other words, this component combined with the MCMC methods leads to the most probable values of the parameters x and the smallest uncertainty of then included in the prediction error regarding the experiments, so that the model has the best fit to the experimental data. In this way, the resulting posterior probability can then be used to robustly quantify the uncertainty in the model predictions. More details about development of this code are exhibited in [8].

2.2.2.B TMCMC sampling method

The practical value and computational cost of the Bayesian framework is largely determined by the effective way of sampling the resulting posterior distribution. MCMC is the key step to implement the Bayesian method in the case of complex distributions. In the last decades a number of software have been developed of the purpose of the most efficient sampling by using Markov Chain Monte Carlo or other improved concepts of it like transitional MCMC(TMCMC) or manifold transitional MCMC(mTMCMC). These sampling algorithms generate a large number of samples originated from the optimal posterior distribution following specific steps. The posterior of the parameters x depends on the likelihood, which is not a Gaussian while it has a term of the model inside it.

We used two types of MCMC software – the TMCMC and the mTMCMC. We started with the TMCMC but as we will describe later in chapter 3, mTMCMC gives us better results including more information. The main difference between of them is that the mTMCMC takes into consideration the derivatives of the posterior with respect to each parameter and introduces a new quantity, the Fisher information matrix which hides the mean of the squared gradient of the model. As the prior is uniform, the derivative of the prior vanishes and the derivatives of the posterior transformed to the gradient of the log-likelihood. As this extensive method needs to be described fastidiously and it is not the purpose of this thesis, more details can be found in paper [17].

The sampling part of the code is extremely computationally expensive. As the number of the unknown parameters increase in the model, the number of the samples also increases. The user should choose a large number of samples so that accurate results are obtained without losing significant information. It was found in this research that this task is a great challenge because the problem is unidentifiable. The unidentifiability arises from the fact that a large number of parameters exist that are difficult to be estimated due to the limited available information originated by the experimental data. The model parameters are eight plus the variance of the prediction error. The number of samples considered reached 100000. Consequently, this is exhaustively expensive and it cannot guarantee that we will get accurate results,

characterized by uniformly generated samples in the whole range-domain of the posterior distribution.

This is the reason why we seek for a way to reduce the parameter dimension in this model or uncertainty of the model. At first sight, we understand that we cannot choose inconsiderately the parameters that need to be rejected. This decision can be based on the variance that characterizes the multiple optimal solutions from the optimization process. This is also described in detail in the next chapter.

2.3 Sensitivity analysis

We have also implemented a global sensitivity analysis based on Sobol indices. The results of it can help us to understand the importance of each parameter and how it influences the output QoI of the model. In this way the analysis of the results can be enhanced, as we can explain the most probable values and the variances of the marginal distributions of the parameters. The current analysis is presented in the next paragraph.

2.3.1 Sobol analysis

Sobol analysis calculates the sensitivities S_i, S_i^{tot} of the QoI to the i-th parameter, which is given by:

$$S_i = \frac{\text{var}\{\text{E}[\sigma \mid \theta_i]\}}{\text{var}\{\sigma\}} \qquad (1.26)$$

This quantity represents how much the variability in a parameter value can influence the model output. Noticing the values of the sensitivities, we can separate the important parameters, based on our perception. The small values of the sensitivities mean less importance of the associated parameters in the output. There is also a table shown below and taken from the paper[18] that advices us how we can distinguish the less sensitive parameters from the important ones.

Table2.1: Relevance of an input parameter from its global sensitivities

Very important	$0.8 \leq S_i, S_i^{tot} \leq 1$
Important	$0.5 \leq S_i, S_i^{tot} \leq 0.8$
Unimportant	$0.3 \leq S_i, S_i^{tot} \leq 0.5$
Irrelevant	$0 \leq S_i, S_i^{tot} \leq 0.3$

At first, knowing the results from Sobol, we can examine the results of the Bayes framework, like the most probable values and the variance of each different parameter. This method helps us to improve our perception about the parameters values, their variance and the impact of them on the model, lead us to more informed conclusions. As a final step, one can say that small divergences of the optimal values in the most insensitive parameters cannot change the results given by the Bayes analysis, while we can conclude the exact opposite about the important parameters. The analysis is described in aforementioned paper.

CHAPTER 3

Applications

In this chapter were present the applications of the theory developed in this research. The first section illustrates the experiments that are used for the purpose of optimization and Bayes framework implementation. In the next sections, we present the result of each different application and we examine them. The analysis is enhanced by the Sobol analysis results that they are also described in this chapter. Specifically, the sections are developed with regard to the experiments. Thus, the Section 3.1 is about the first experiment taken from [1] and the Section 3.2 is about the second selected from [2], according to the Table in the Appendix A. In the following section, we investigate the species variability that is based on the nature of the system.

3.1 First experiment selected from the paper of Hawkins and Bey [1]

The stress-strain relationship from the experiment is illustrated in Figure 3.1.
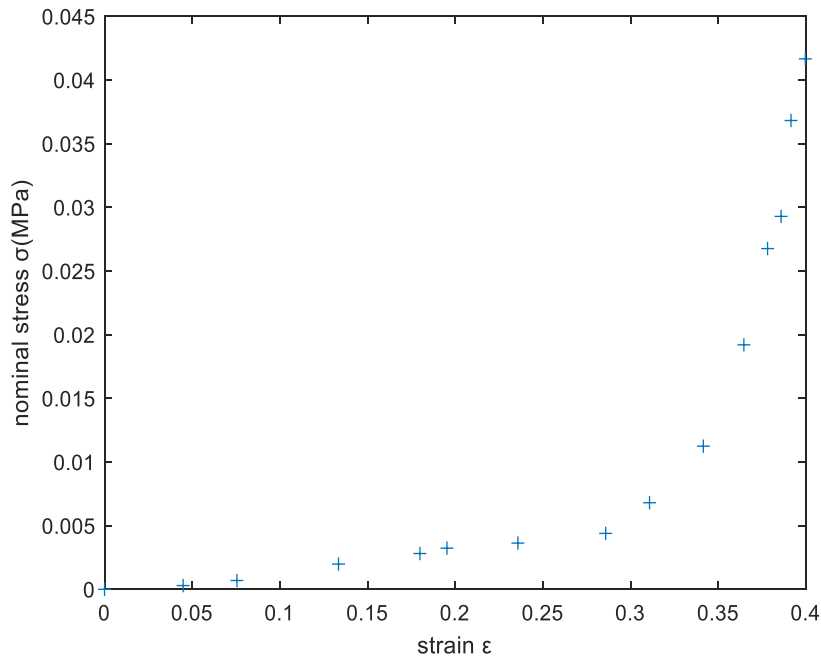
Figure 3.1:Hawkins and Bey's experiment, stress-strain relationship

3.1.1 Optimization process

Comparing the model with the experiment we get multiple solutions. Let's note that Hawkins and Bey [1] propose a specific value for the variable ε_{opt}=0.192 which is directly obtained from the experimental data of their experimental study. Thus, we use this recommended value. We run the optimization framework which is CMA-ES and its procedure and methodology has been described before. In particular, we execute the same code with the same inputs and options several times. The Figure 3.2 indicates the curve of the model and the experimental data. As it is shown, in all the executions the model approaches in the same "global" way the experimental data, managing to reduce the error between them. The figures below show the variance in the optimal parameter solutions. It is worth noting that we choose to illustrate only the trials that give us the same optimal objective function, which is the global minimum of it. It seems there is a variety of combinations of the optimal parameter values that identify the minimization of the objective function. However, there are several runs that could not give us this optimal result, trapped in local minima, or cannot converge. Thus, it seems that this method is not always able to give accurate information about the appropriate optimal values of parameters that fulfill simultaneously the physical conditions and the mathematical global optimization. Consequently, sometimes we need either to filter the results or interfere. In this case, we exhibit only the global minima.
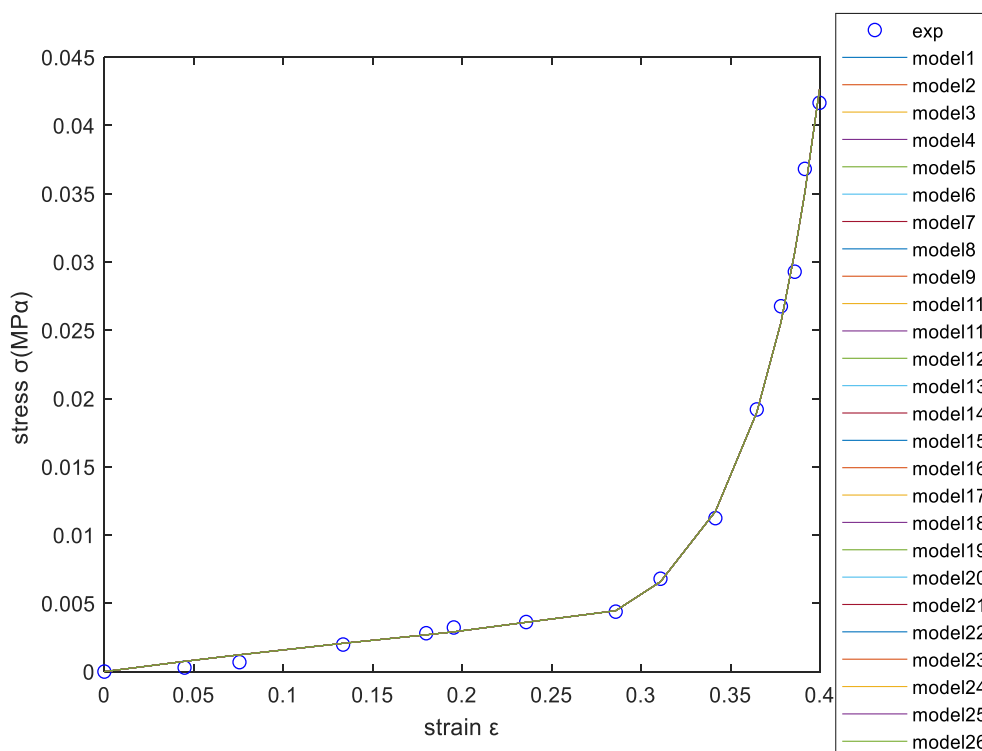
Figure 3.2: Optimized model curves,model propagation for the experiement

In the Figures 3.3, we present the optimal values of each parameter and the fact that they are characterized by a variance in each different execution. As we can observe, there are some important differences in the results of point-based parameter estimation.

(a)

(b)

(c)

(d)

(e)

(f)
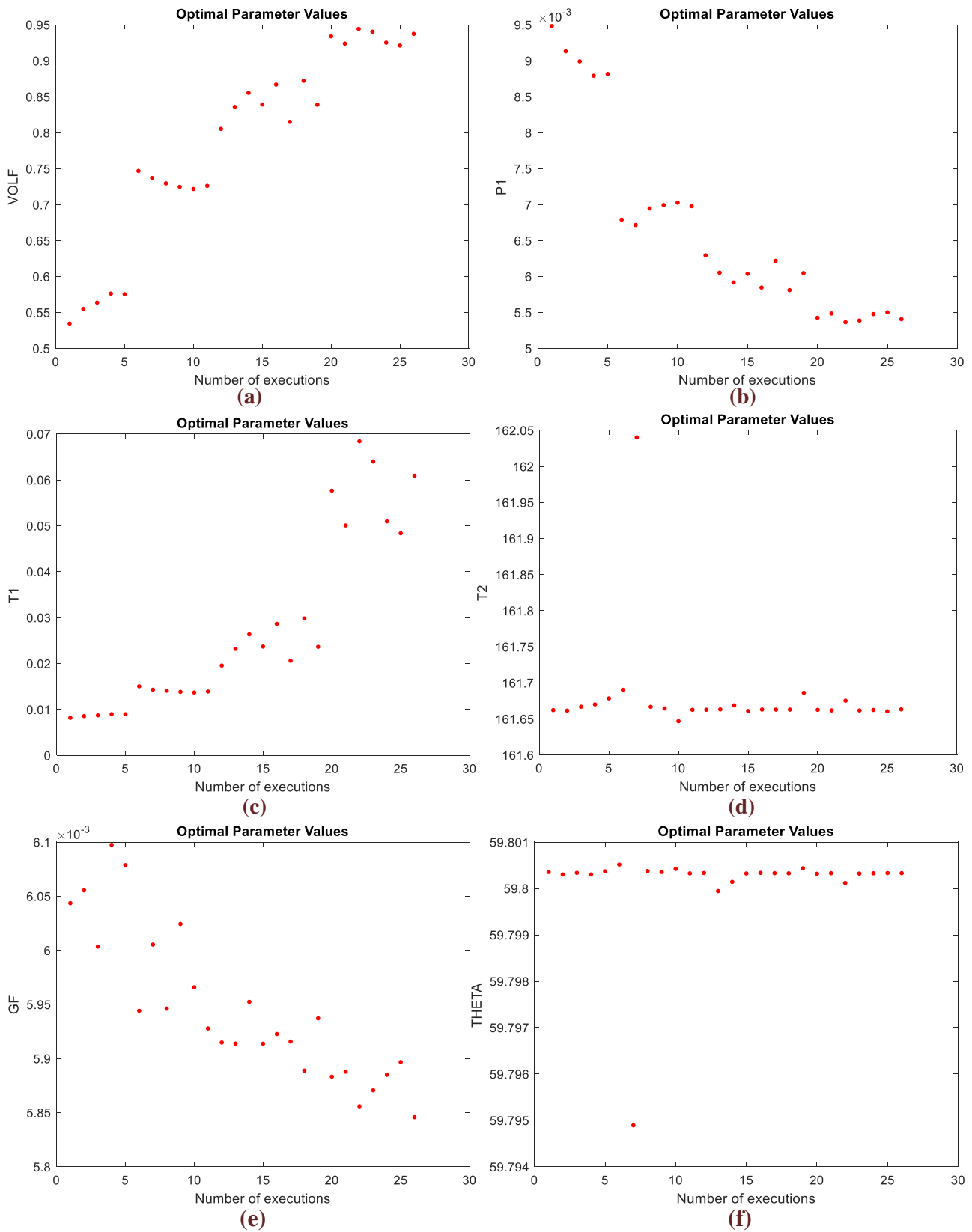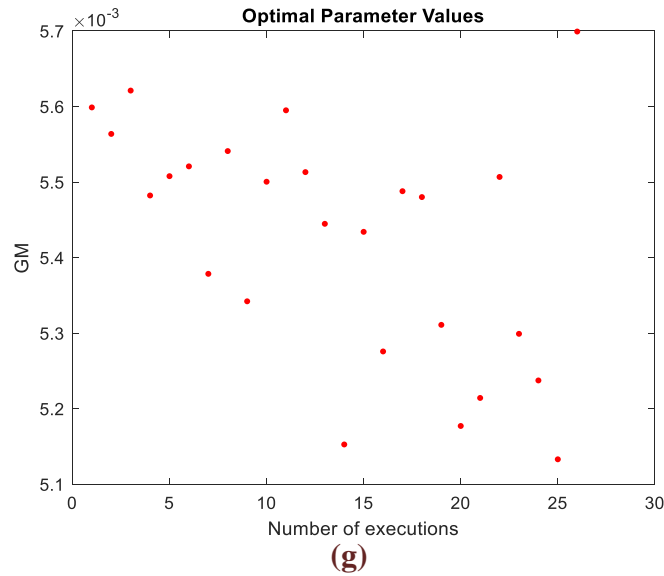
Figure 3.3: Variability of the optimized parameter values for the first experiment, (a)VOLF: fiber volume fraction, (b)P1: fiber elastic modulus, (c),(d)T1,T2: mathematical parameters related to the CME's response, (e)THETA: angle between collagenous fibrils and myofibrils, (f),(g)GF,GM: fiber and connective tissue shear modulus

The purpose of this section is to investigate the variability of the optimal parameter values. We illustrate the results about this experiment so that we can focus on the point of this statement and the next step which is also a greatly important part of the research. Realizing that this variability cannot give us the whole information that we seek, we need to search in other methods. Moreover, implementing this framework we were confronted with the obstacles regarding the local minima. As the point based estimation loses accuracy, the Bayesian seems to be the solution. It is able to give us not only the optimal parameters values but a measure of the uncertainty by representing the support of the posterior distribution. In the next section, the results of the Bayesian approach are illustrated for each different experiment.

At first sight, another attribute that someone can notice is that there is variability, large in some and small in other parameters. This is an interesting characteristic that may be allied with the sensitivity of the model to each different parameter. This feature will be discovered by implementing a more evaluate method, called Sobol analysis.

3.1.3 Bayesian framework

Firstly, we present some results of the Bayesian analysis using this experiment. In these results, as it is shown we used only four variables of the unknown parameter set. These four parameters were chosen regarding their variances, while examining the optimization process results. In the next step, we will explore the 8th dimension of the unknown model parameters. However, the results of the current parameter set which is θ= [VOL T1 GF GM σ], are also worth to be noted. Although it is vital to implement this framework for all the parameters, searching about less parameters than eight has some advantages. We manage to reduce the exhaustive computational cost of the sampling task and subsequently the time that every single execution needs. Moreover, we limit the model uncertainties and we can handle and estimate the results at the first sight.

As we mentioned in the chapter 2, section 2.2.2B, we developed two frameworks based in MCMC (Markov Chain Monte Carlo). The figure 3.4 shows the results of the TMCMC. Each different plot has a meaning. The diagonal plots are the marginal distributions of the parameters. Under the diagonal, the contour plots in 2D space of a parameter set $\theta = [\theta_i, \theta_j], i \neq j$ are shown. The yellow points are the most probable values of the parameters. Upper than the diagonal, there are the samples of the optimal parameter values. In these plots we can also notice the correlation between the parameters. The mTMCMC plots are similar.
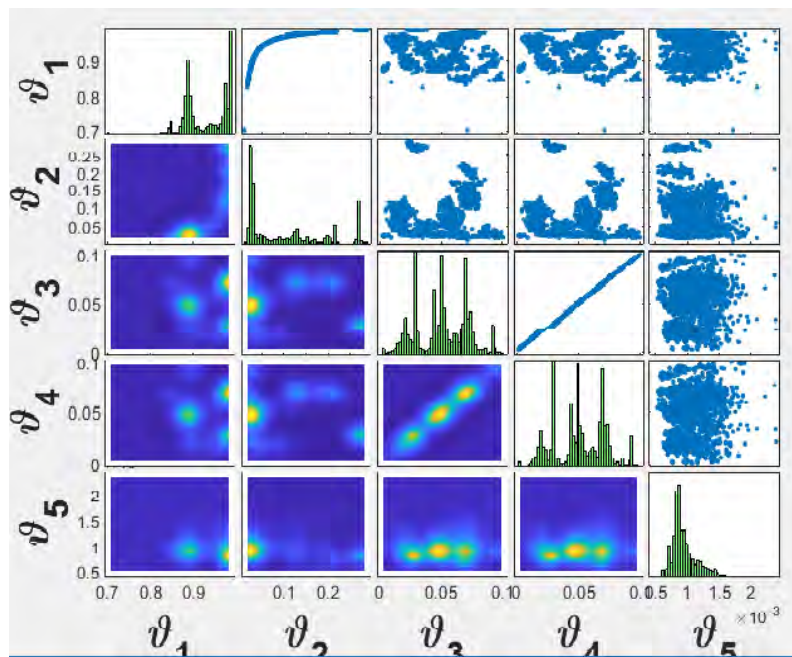
Figure 3.4: TMCMC results about 5 parameters

As we can observe in the Figure 3.4, the TMCMC algorithm is unable to produce samples from the posterior distribution. It has a difficulty in generating uniformly samples in the whole parameter space and subsequently it cannot provide good quality marginal distributions of the parameters because the model is highly unidentifiable.

Furthermore, it seems that it does not have the capability to gives us the contour plots of the most probable values in the whole parameter domain, as they are centered in some points. This is also the explanation of the multiple picks that the distributions have. Another point that needs to be noted is that these results can be different in several same runs because of the demanding task of sampling method, leading us not to trust each result. However, this framework can give us a good quality of model predictions, while using the generated samples the model's response approaches efficiently the experimental data. Consequently, we implement another improved version of MCMC which is called manifold TMCMC and it delivers more accurate results. The results of this method are illustrated in Figure 3.5.
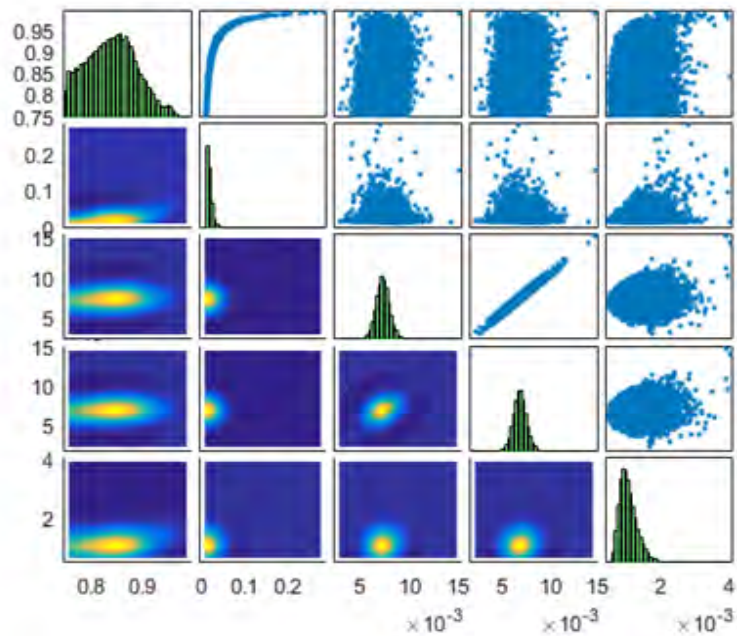
(a)
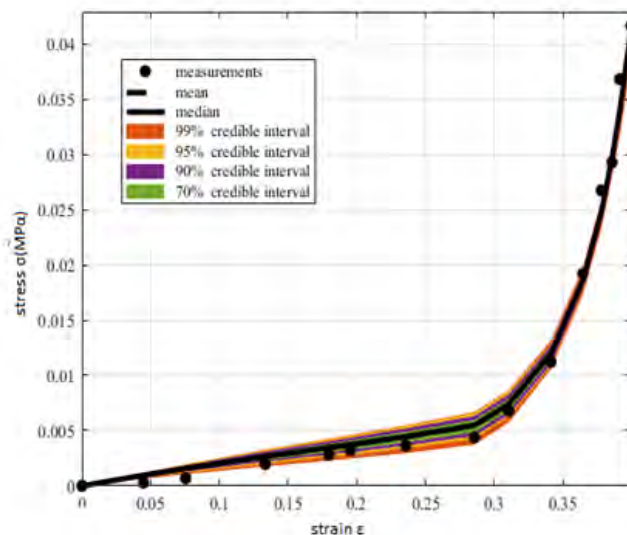
(b)

Figure 3.5: (a)mTMCMC results and (b)current model uncertainty propagation

These plots illustrate the most probable values of the parameter set. Let us remind ourselves that the considered model parameter set is $\theta = [\text{VOLF}, \text{T1}, \text{GF}, \text{GM}]$ and the subplots are distributed appropriately. These values can give efficient model propagation with a small variance as it is shown in the bottom plot of Figure 3.5. As we mentioned before, the diagonal elements-plots are the marginal distributions of each parameter. For instance the plot (1,1) illustrates that the parameter $\theta 1$ (fiber volume fraction)can take value in the range [0.75-0.99] with some possibility. The most possible value is in the range [0.8-0.9], as it seems not only from the distribution but from the contour plots, too. However there are also some other samples over this range that can give equally the best model fitting with the experimental data. Consequently, someone can say that the first parameter can take values inside the range [0.75-0.99] such that the model is able to approach the data.

Let's introduce the second parameter in our analysis. This parameter represents a mathematical parameter, related to the connective tissue's response. Let's give some emphasis to the plot (1,2) that determines a correlation between the first and the second parameter . It says that if someone chooses a specific value of the first, then he should follow this thin and strict parabolic curve. Every combination outside of this curve cannot give the same efficient approximation of the experimental data. Furthermore, the most probable values of the shear modulus came from the contour plots where are yellow in a specific area around the value 0.006.

Regarding all these points, we can say that the suitable ranges of the parameters are:

Table 3.3: Suitable parameter ranges

PARAMETERS	RANGES
VOLF	[0.75-0.99]
T1	[0-0.3]
GF	[0.005-0.01]
GM	[0.005-0.01]

The probable values are:

Table 3.4: Probable parameter values

PARAMETERS	MPV
VOLF	Multiple
T1	Multiple
GF	~0.006
GM	~0.006

This conclusion can be proved also comparing the optimization results with mTMCMC results. The Figure 3.6 illustrates the CMA points and the mTMCMC samples in the same plots and the accuracy of each different result. CMA points are generated while we execute optimization framework only for the interested

parameters and the others are fixed in their globally values proposed by the Figures 3.3.
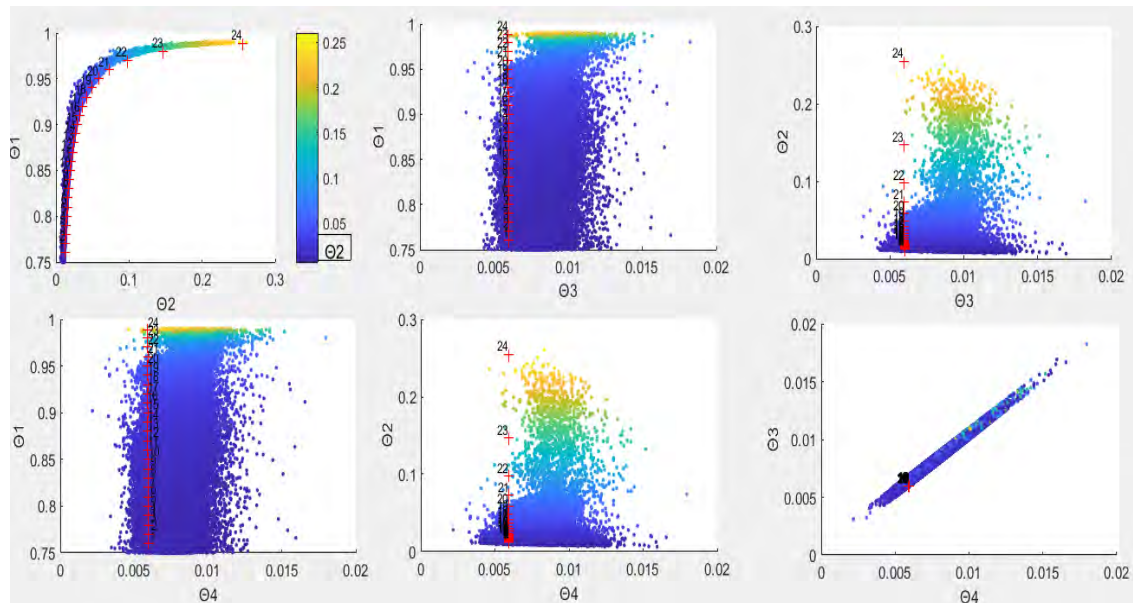
Figure 3.6: mTMCMC and optimization results

The red points are generated by the optimization framework and the others are painted with different color with respect to the values of the $\theta 2$. It is noticeable in the Figure 3.6 that the two analyses converge in the global solutions, as the CMA results coincide with the mTMCMC results. So, it is recommended to compare, combine and take into account all these results so as to make a conclusion about the most suitable parameter values which are capable to give model prediction that approximates efficiently the realistic behavior.

Regarding the optimization results, it is proved that the fiber volume fraction can take a value inside the range [0.5-0.99]. However, if this experiment refers to a healthy rat, this means that the fiber volume fraction should take values only inside the range [0.9-0.99]. This is a physical limitation that needs also to be considered. Consequently, the second parameter needs to satisfy the parabolic relationship and the shear moduli can be equal to 0.006. This parameter estimation includes typical parameter values proved that the model response fits the Hawkins experiment very well.

Parameter set θ=[VOLF P1 T1 T2 THETA GF GM s]

Let's direct our attention to the eight-parameter inference, so we can make some accurate conclusions for all the model parameters. The Figure 3.7 indicates the mTMCMC results about the whole parameter set which is θ= [VOLF P1 T1 T2 THETA GF GM s]. The figure 3.8 illustrates the samples of the posterior colored with respect to the first parameter (fiber volume fraction). In the same figure there are also the optimal parameter sets generated by the optimization process.
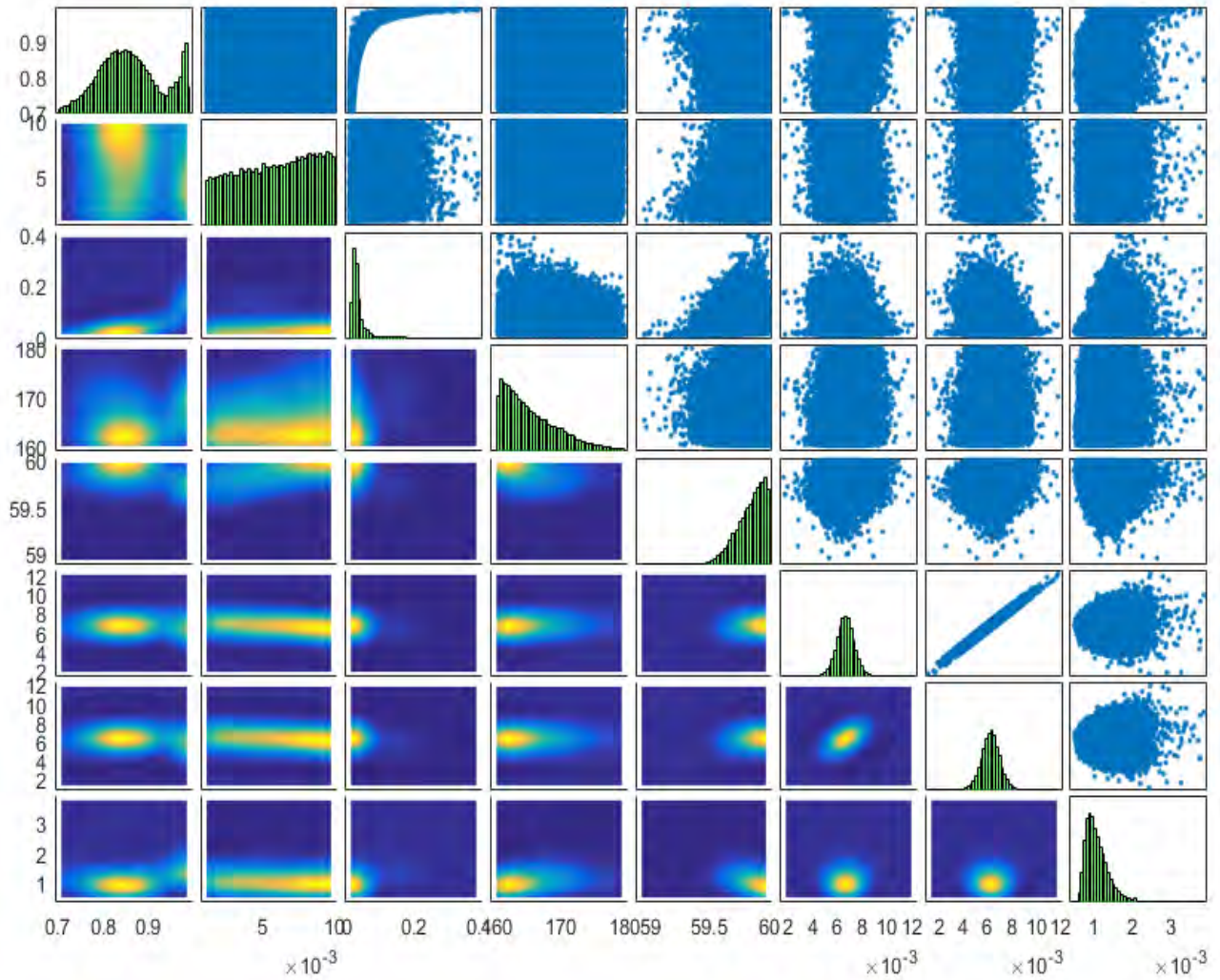
Figure 3.7: mTMCMC results for parameter set θ=[VOLF P1 T1 T2 THETA GF GM s]
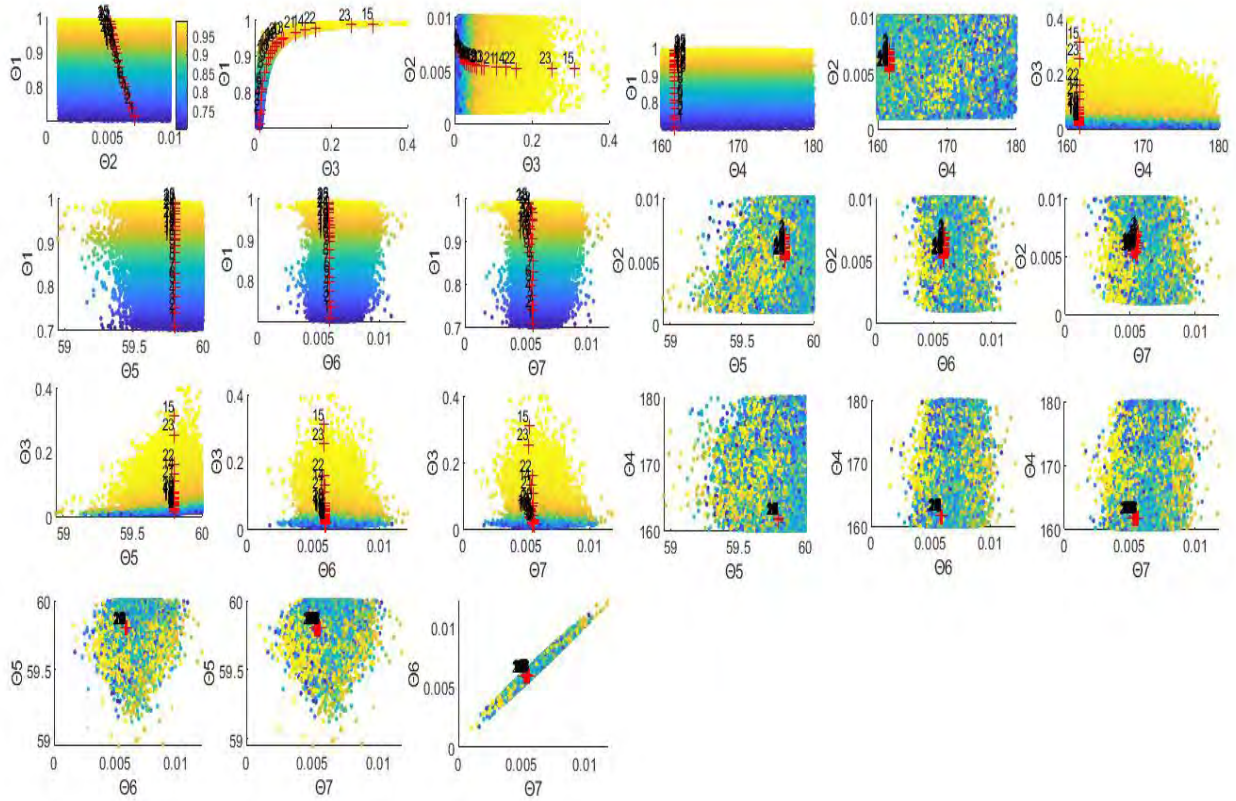
Figure 3.8: mTMCMC results, colored with respect to the VOLF, and CMA results
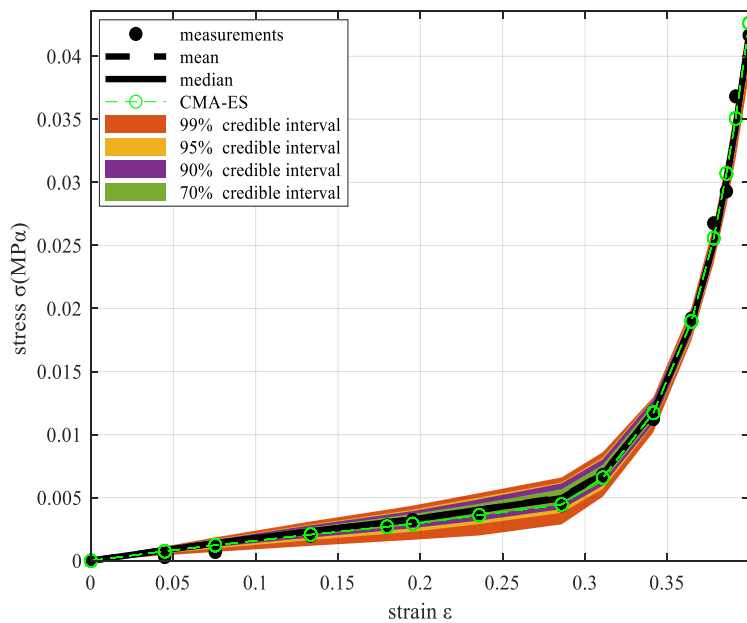
Figure 3.9: Model uncertainty propagation, resulted from mTMCMC

The Figure 3.8 illustrates the accuracy of both analyses, as the CMA points are included in the mTMCMC results. This figure has the whole information about the model parameter set. It advices us what are the optimal parameter values and it gives us also some instructions about the support of the posterior. The values of the model parameters match with specific values of the other parameters, as they are colored with respect to the VOLF. That means that every appropriate optimal parameter set of the colored mTMCMC results can give very good model propagation with a small uncertainty. This fact is also proved by the Figure 3.9, which illustrates the model prediction using not only the samples from the posterior of the model parameters but also the prediction error. Consequently, examining this figure, one we can say, that the discrepancy between model and experimental data using the samples from the mTMCMC or from the CMA is very low.

In the Figure 3.8, the samples of the optimal posterior are colored with respect to the VOLF's values. Examining them, the values of this parameter match with specific values of the others. So, if the fiber volume fraction is chosen to be equal or around to 0.97 (yellow point), the other parameter should take a value of a yellow sample, approximately close to the values, shown in Table 3.5:

Table 3.5: Probable parameter values

PARAMETER	SUITABLE VALUES	EXPLANATION
Eopt	0.192	Hawkins's recommendation
P1	~[0.0001,0.01]	Uniform distribution, range: [0.0001, 0.01]. There are yellow points in the whole domain. One can follow the instruction of the literature about this parameter.
T1	~[0.1,0.4]	1 dimensional manifold ,strict correlation(figure 3.10)
T2	~162	Highest probability at this value(figure 3.7), gradually reduced
THETA	60	Marginal distribution centered on this value(59.8 proposed by the optimization)
GF	0.006	Marginal distribution centered on this value
GM	0.006	Marginal distribution centered on this value

We continue our analysis by discovering the strict correlation between the fiber volume fraction and the T1 by using the CMA-ES framework. Particularly, we generate CMA points of the optimal parameter values with an automated way by doing multiple executions of the CMA-ES framework and changing the bounds of the fiber volume fraction in each different time. The way that we change the bounds is described below:

%Total bounds of the VOLF: [0.5-0.99]

$$di : \text{step}(\text{user's choice})$$

$$Upper\_bound_i = lower\_bound_i + di$$

We choose the VOLF because it has a great meaning for each leaving organism and as it seems the model can approach efficiently each realistic mechanical behavior using several different values of this parameter. This attribute is noticed also in some other parameters as it is illustrated in the Figure 3.3.

The Figure 3.10 indicates the trend line of the CMA-ES results about the fiber volume fraction and the T1 parameter. We use the cubic spline interpolation and we can approach the CMA-ES points, as it is shown in the figure. In order to follow this correlation, someone needs to choose the appropriate constant terms of the cubic function which is:

$$C_i = a_i + b_i x + c_i x^2 + d_i x^3$$

In the appendix B, one can find the basic theory of cubic spline interpolation and the optimal values of the considered constants.
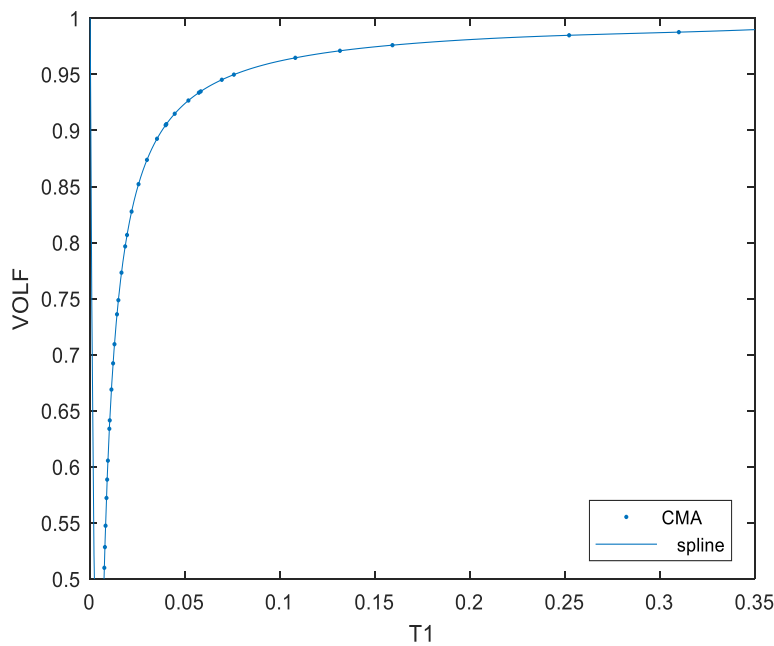
Figure 3.10: Trend line satisfying the strict correlation VOLF-T1

We can observe in the Fig. 3.8 that the samples of the parameters THETA, GM and GF are chaotically distributed and they are not lined up respect to the color (blew, cyan, green, yellow).This is related to the fact that the marginal distributions and the contour plots are centered on a specific value. So, the most of the generated samples of these parameters are point-centered but characterized by a standard deviation. The standard deviation of the GM and GF's marginal distribution is larger than the THETA's. Another parameter that has a great variance is the P1, which approximately

follows a uniform distribution. The variance of the GM, GF and P1 is related to the model's sensitivities. As it is proved by using the Sobol analysis, the model has low sensitivity on the mentioned parameters. For this reason, a recommended value can be specific but any other small divergence from this value cannot considerably influence the output, remaining the accuracy in a high level. Specifically, the Sobol analysis results are shown in the next paragraph.

Sobol analysis results: The Table 3.6 indicates the sensitivities, listed in descending order.

Table 3.6: Sobol results

Parameters	Relevance
THETA	Great important
T1	Important
VOLF	Important
T2	Partially important
P1,GM,GF	Irrelevant

Seeing this result, we can conclude that the P1, GM, GF are so unimportant that any discrepancy of a specific value cannot change the output QoI. Consequently, the optimization process can give various solutions especially for the unimportant parameters such that give the same global value of the objective function. It would be useful to proving this variability once more, by running the optimization (CMA-ES) while we keep the fiber volume fraction (VOLF) fixed in an optimal value. The choice of VOLF to be standard seems appropriate as it has a great meaning for the living beings and the final mechanical behavior of the muscle. The Figure 3.11 illustrates five different optimal values of the GF and GM respect to each execution, which gives the same global minimum of the error between model and experiment.
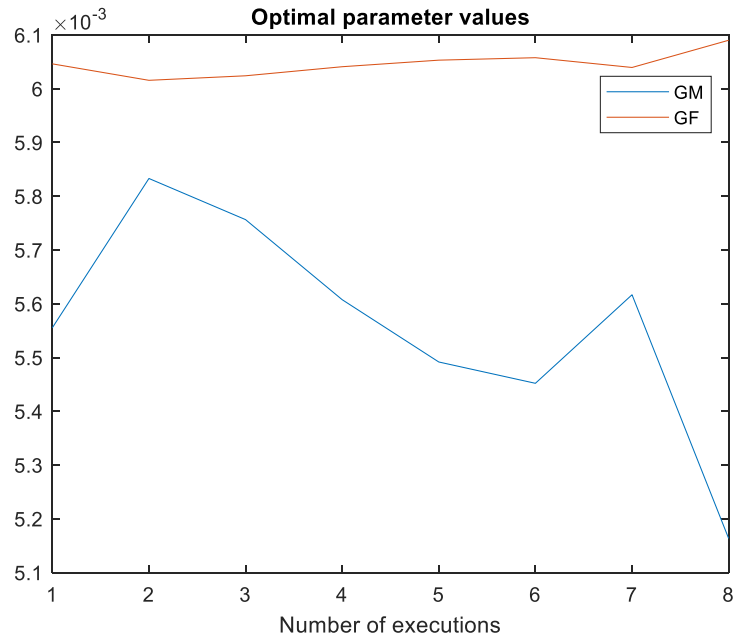
Figure 3.11: GM and GF optimal values to each execution, measure of variability

This result is combined with the Sobol results and explains one more time the variance of the GM, GF marginal distributions. Sobol also proves us the approximately uniform distribution of the P1. Thus, the P1 can take any values inside the considered range without losing the efficiency of the model propagation and the user's decision depends on his knowledge or previous information.

On the other hand, examining the Sobol results, the parameter THETA has a great effect on the output quantity of interest, fact that is also proved by the optimization problem (Figure 3.3) and by the sensitivity analysis. It is also inferred in [15]. This is the reason why the PDF of THETA has smaller standard deviation and subsequently high probability in the most probable value. So, the parameter THETA must be in the strict range of [59.7, 60] and particularly a recommended value is 59.8 so that we can take a good model propagation.

In order to underline this attribute and to enhance the result analysis, we implement the Bayes framework for the three most important parameters which are VOLF, T1 and THETA, while the others are fixed in some typical values.
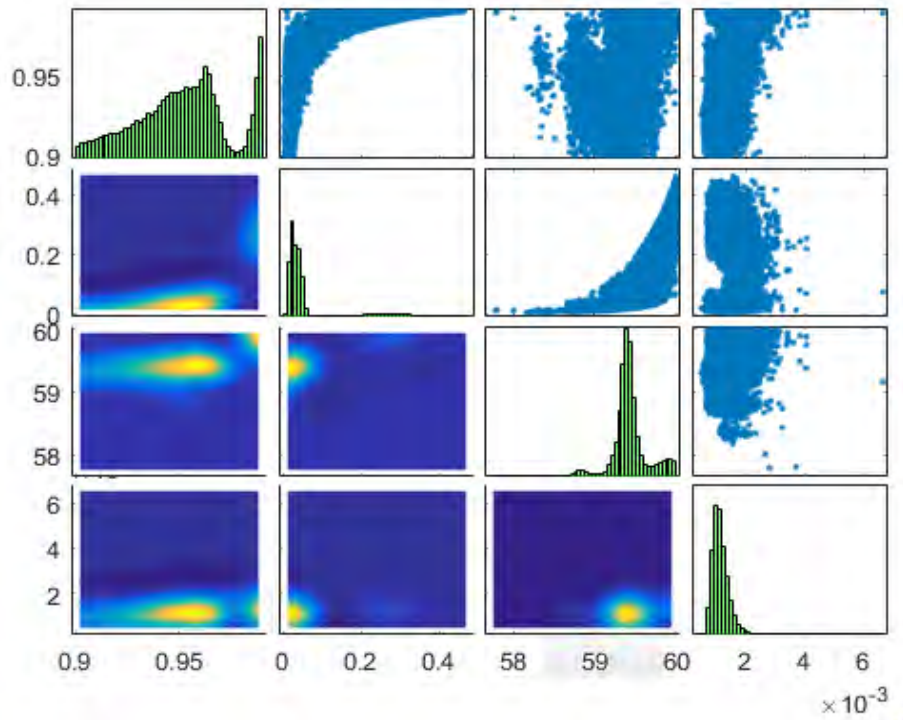
Figure 3.12: mTMCMC implementation about θ= [VOLF T1 THETA]

The software results in the best likelihood, found at VOLF=0.989, T1=0.265, THETA=59.8. Noticing the results, we can prove once more what we analyze before .It becomes evident that the fiber volume fraction for healthy species can take any value inside the range [0.9-0.99], the T1 parameter needs to satisfy the correlation and the THETA must be equal to the value 59.7.

Another notation that should be done, is that it is finally undeniable after finishing the whole analysis that the fiber volume fraction can take any value inside the range given by the physical limitation which is [0.5-0.99]. The model can approach the mechanical behavior of a skeletal muscle about either a healthy or an unhealthy organism. Consequently, the value of it depends on the purpose of each research and the researcher's decision.

3.2 Experiments selected form the paper of Calvo et al. [2]

Let's continue with another experiment. It is also a rat and the same type of muscle (Table in the Appendix A). We implement the same analyses and we will see if the results about the rats can match, so that we can result in a general conclusion about these species. These experiments are five and the experimental data are illustrated in the Figure 3.13. A great advantage of this group of experiments is that they are five rats that are grown up in the same environment with the same conditions and treatment. Seeing this, we can ensure that any conclusion resulted from the analyses about this group include specific uncertain factors, like measurement uncertainty, and we know that these factors cannot change in each different experiment. This measurement uncertainty may arise from variability in set up of the experiment, several errors in the measuring equipment or errors in the measuring procedure.
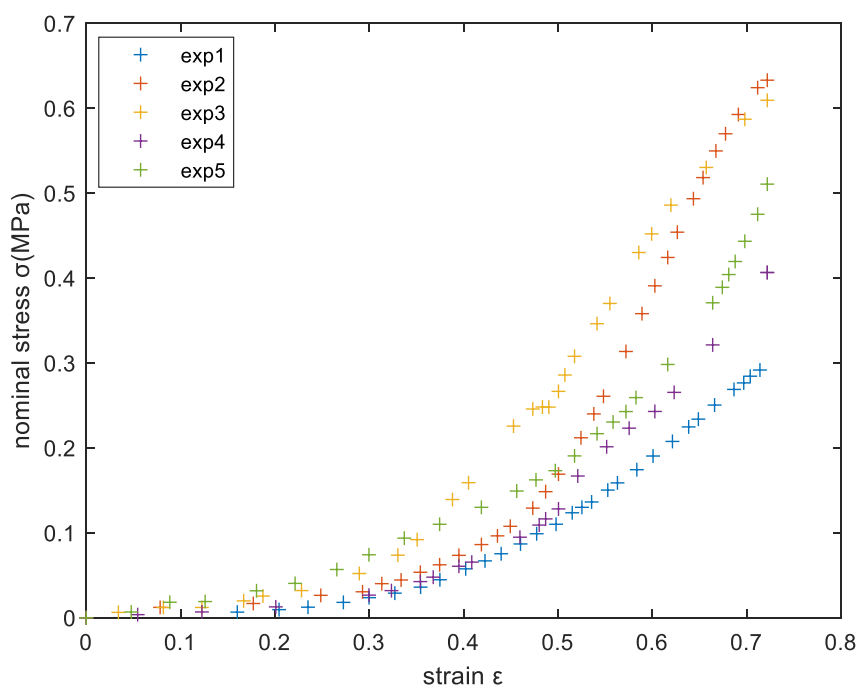
Figure 3.13: Experiments from the paper of Calvo et al.

As we can see, there is a great difference along the experimental data, despite the fact that the same species are objected to the same experimental conditions and equipment. For this reason we implement all the methods for each case as we expect some divergence in the results, too. As it seems with a first sight, there may be different optimal model parameters such that the model can efficiently identify this variety of mechanical responses.

3.2.1 First experiment

In the next paragraphs 3.2.1.1 and 3.2.1.2 we analyze the results from the CMA-ES and mTMCMC frameworks, executed for the first experiment from [2], respectively.

3.2.1.1 Optimization analysis

We run the optimization process for this experiment and we get multiple solutions once more. We implement the CMA-ES by changing every time the bounds of the fiber volume fraction to smaller bounds than [0.5, 0.99] with a step of 0.01. Doing this, we gain a lot of different optimal parameter values that give the same global minimum of the error, as it is shown in Figure 3.14 (model with solid line). We are interested in the strict correlation between the fiber volume fraction and T1 as it is proved in the previous experiment. In the next figure the multiple optimal parameter values are illustrated. Moreover, seeing this solution the next step is the Bayes framework implementation.
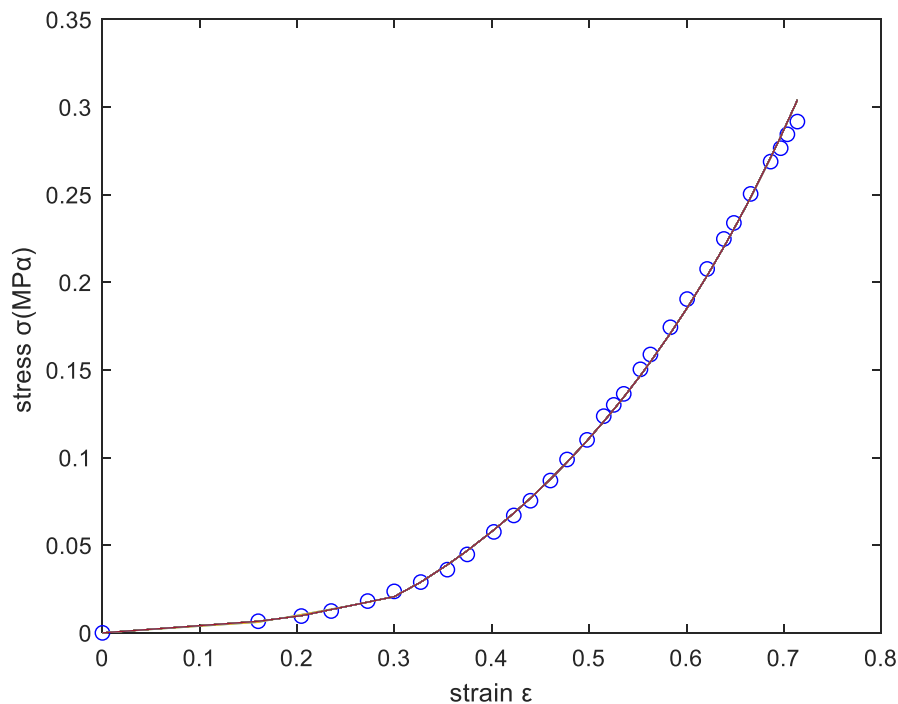
Figure 3.14: Global model approximation of the 1ˢᵗ experiment from [2]

The multiple solutions are illustrated in a clear way in the next Figures 3.15
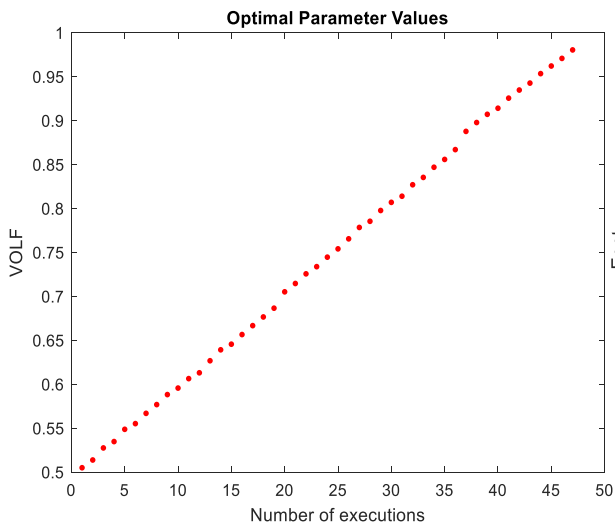
(a)
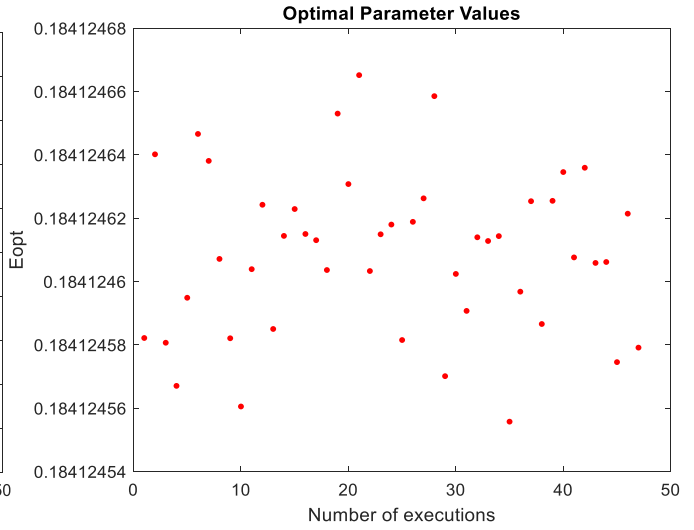
(b)
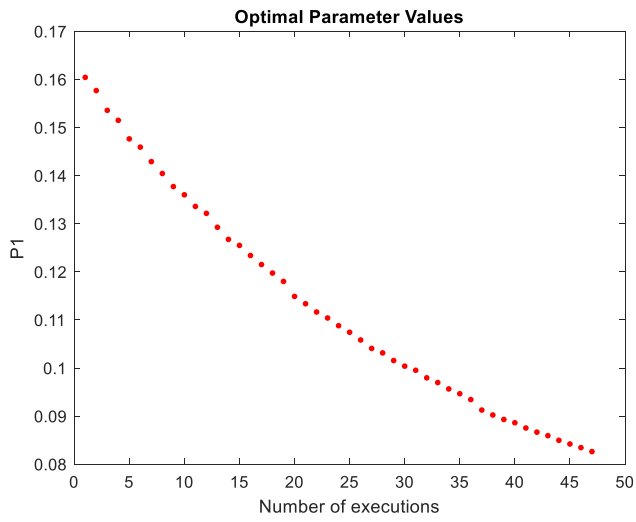
(c)
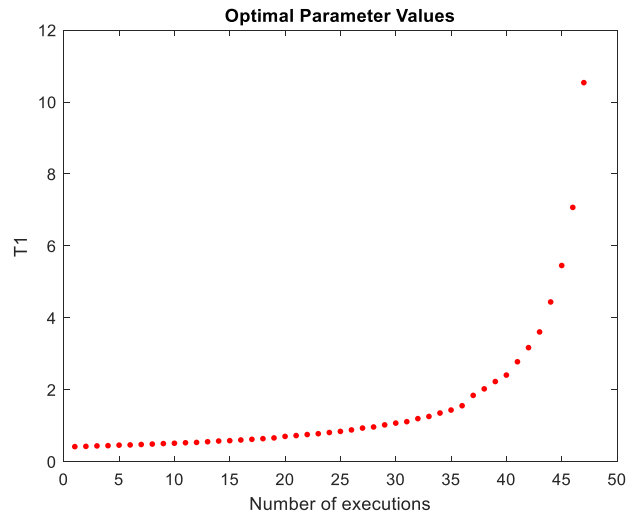
(d)
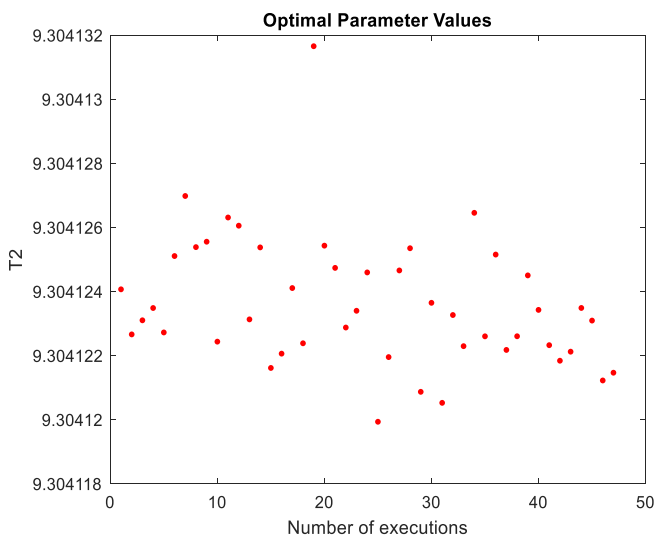
(e)
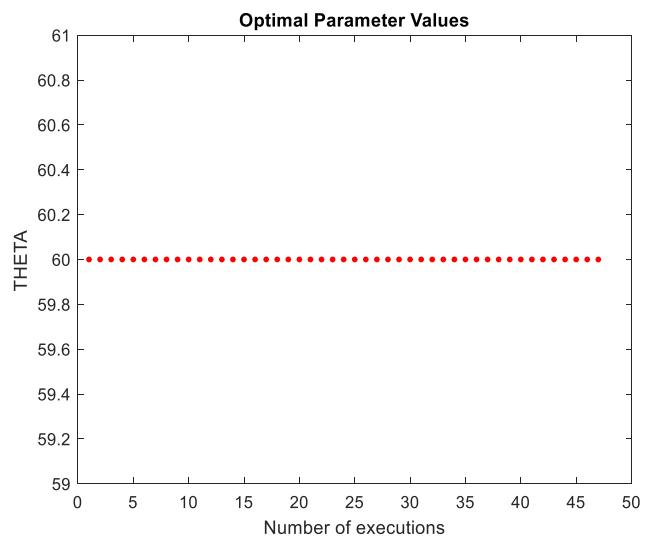
(f)
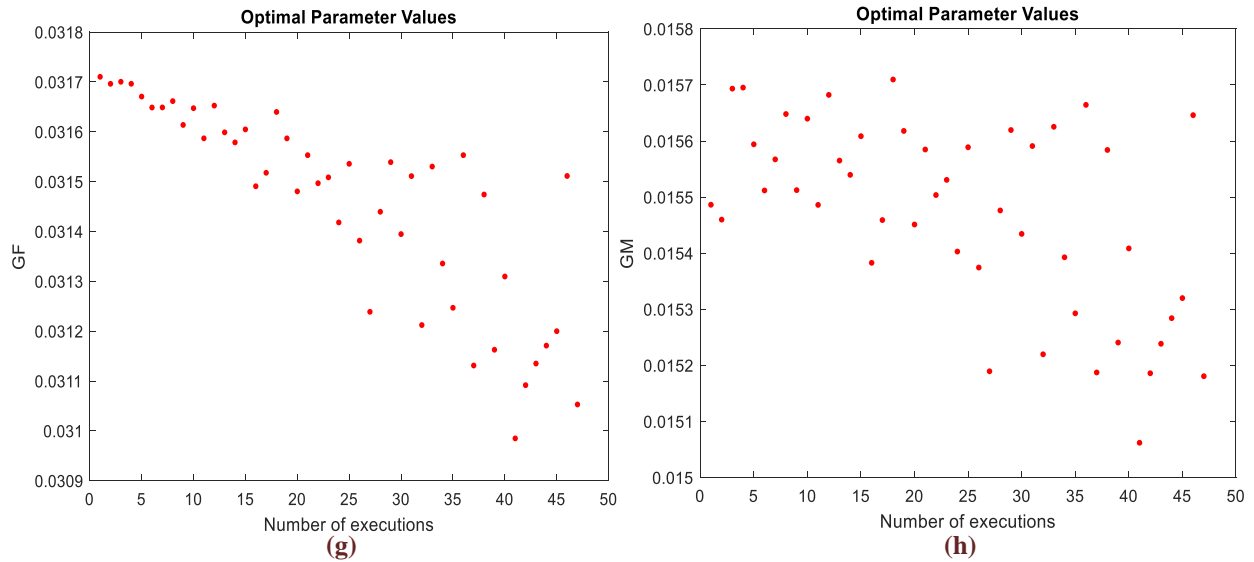
Figure 3.15: Variability of the optimized parameter values for the first experiment from [2], (a)VOLF: fiber volume fraction, (b)Eopt: optimal fiber strain, (c)P1: fiber elastic modulus, (d),(e)T1,T2: mathematical parameters related to the CME's response, (f)THETA: angle between collagenous fibrils and myofibrils, (g),(h)GF,GM: fiber and connective tissue shear modulus

Examining the results of the CMA-ES framework, we can notice that the VOLF, P1, T1 have a great variance, GF and GM have middle and Eopt, T2 and THETA have a null variance. Regarding also the Sobol analysis that we have already run, the P1 has irrelevant influence in the model. So, it is recommended to start the Bayesian analysis for VOLF, T1, GF and GM.

3.2.1.2 Bayesian framework

As we explained before, we choose the parameter set θ=[VOLF T1 GF GM] and we execute the mTMCMC framework. The results are the following.
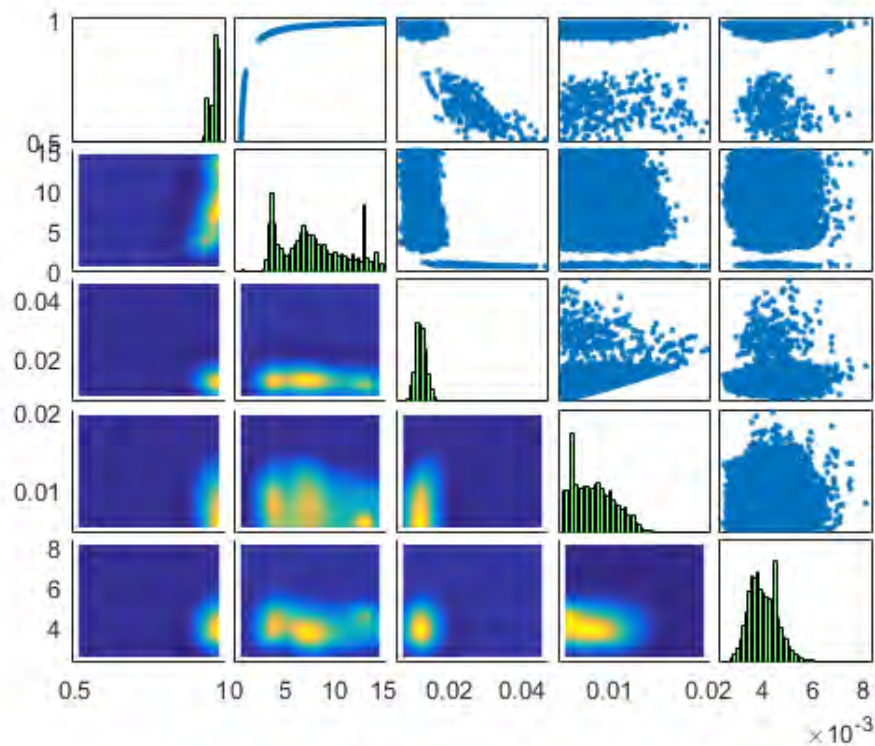
Figure 3.16: mTMCMC results for the 1st experiment, θ=[VOLF,T1,GF,GM]
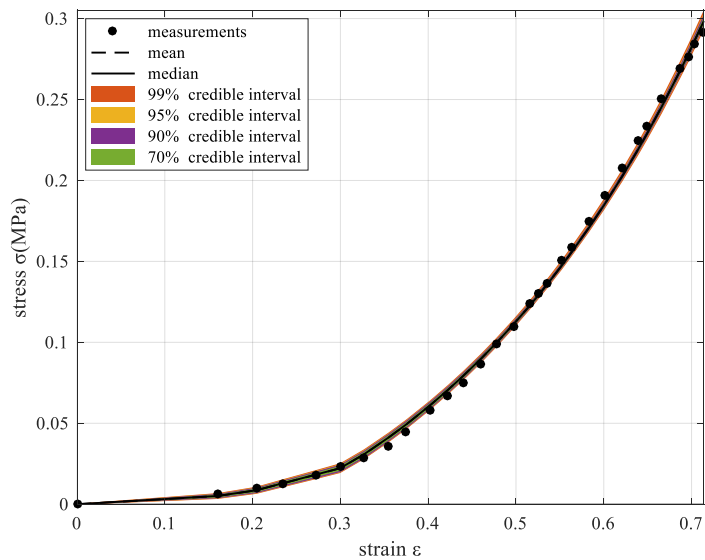
Figure 3.17: Model uncertainty propagation using mTMCMC samples, θ=[VOLF T1 GF GM]

As it seems the software generate samples in several different spaces, without getting uniformly distributed samples. This is because the model is highly identified by several parameters, regarding the available data that can give us some information. Realizing this difficulty of our model, we run again the mTMCMC but we separate the prior bounds of the volume fraction in smaller ranges. In this way we hope to get more accurate samples. The first case is about the bounds [0.5-0.75].
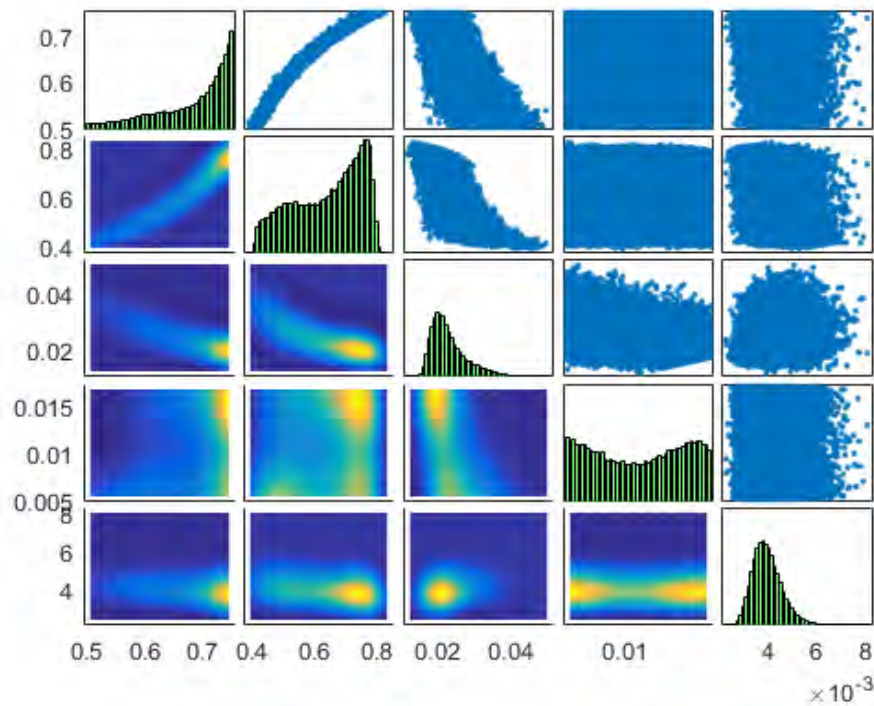
Figure 3.18: mTMCMC results for VOLF bounds [0.5-0.75]
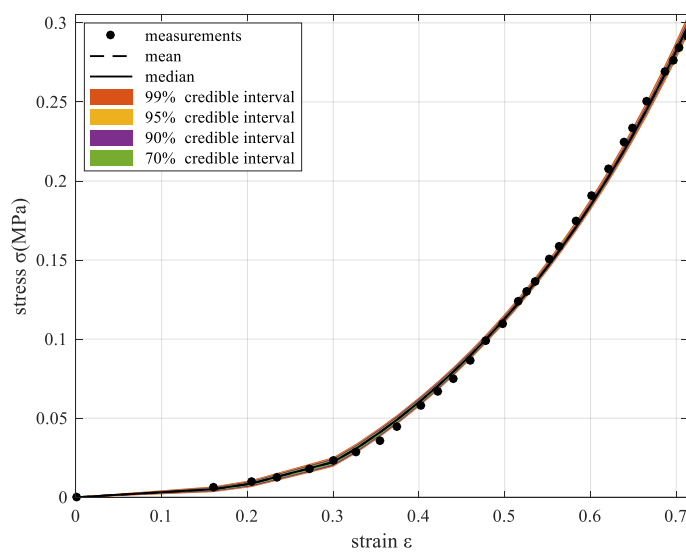
Figure 3.19: Model uncertainty propagation using mTMCMC samples, θ=[VOLF T1 GF GM], VOLF [0.5-0.75]

The next case is about the bounds [0.75-0.92]
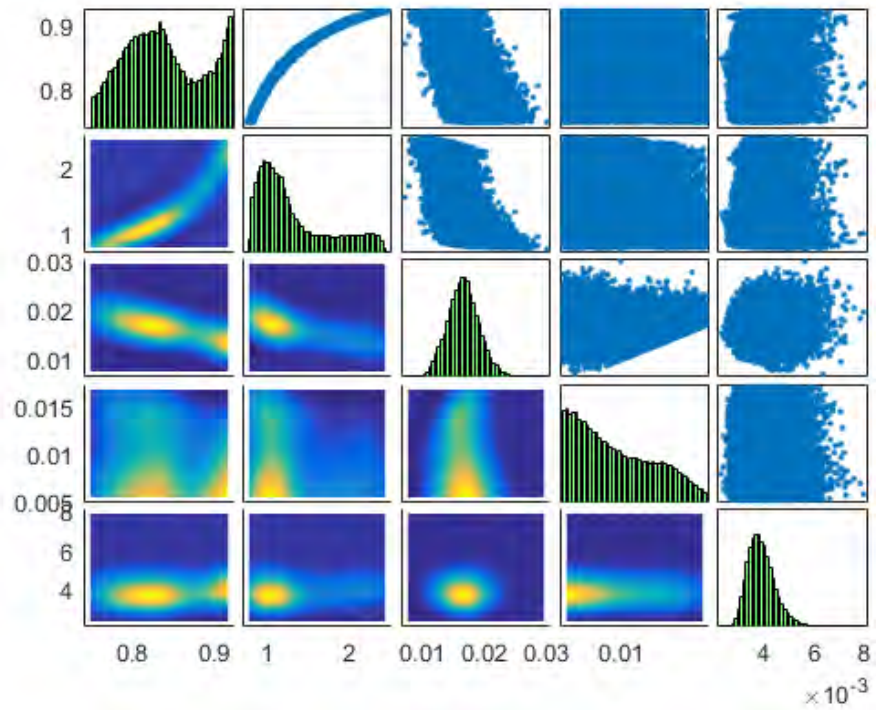
Figure 3.20: mTMCMC results for VOLF bounds [0.75-0.92]
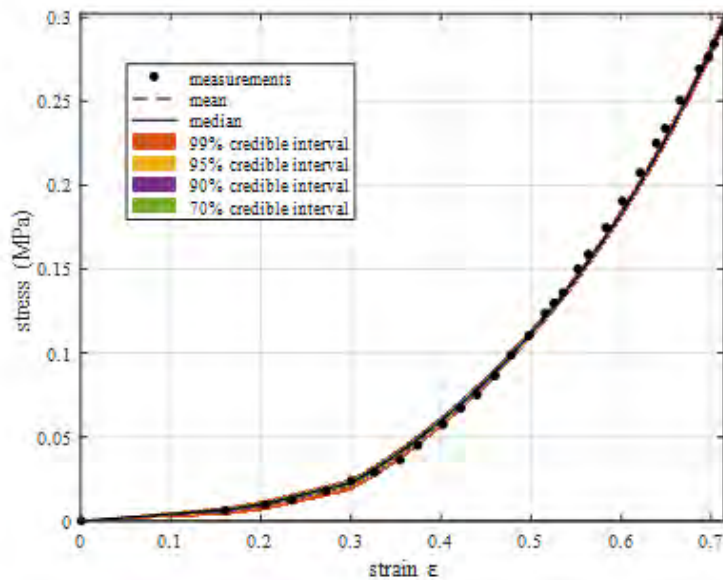
Figure 3.21: Model uncertainty propagation using mTMCMC samples, θ=[VOLF T1 GF GM], VOLF[0.75-0.92]

The next case is about [0.92-0.99]
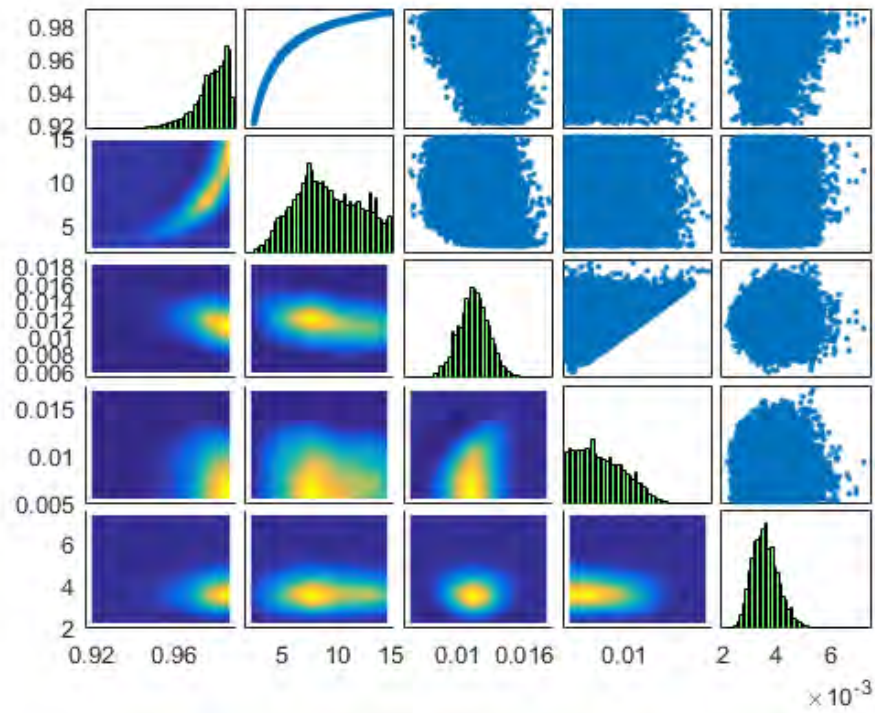
Figure 3.22: mTMCMC results for VOLF bounds [0.92-0.99]
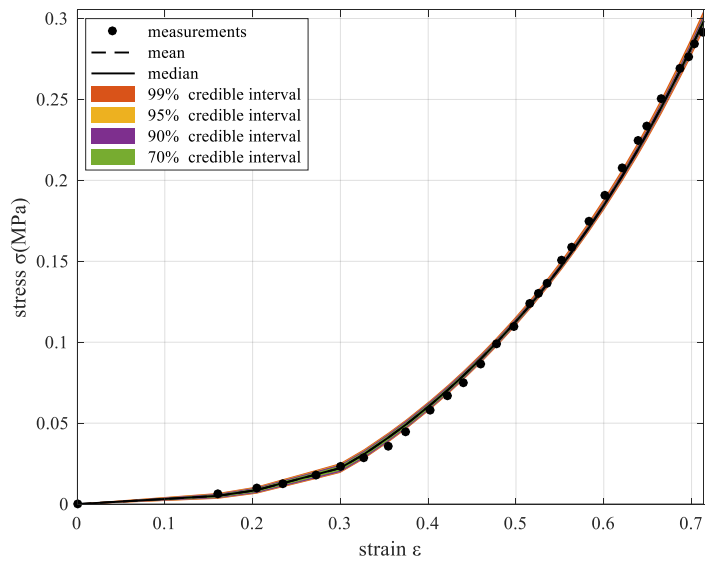
Figure 3.23: Model uncertainty propagation using mTMCMC samples, θ=[VOLF T1 GF GM] and VOLF[0.92-0.99]

Noticing the result from the mTMCMC, we can say that the generated samples are able to give perfect model propagation with a slight quantile space, which means that the discrepancy between model and experiment, expressed by the prediction error is greatly low. The first figures (3.18, 3.20, 3.22), as we analyzed in the other experiment from [1], illustrate the support of the posterior distribution and give us wide information about the appropriate values of the parameters. So, the recommended values of the parameters are exhibited in the next tables.

Table 3.7: Suitable parameter ranges

PARAMETERS	RANGES
VOLF	[0.5-0.99]
T1	[0-15]
GF	[0.005-0.03]
GM	[0.0001-0.02]

Examining all the results, we would say that the most suitable values are not random. If someone needs to give in the fiber volume fraction a value inside the range [0.5-0.75], [0.75-0.92] or [0.92-0.99], then he needs to bear it in his mind so that he can make a decision about the T1, the shear modulus' values. For instance, if the VOLF takes a value inside the [0.5-0.75], then the most appropriate value of the fiber shear modulus is around 0.02. However, if the VOLF is inside [0.92-0.99], then the GF should be around 0.012.

Table 3.8: Probable parameter values

PARAMETERS	MPV
VOLF	Multiple (User's choice)
T1	Strict correlation
GF	Multiple, depends on VOLF
GM	Multiple, depends on VOLF

It is noticeable that the strict correlation between the fiber volume fraction and the T1 is a characteristic of our model and it is not dependent of the experiment. For this reason, we expect a similar relationship in each different case of the experiments. After implementing the appropriate analyses for the group of these experiments, we will have an interest in discovering these correlations and comparing them among the different specimens. This task is accomplished and described in the paragraph 3.3.6.

Let's direct out attention to the other parameters, too. Considering that the other parameters do not have a large variability (Figures 3.15), we take advantage of it and we reduce the bounds of the prior. In this way, we hopefully ensure the accuracy of the results. The parameter set is θ= [VOLF Eopt P1 T1 T2 GF GM]. We also consider

that THETA=60 as the variance of the CMA results is zero and the Sobol has shown that any discrepancy of this value has a great impact on the output.
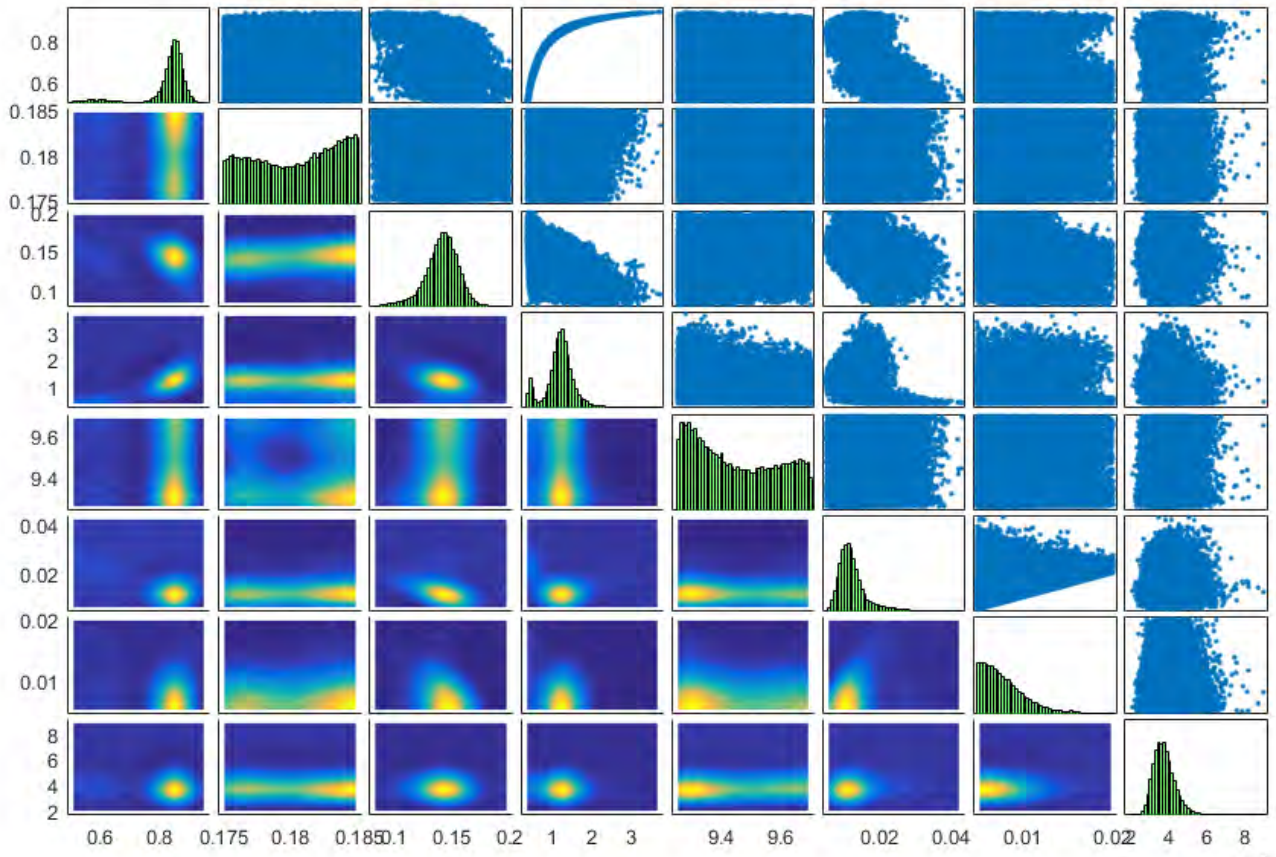
Figure 3.24: mTMCMC results for parameter set θ=[VOLF Eopt P1 T1 T2 GF GM]
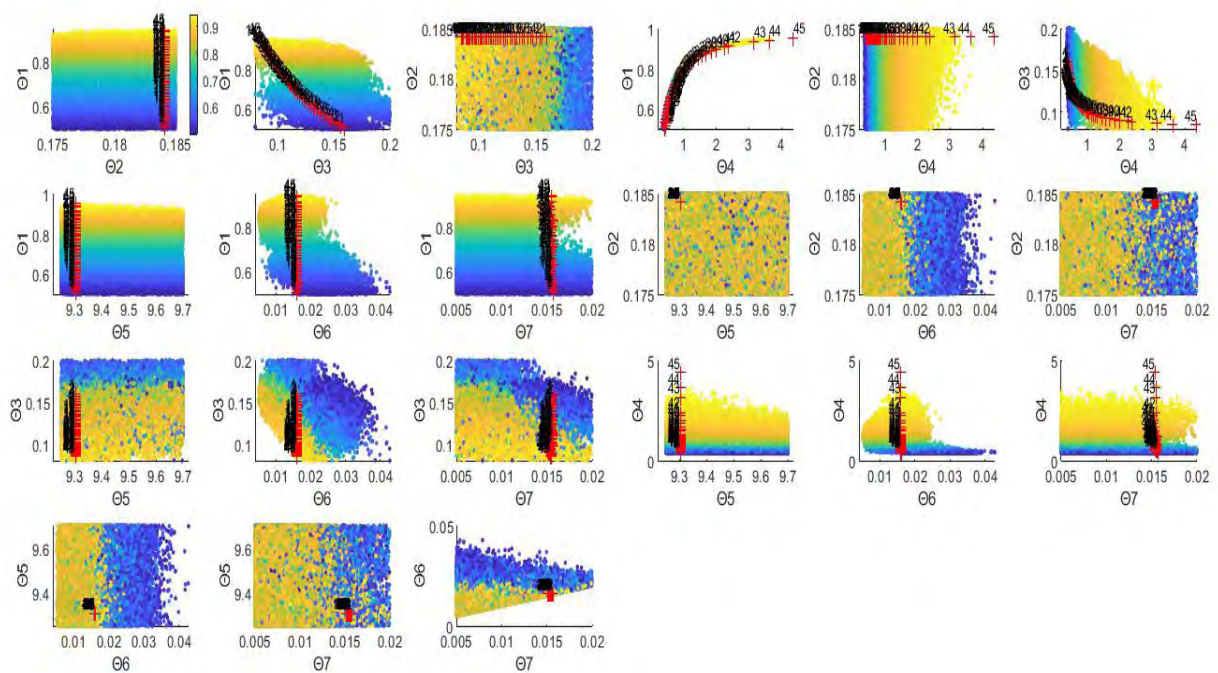
Figure 3.25: colored mTMCMC results and CMA points

Examining the results, we can make the next conclusions, included in the next table:

Table 3.9: Most probable parameter values

PARAMETERS	SUITABLE VALUES	EXPLANATION
VOLF	[0.5-0.99]	User's choice
Eopt	~0.184	Proved by CMA and mTMCMC, small variance and uniformly distributed samples in this range
P1	~0.13	Yellow contour plot
T1	[0-12]	Strict correlation
T2	9.3	Highest probability in this value
THETA	60	CMA, no variance
GF	~0.012	Recommended values from the figures 3.18, 3.20, 3.22. Depended on the VOLF value.
GM	~0.009	Recommended values from the figures 3.18, 3.20, 3.22. Depended on the VOLF value.

The samples, generated by the mTMCMC, give the model propagation, illustrated in the Figure 3.26. As it seems the mTMCMC achieves to reduce the influence of the model prediction error such that all the samples give a great model approximation of the first experiment from [2]. The CMA points are also very close to the measurements as the mean model propagation using mTMCMC samples does. This figure proves us the accuracy of the analyses' results.
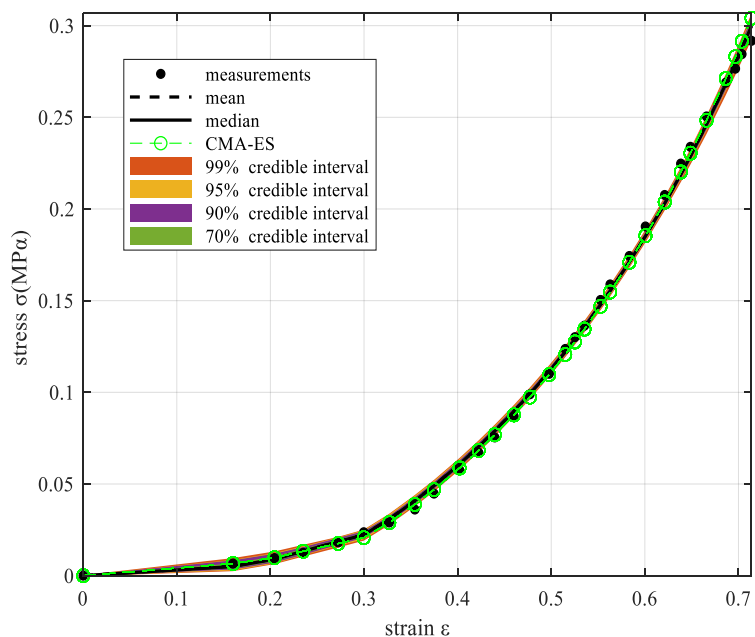
Figure 3.26: Model uncertainty propagation using mTMCMC samples and CMA results

As it is mentioned, the prior bounds in mTMCMC software are defined narrow, bearing in mind the CMA results. In this way we limit the range in which the parameters can take a possible value. If the bounds are extremely small, we finally result in ignoring the considered parameters in the analysis. For this reason, it is better to enlarge the bounds up to a point that the sampling procedure will be completed successfully. These obstacles are standing because of the high dimensional unidentifiable model that we have and few experimental data that are not enough so that we can gain as much information as we need for the parameter identification.

The next figure illustrates another execution of the mTMCMC for the whole parameter set. This time we have enlarged the prior bounds in some parameters.
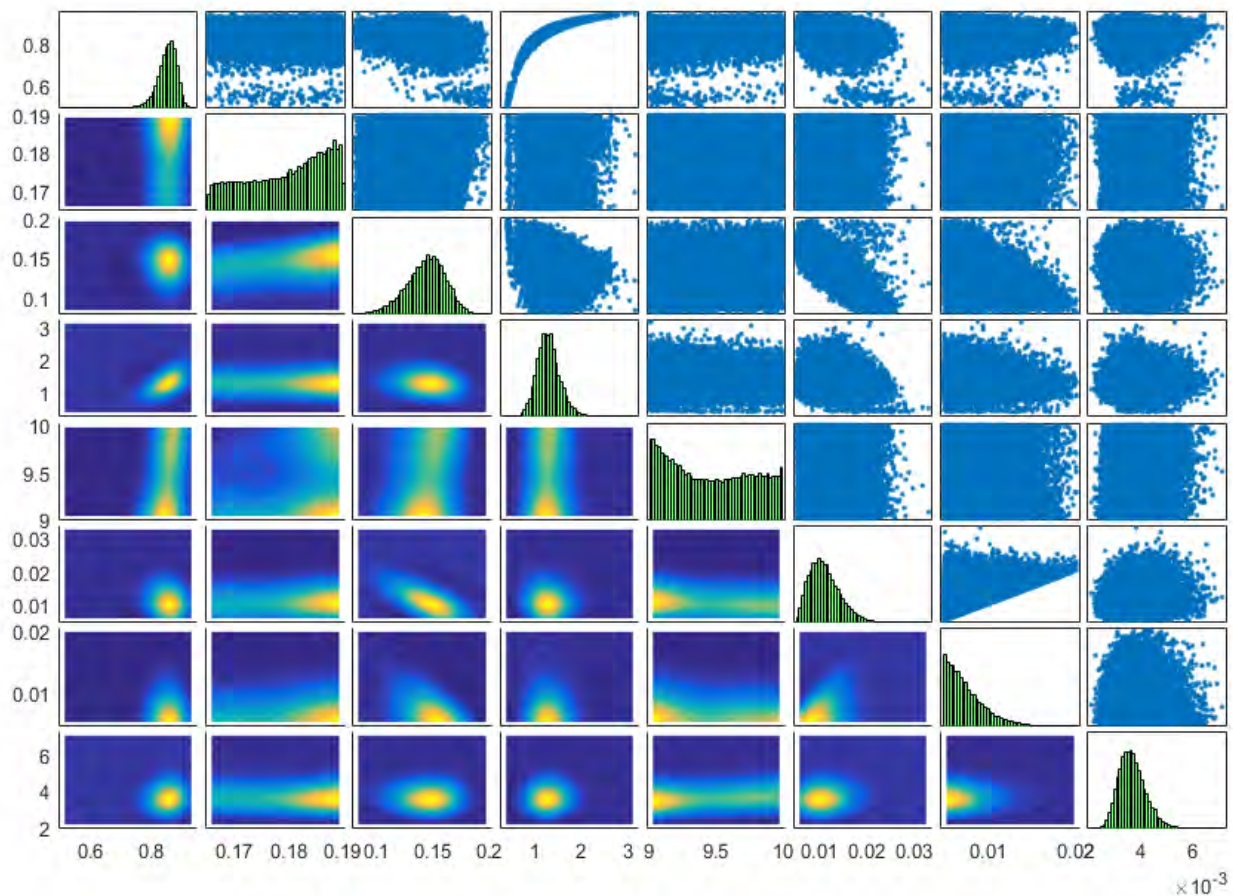
Figure 3.27: mTMCMC with larger prior bounds

Regarding the marginal distributions of the parameters, we can also make some useful conclusions:

1. The fiber volume fraction is recommended to be around 0.9. Seeing the CMA results, we know that the fiber can take a variety of values inside the range [0.5-0.99].
2. The Eopt is characterized by an approximately uniform distribution in the range [0.16-0.19]. The yellow points are centered on the highest values of this range. Moreover, the optimal value of Eopt is around 0.184. However the model propagation shows us that any other value inside this range can give a

good model approximation with a small discrepancy of the experimental data (Figure 3.26).

3. The P1 is more centered on the value around 0.15 but with an important variance. This is explained also by the Sobol analysis.

4. The T1 marginal distribution recommends the 1.5 as the most probable value. This is not accurate as we know that T1 can take a variety of values with the condition the follows the strict correlation that it has with the VOLF.

5. The T2 should take a value around 9.3. However the samples from the optimal posterior distribution generated in the support of it can give an efficient approximation of the experimental data with an extremely small error.

6. The THETA must be equal to 60 as it is shown in the CMA results. Let's also remind that the model is extremely sensitive to this parameter.

7. The marginal distribution of GF is centered on 0.012. However, the Figures 3.18, 3.20, 3.22 recommend as several different values. This attribute is also clear in Figure 3.25 where the colored points are somehow lined up respect to the color. This is also a clue that the value of this parameter is depended on the VOLF's value.

8. The same conclusion with GF we can also make about GM.

3.2.2 Second experiment

In this paragraph we analyze the results from the applied frameworks for the second experiment from [2].

3.2.2.1 Optimization analysis

The optimization framework has given multiple optimal parameter values, shown in Figures 3.29, such that the model fits globally to the experimental data (Figure 3.28).
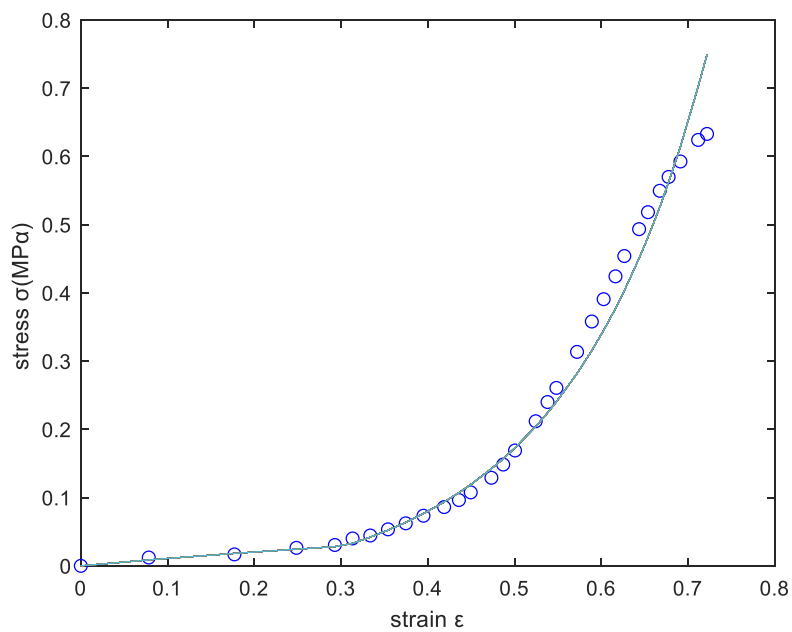
Figure 3.28: Global model approximation of the 2nd experiment

The multiple solutions and their variances are illustrated in a clear way in Figures 3.29.
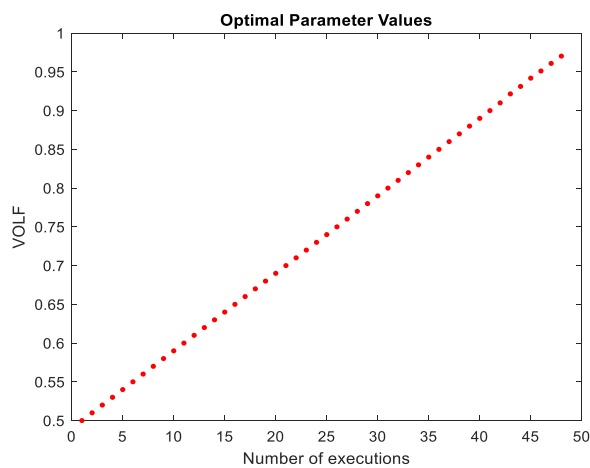
(a)
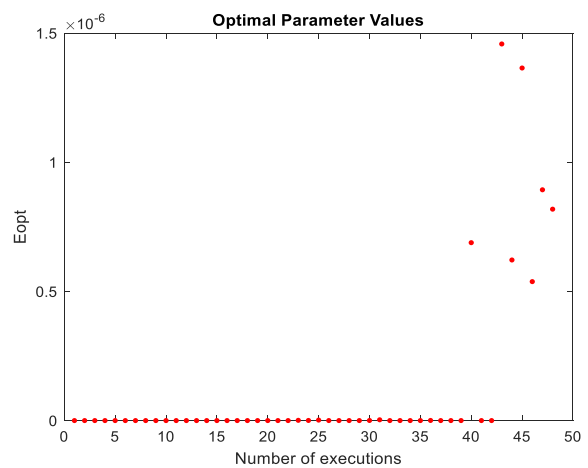
(b)
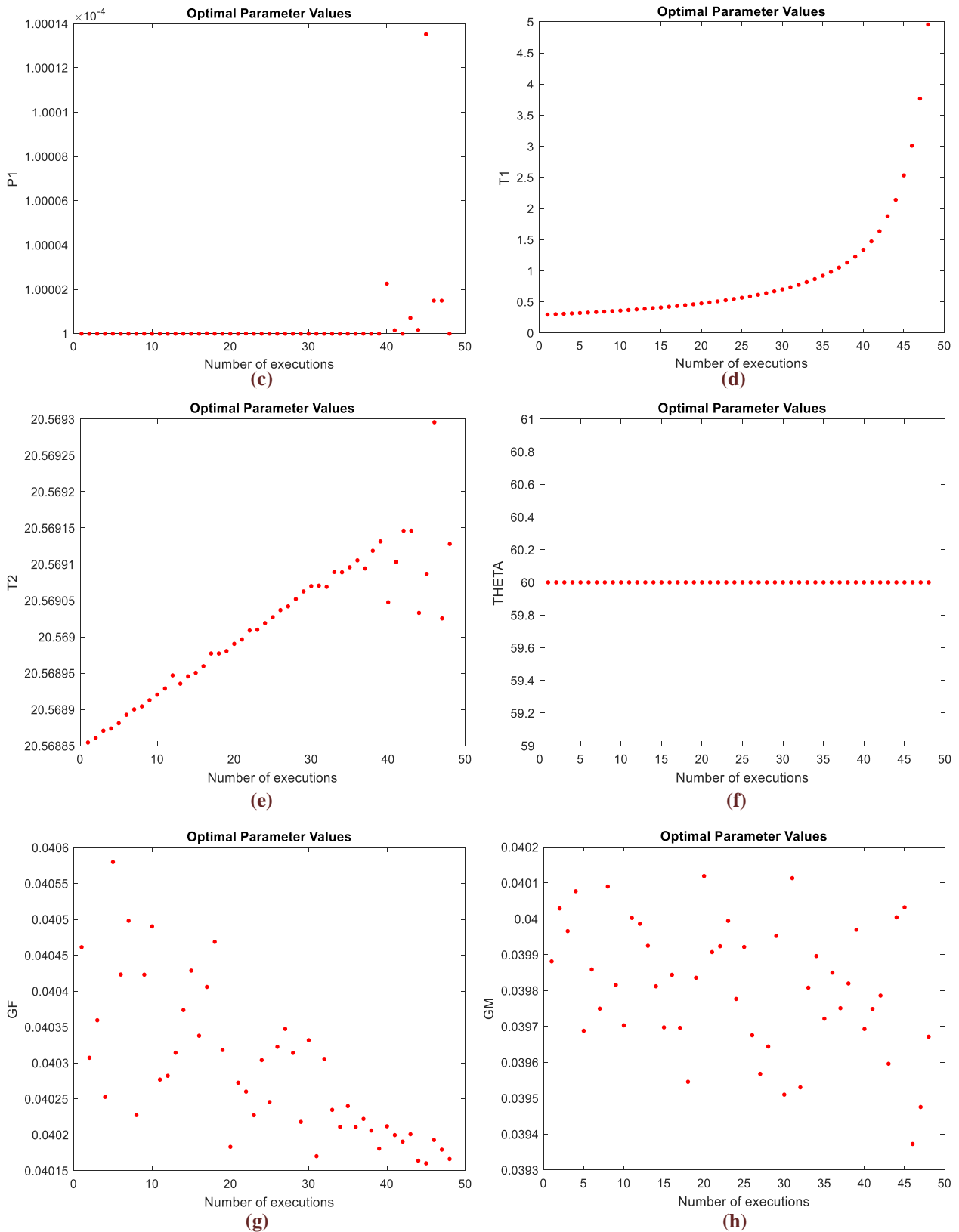
Figure 3.29: Variability of the optimized parameter values for the second experiment, (a)VOLF: fiber volume fraction, (b)Eopt: optimal fiber strain, (c)P1: fiber elastic modulus, (d),(e)T1,T2: mathematical parameters related to the CME's response, (f)THETA: angle between collagenous fibrils and myofibrils, (g),(h)GF,GM: fiber and connective tissue shear modulus

3.2.2.2 Bayesian framework

We execute the mTMCMC framework for the second experiment. The parameter set in which we are interested in is θ=[VOLF T1 GF GM], while the variances of the CMA points of the other parameters are small. The results are exhibited in Figures 3.30 and 3.31.
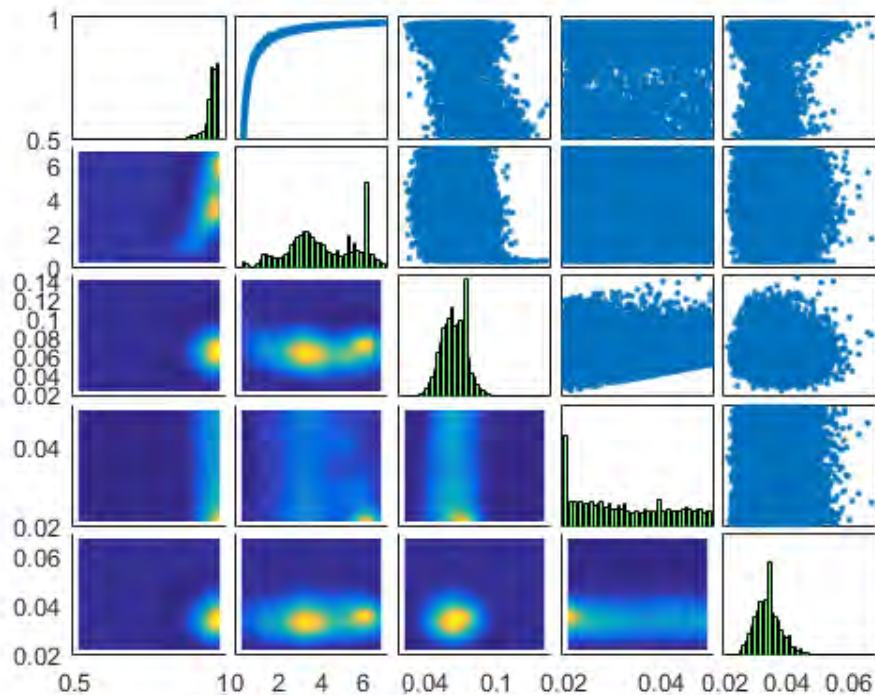
Figure 3.30: mTMCMC results for the 2nd experiment, θ=[VOLF T1 GF GM]
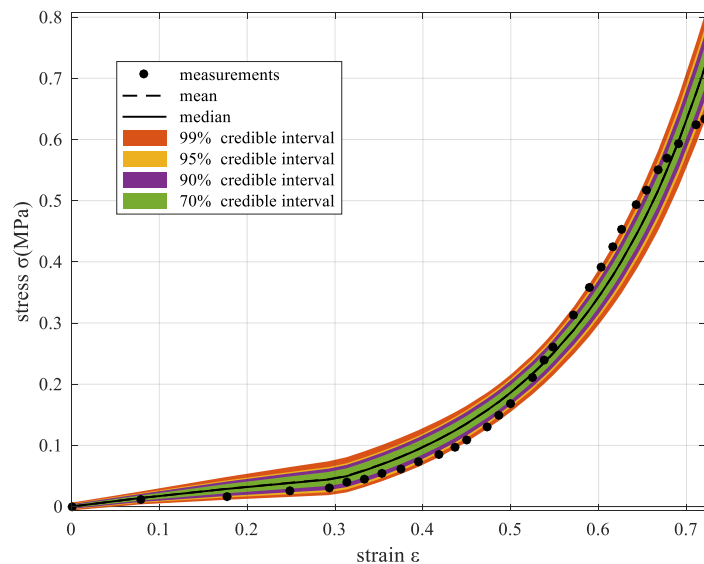
Figure 3.31: Model uncertainty propagation using mTMCMC samples

Examining the results, we gain information about the most probable values of the considered parameter set. It is clear that the VOLF and T1 can take a large number of

appropriate values, only with the condition of satisfying their correlation. Moreover the most probable values of GF and GM are 0.06 and 0.02, respectively. Let's remind ourselves that the other parameters are fixed in the values, proposed by the CMA results. It also needs to be noted that the discrepancy between model and experimental data is larger than other case possibly because of the measurement errors.

We continue with the whole parameter set θ=[VOLF Eopt P1 T1 T2 THETA GF GM]. The results are illustrated below.
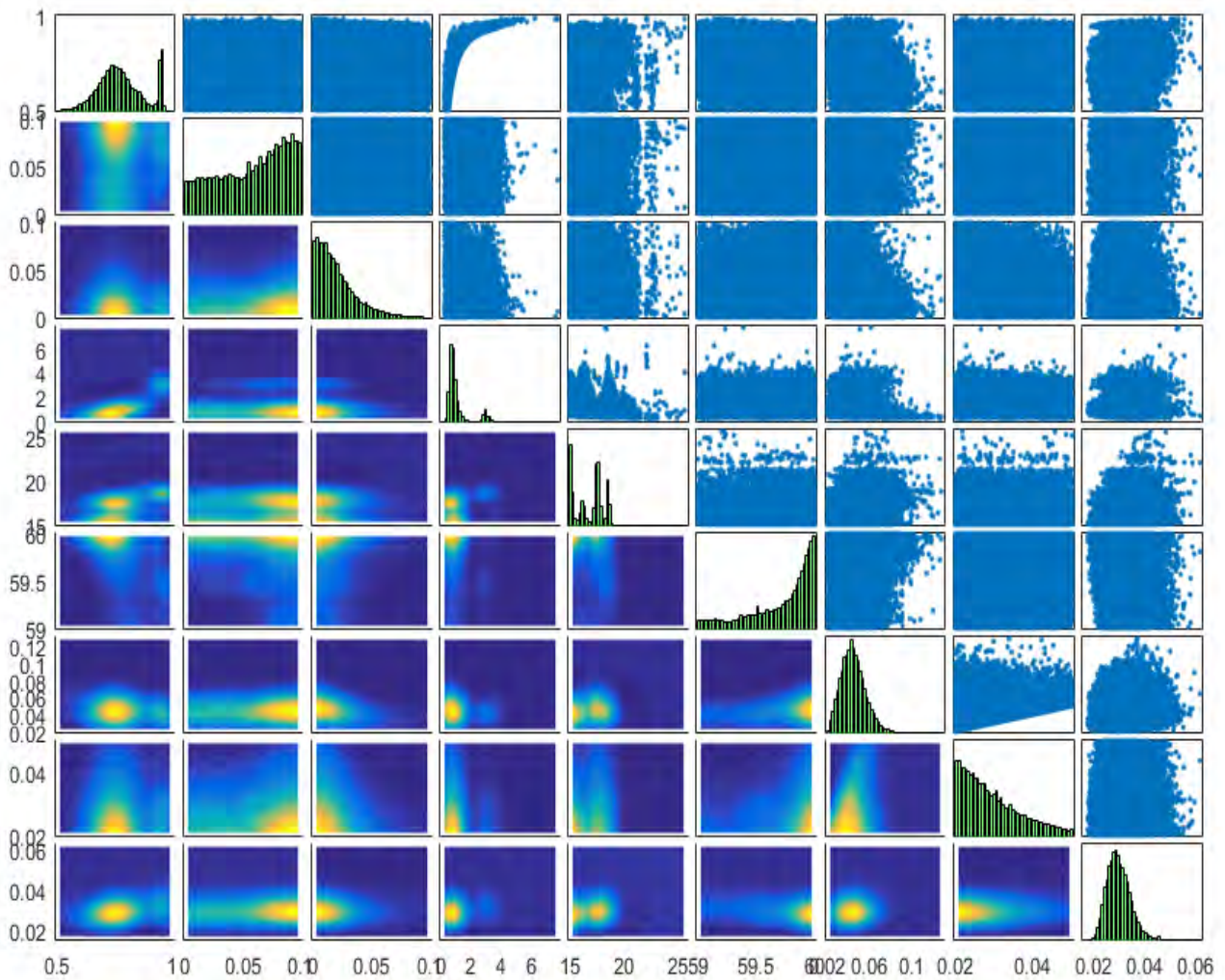
Figure 3.32: mTMCMC results
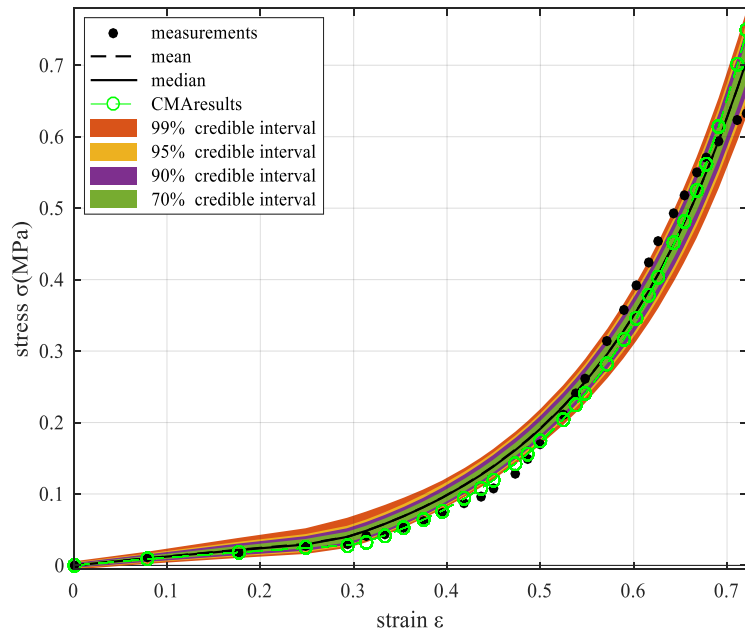
Figure 3.33: Model propagation using mTMCMC samples and CMAresults

As it seems, the mTMCMC cannot manage efficient sampling of the T2 parameter. Another disadvantage of the execution is that the optimal solution resulting from the CMA software can approach the data better than the model propagation originated by the mTMCMC results. In the next figure, the results from a second execution are exhibited.
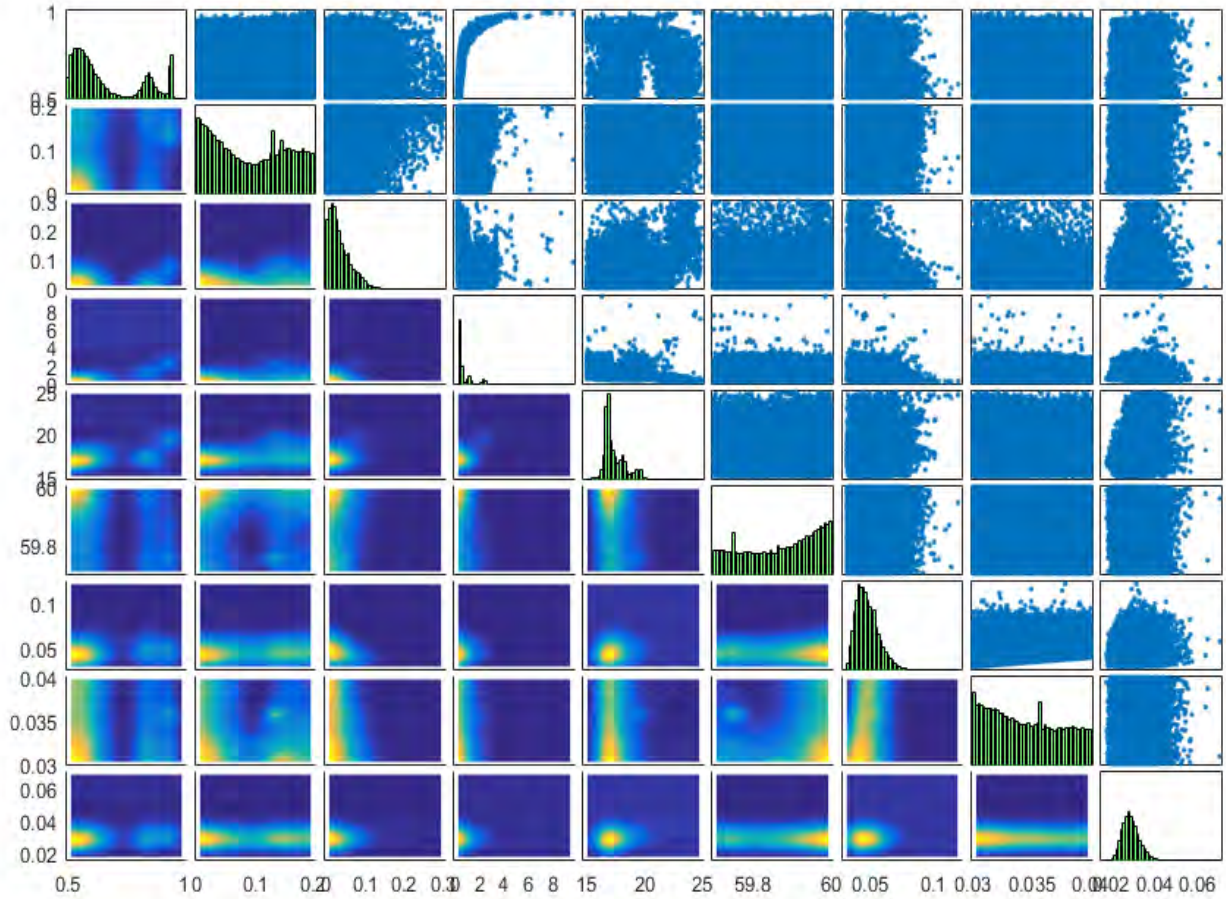
Figure 3.34: mTMCMC results
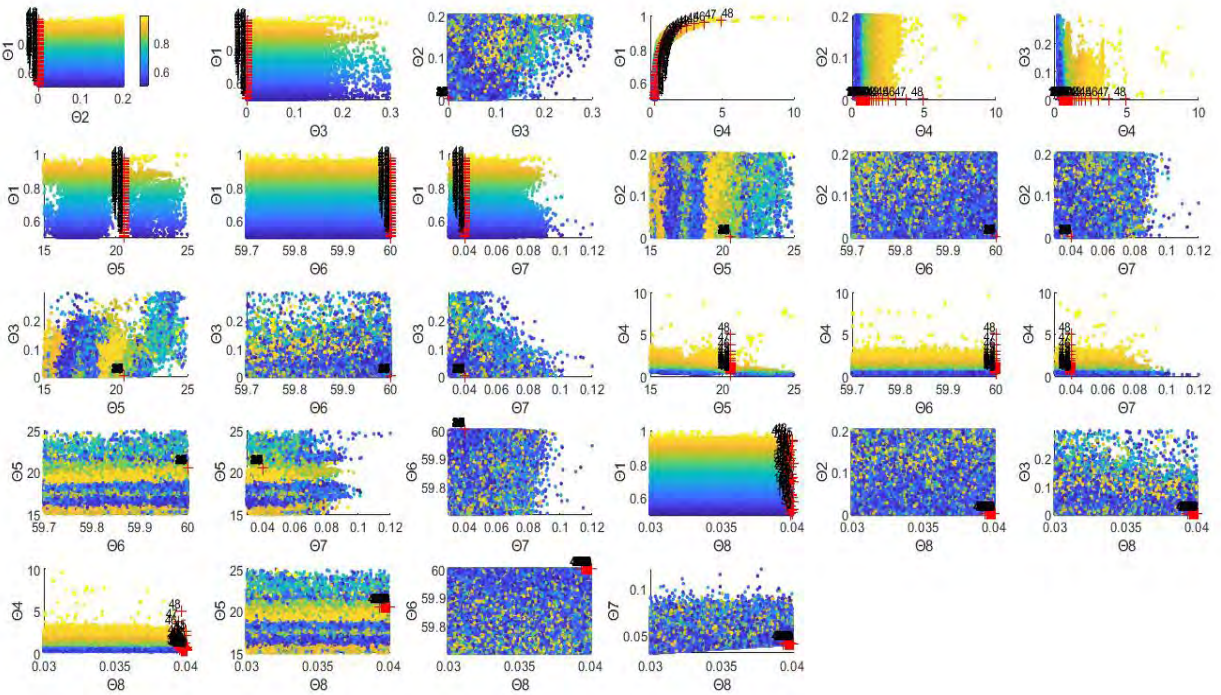
Figure 3.35: Colored mTMCMC samples and CMA points
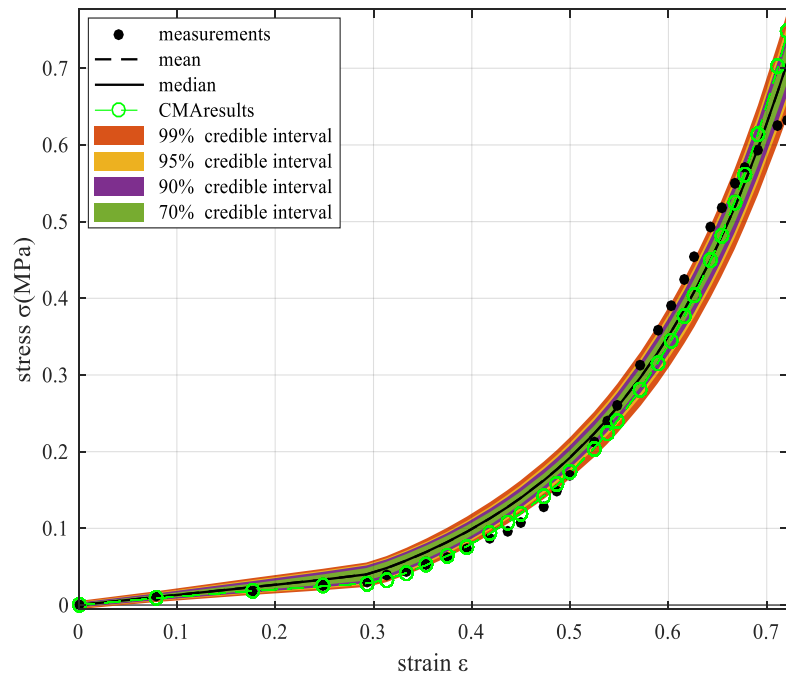
Figure 3.36: Model uncertainty propagation using mTMCMC samples and CMA results

Examining the results, the conclusions are:

1. The VOLF can take a large number of values inside the range [0.5-0.99]
2. The most probable values of the Eopt are less than 0.1. CMA recommends the value 0. However, the uncertainty of the posterior is large enough so that the marginal distribution of it approximates a uniform distribution.
3. The marginal distribution of P1 is centered on the values around 1e-4. The CMA points are also the same.
4. The T1 must follow the strict correlation that has with the VOLF
5. The T2 is extremely centered on the value 16.
6. The THETA must be equal to 60.
7. The most probable value of GF is 0.035
8. The most probable value of GM is 0.03. As the yellow points are distributed uniformly in the considered range, we can say that the range is to small and all the values inside it can give a good model propagation

3.2.3 Third experiment

Now, we present the same result for the third experiment from [2].

3.2.3.1 Optimization analysis

We exhibits the results from the automated multiple executions of the CMA-ES framework. In the first figure, we prove that we get only the global optimal parameter values that give the optimal model propagation.
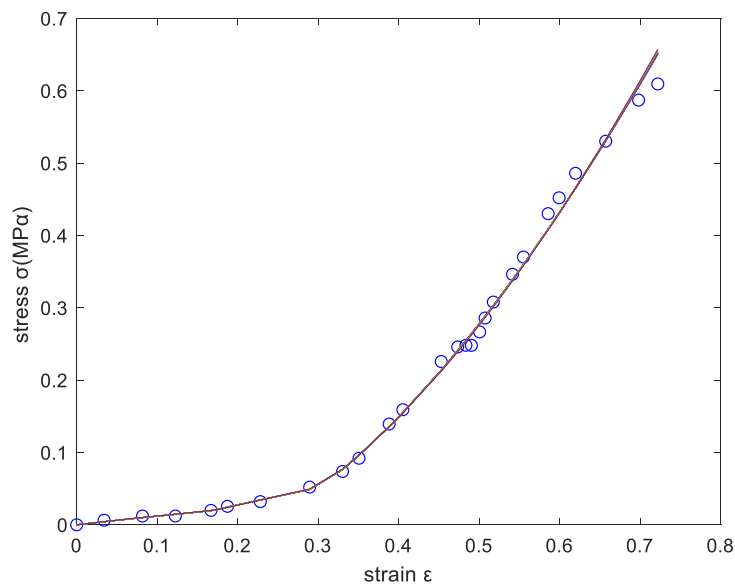
Figure 3.37: Global model approximation of the 3ʳᵈ experiment

The multiple solutions are illustrated in a clear way in Figures 3.38.
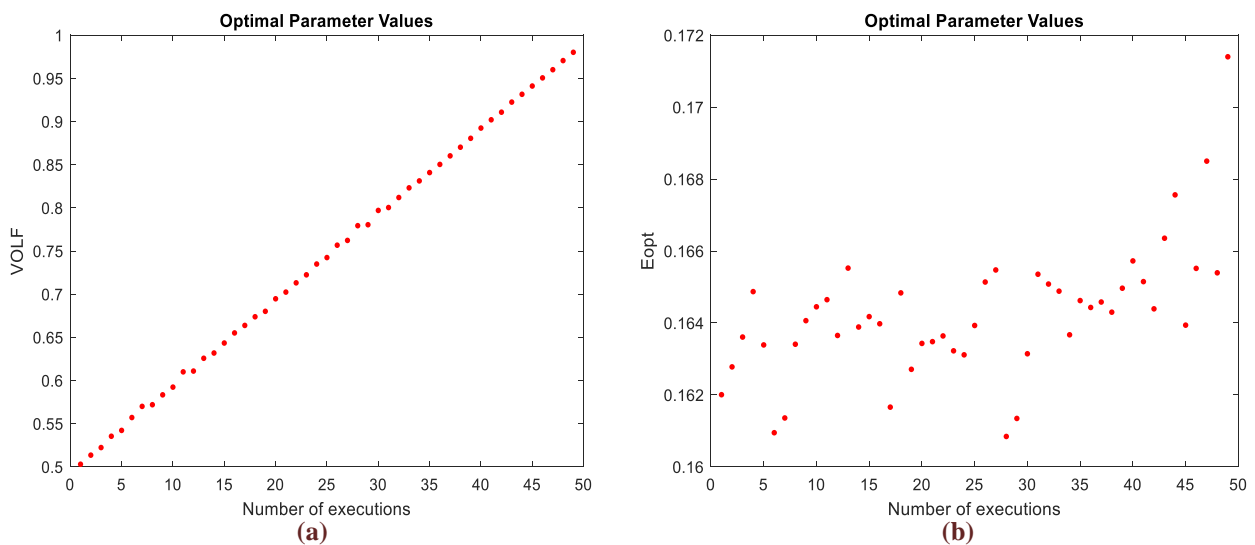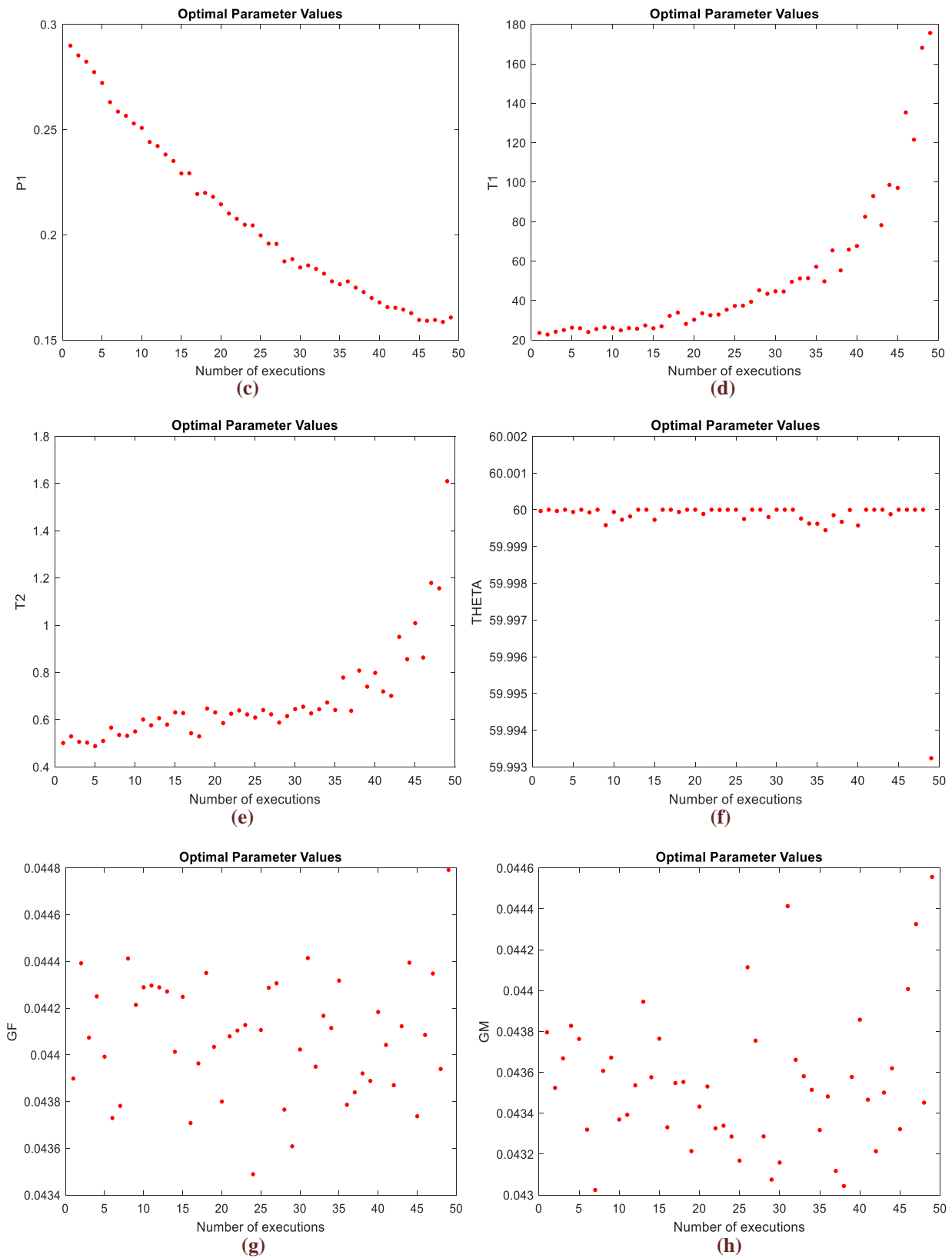
Figure 3.38: Variability of the optimized parameter values for the third experiment, (a)VOLF: fiber volume fraction, (b)Eopt: optimal fiber strain, (c)P1: fiber elastic modulus, (d),(e)T1,T2: mathematical parameters related to the CME's response, (f)THETA: angle between collagenous fibrils and myofibrils, (g),(h)GF,GM: fiber and connective tissue shear modulus

3.2.3.2 Bayesian framework

The parameters set that is characterized by some variance in the CMA results is θ= [VOLF P1 T1 T2 GF GM]. Thus, we execute the Bayesian framework for this parameter set. The results are below.
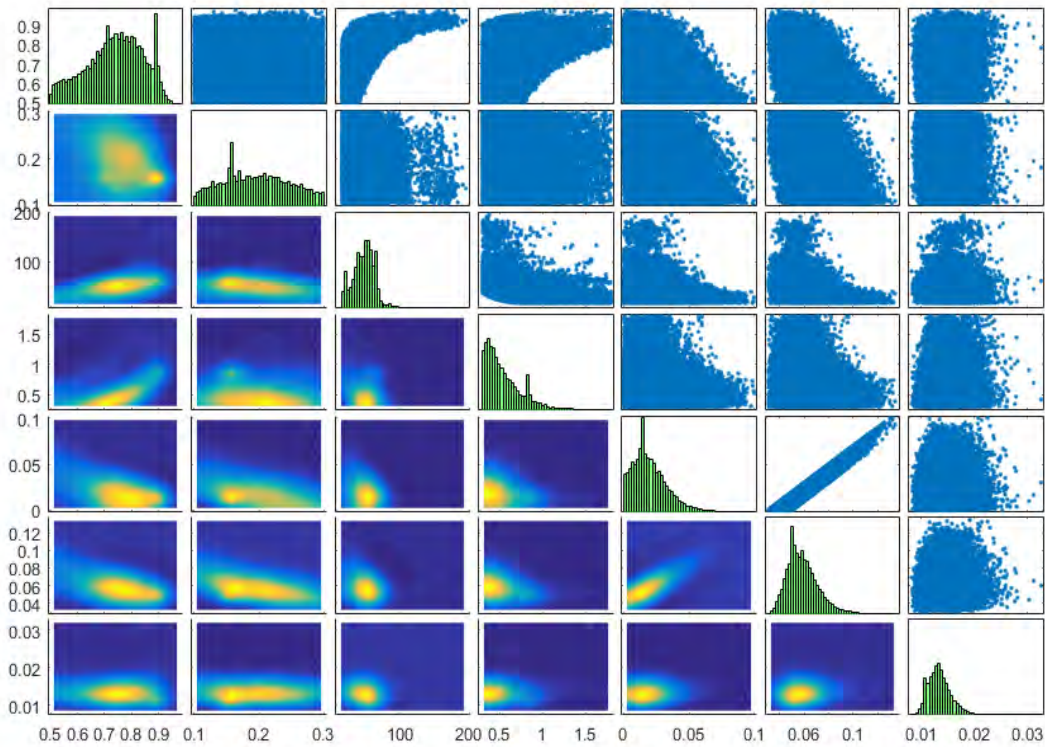
Figure 3.39: mTMCMC results for the 3rd experiment, θ= [VOLF P1 T1 T2 GF GM]
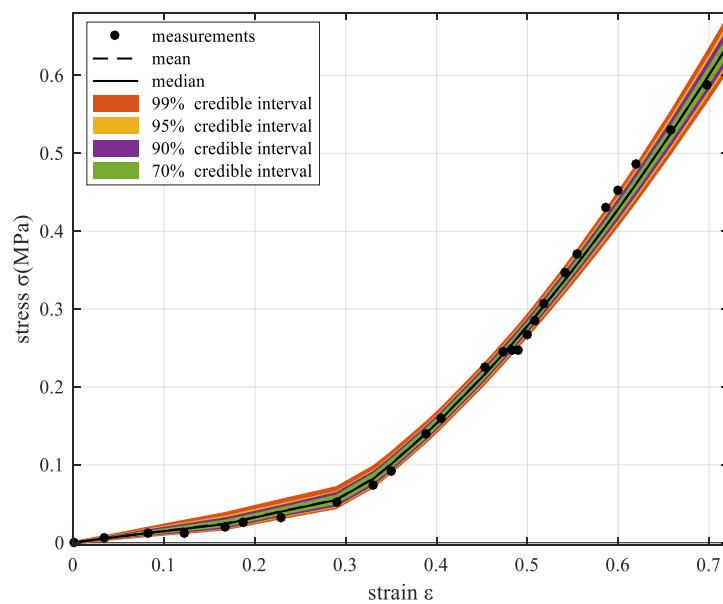
Figure 3.40: Model uncertainty propagation using mTMCMC samples

Table 3.10: Probable parameter values

PARAMETERS	MPV
VOLF	Multiple (User's choice)
P1	Depends on the VOLF
T1	"Surface" correlation
T2	"Surface" correlation
GF	~0.06
GM	~0.02

As it seems, the correlation between VOLF and T1 is not a line but a surface. In other words, one specific value of fiber volume fraction doesn't correspond to a specific value of T1 but to a variety of values. Let's discover this characteristic by using the CMA points and mTMCMC results.
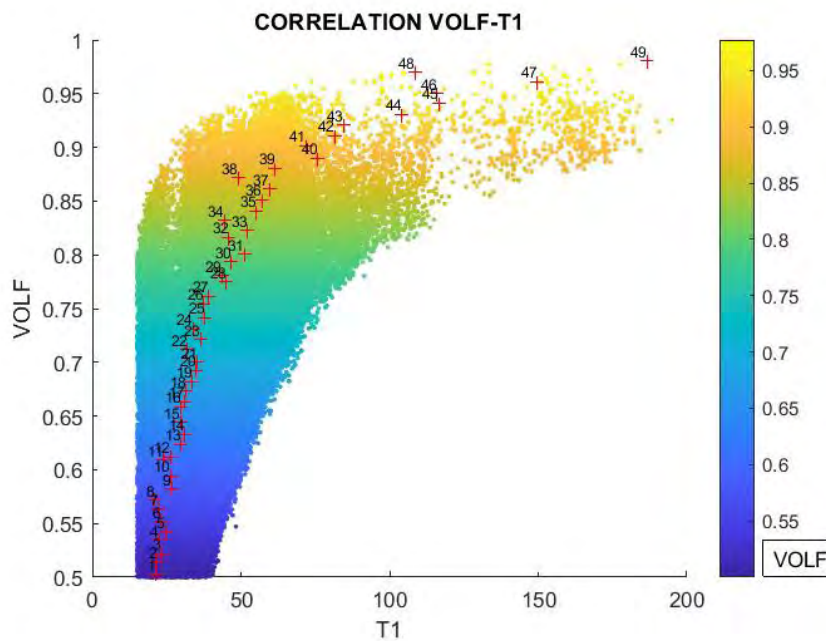
Figure 3.41: Correlation between VOLF-T1 for the 3rd experiment

Now, we run the CMA again keeping the T1 fixed on the values 30, 50, 60, 80. If the VOLF gives multiple values with the same global minimum of the objective function, then we have proved the "surface" characteristic.
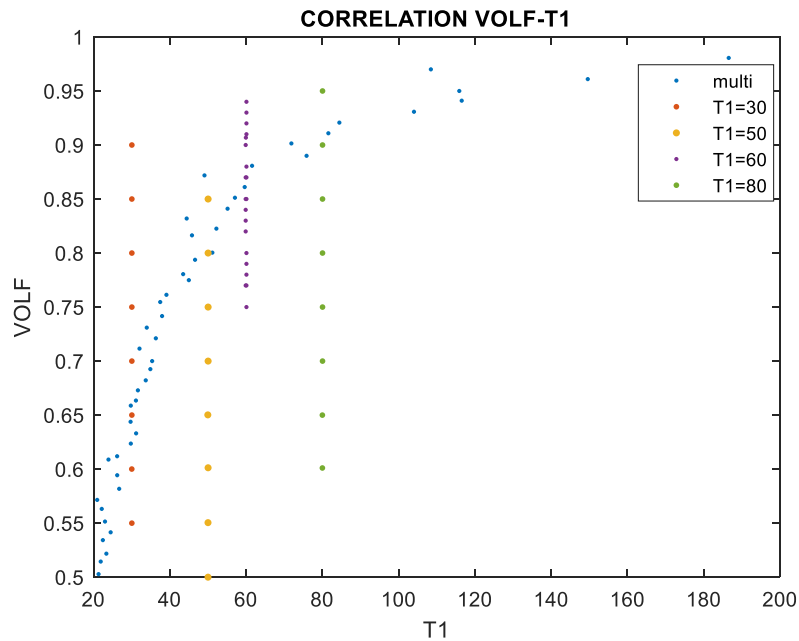
Figure 3.42: Correlation between VOLF-T1, surface characteristic using CMA points

Another fact that can be easily proved is the correlation between VOLF and T2, too.
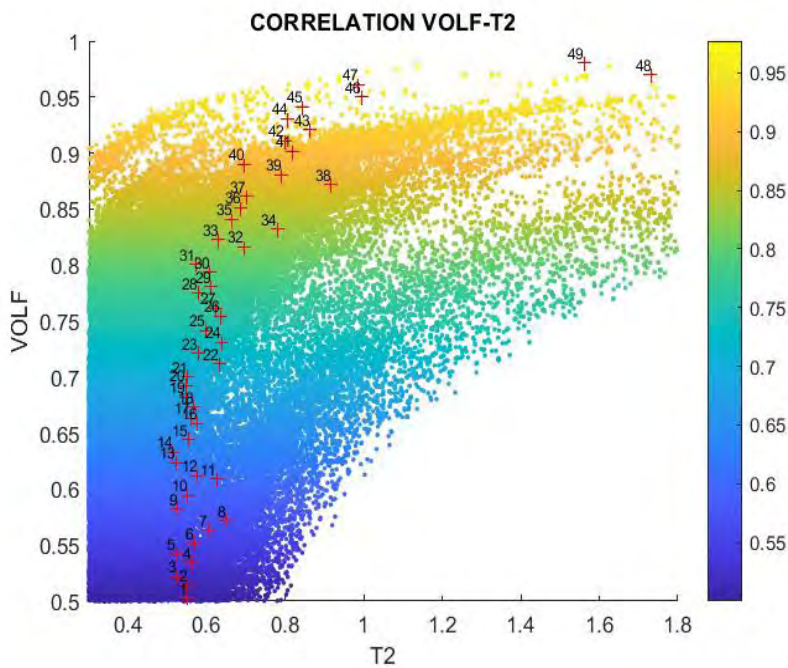
Figure 3.43: Correlation between VOLF-T2 for the 3rd experiment

Now, we execute the mTMCMC framework for the parameter set θ= [VOLF Eopt P1 T1 T2 THETA GF GM].
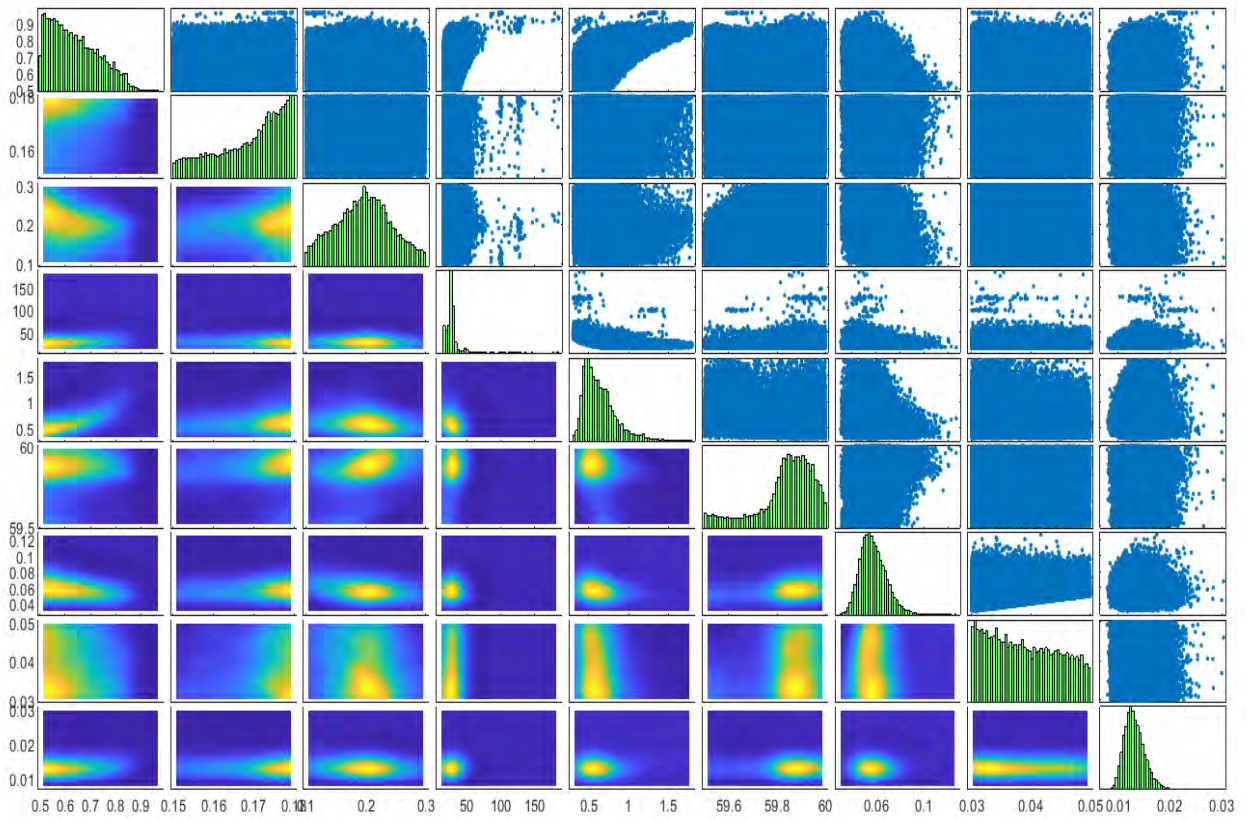
Figure 3.44: mTMCMC results for the parameter set θ=[VOLF Eopt P1 T1 T2 THETA GF GM]
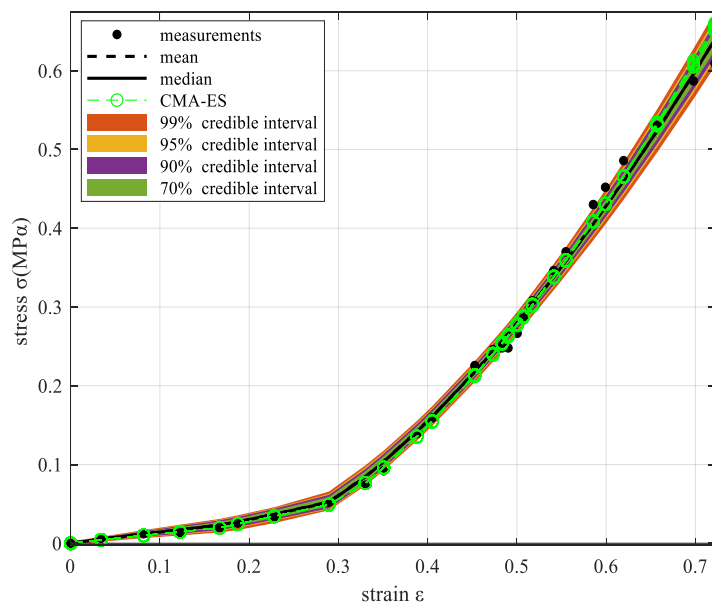
Figure 3.45 Model uncertainty propagation using mTMCMC and CMA results

59

The samples generated by the mTMCMC are illustrated in Figure 3.33. They give efficient model propagation with small error. However, an important disadvantage of the results is that the mTMCMC could not generate sample for the highest values of VOLF. As it is proved by CMA, the values inside the range [0.8-0.99] can also be accepted despite the fact that mTMCMC has not generated samples in this range.

Thus, we execute the mTMCMC framework once more. The bounds of the VOLF are defined to be [0.8-0.99]. The results are illustrated in the next figure.
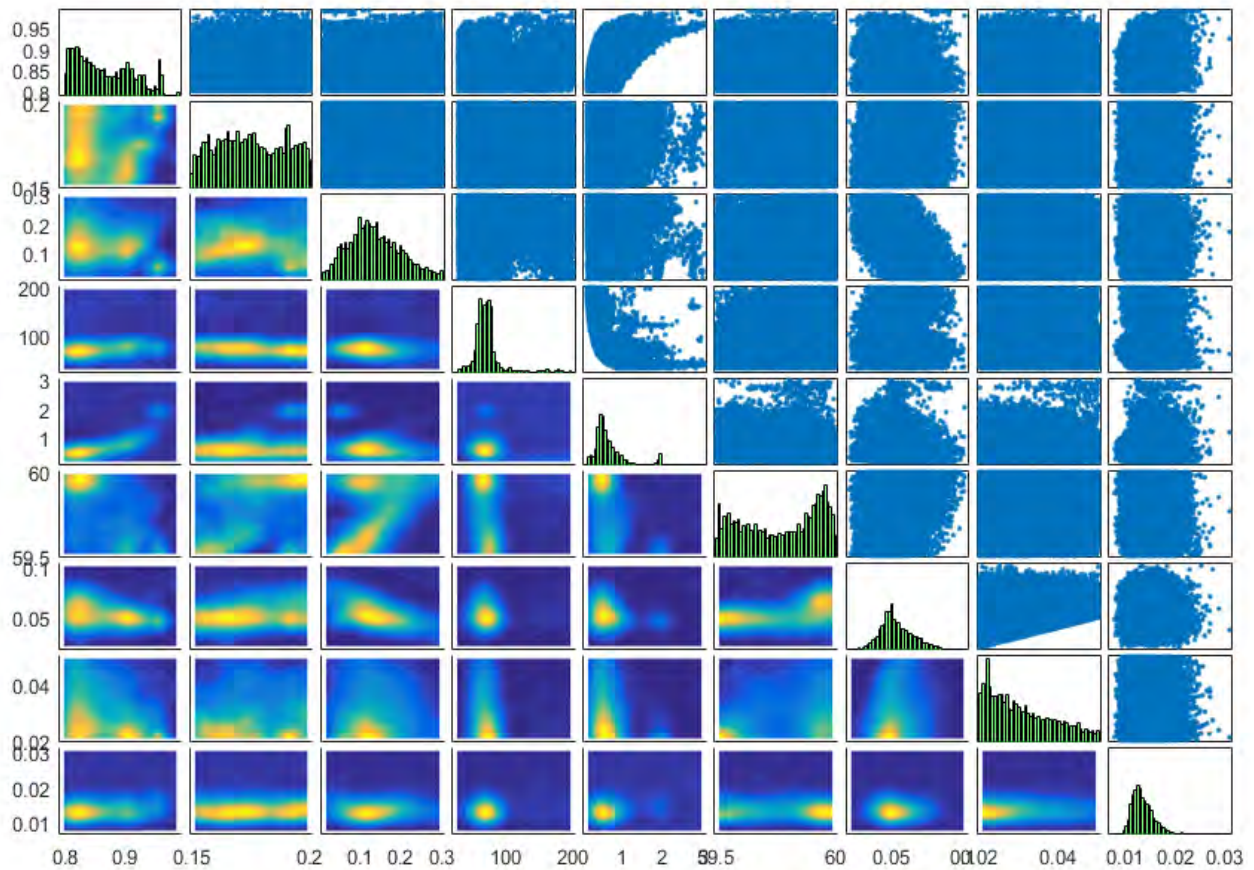
Figure 3.45: mTMCMC results for VOLF [0.8-0.99]

The sampling task is highly demanding for this experiment .As it is mentioned the correlation between VOLF and T1 is wider than for the other experiments .That means that the optimal parameter values are increased and the problem become more unidentifiable. For this reason, generating samples in the whole domain is more difficult to be accomplished.

Examining the results from both analyses, some conclusions can be done:

1. The VOLF takes a variety of values. So, it is researcher's choice.
2. The Eopt should take a value larger than 0.16. CMA recommends the value around 0.16, but mTMCMC propose more probable values that can give model propagation with small uncertainty.
3. The P1 takes also a large account of values such that the model propagation is very good. This attribute is also explained by Sobol.
4. The T1 should follow the correlation. However, as it was previously proved, this correlation is not too narrow to reduce the options of the optimal values.
5. The T2 takes also a large number of values. It also has a correlation with the VOLF
6. The THETA must be equal to 60.
7. The GF should be around 0.04. However, its value depends on the VOLF's value, as it is noticed through the different executions.
8. The GM should be around 0.04. However, its value depends on the VOLF's value, as it is noticed through the different executions.

3.2.4 Fourth experiment

In the next paragraphs, we exhibit the same result for the fourth experiment from [2].

3.2.4.1 Optimization analysis

We follow the same procedure once again. In the next figures we present the results from the automated multiple executions of the CMA-ES framework. In the first figure, we prove that we get only the global optimal parameter values that give the optimal model propagation.
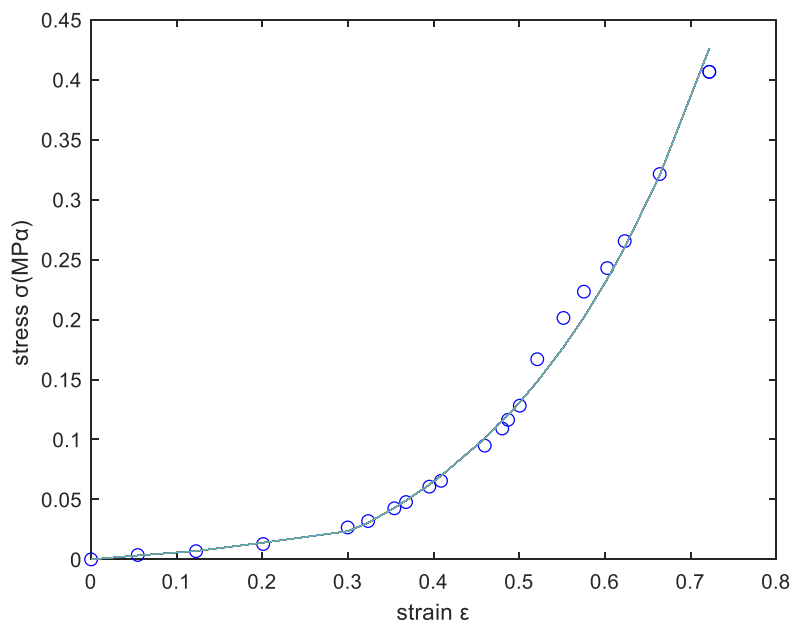
Figure 3.46: Global model approximation of the 4th experiment

The multiple solutions are illustrated in a clear way in Figures 3.47.
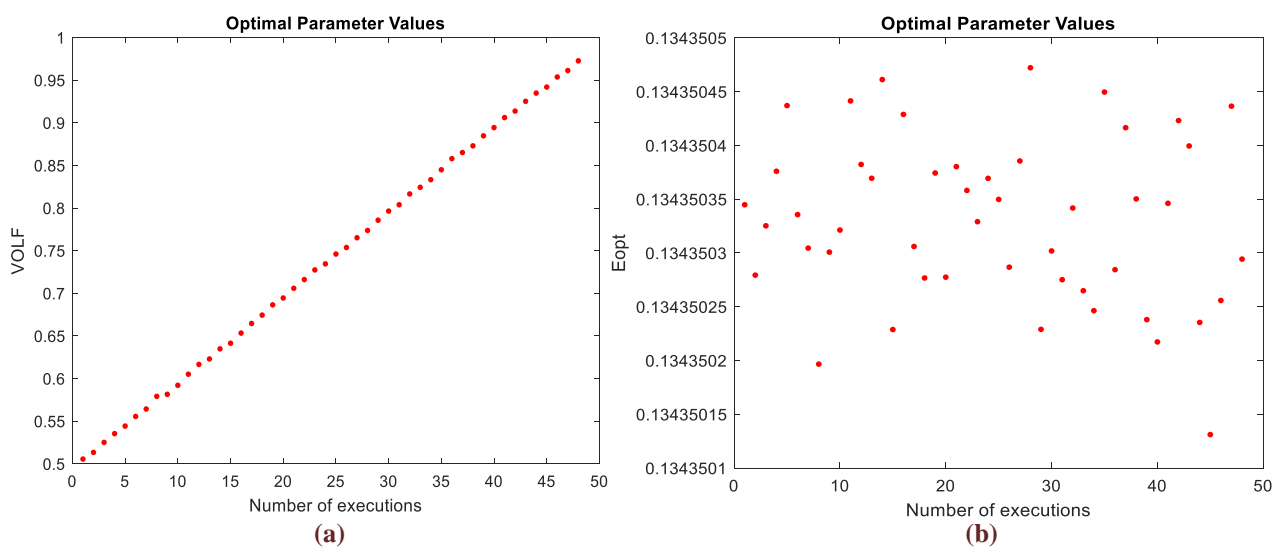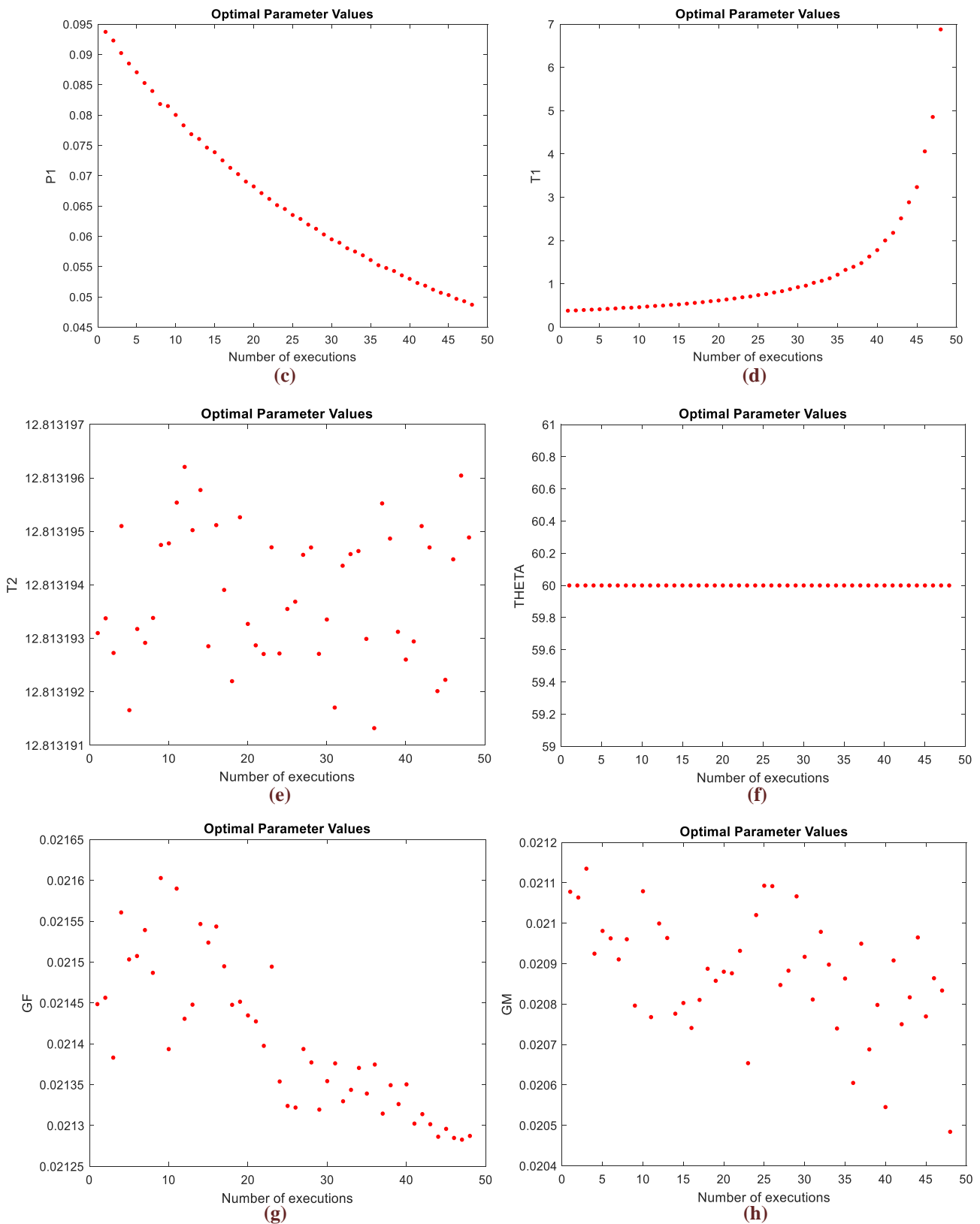
Figure 3.47: Variability of the optimized parameter values for the fourth experiment, (a)VOLF: fiber volume fraction, (b)Eopt: optimal fiber strain, (c)P1: fiber elastic modulus, (d),(e)T1,T2: mathematical parameters related to the CME's response, (f)THETA: angle between collagenous fibrils and myofibrils, (g),(h)GF,GM: fiber and connective tissue shear modulus

3.2.4.2 Bayesian framework

The model parameter set we are interested in is θ = [VOLF P1 T1 GF GM]. The results from the mTMCMC framework are exhibited below.
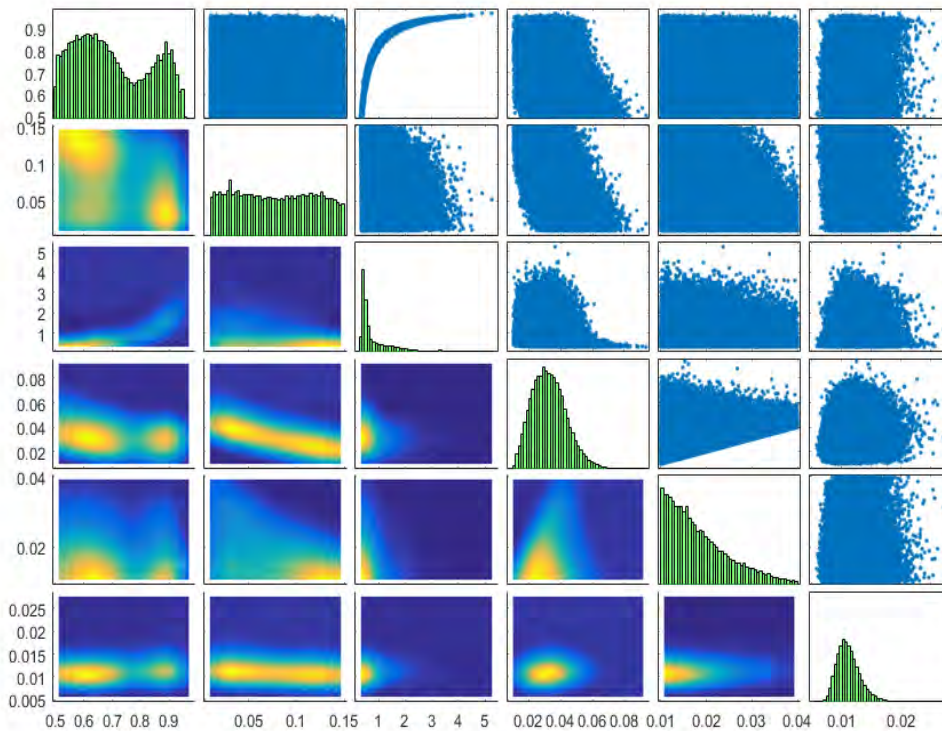
Figure 3.48: mTMCMC results for the 4th experiment, θ = [VOLF P1 T1 GF GM]
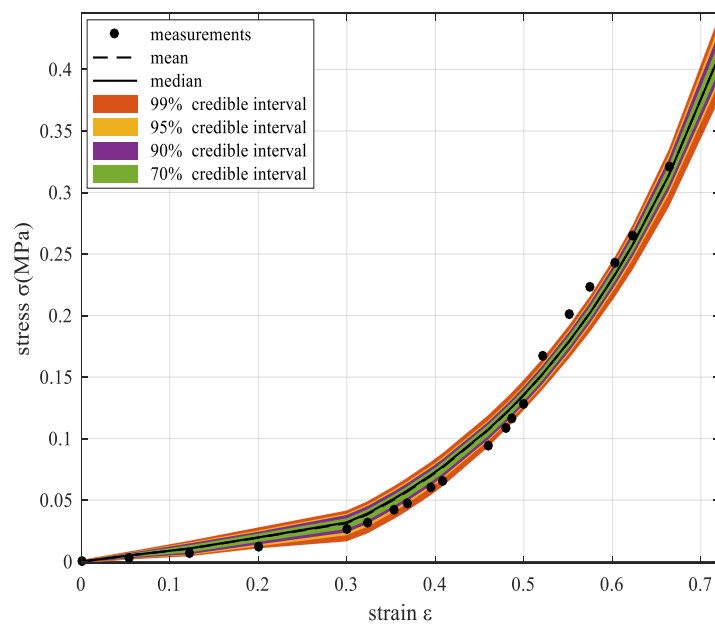
Figure 3.49 Model uncertainty propagation using mTMCMC

Table 3.11: Probable parameter values

PARAMETERS	MPV
VOLF	Multiple (User's choice)
P1	Depends on VOLF
T1	Strict correlation
GF	~ 0.03
GM	~0.02

Now, we develop the same analysis for the whole parameter set.
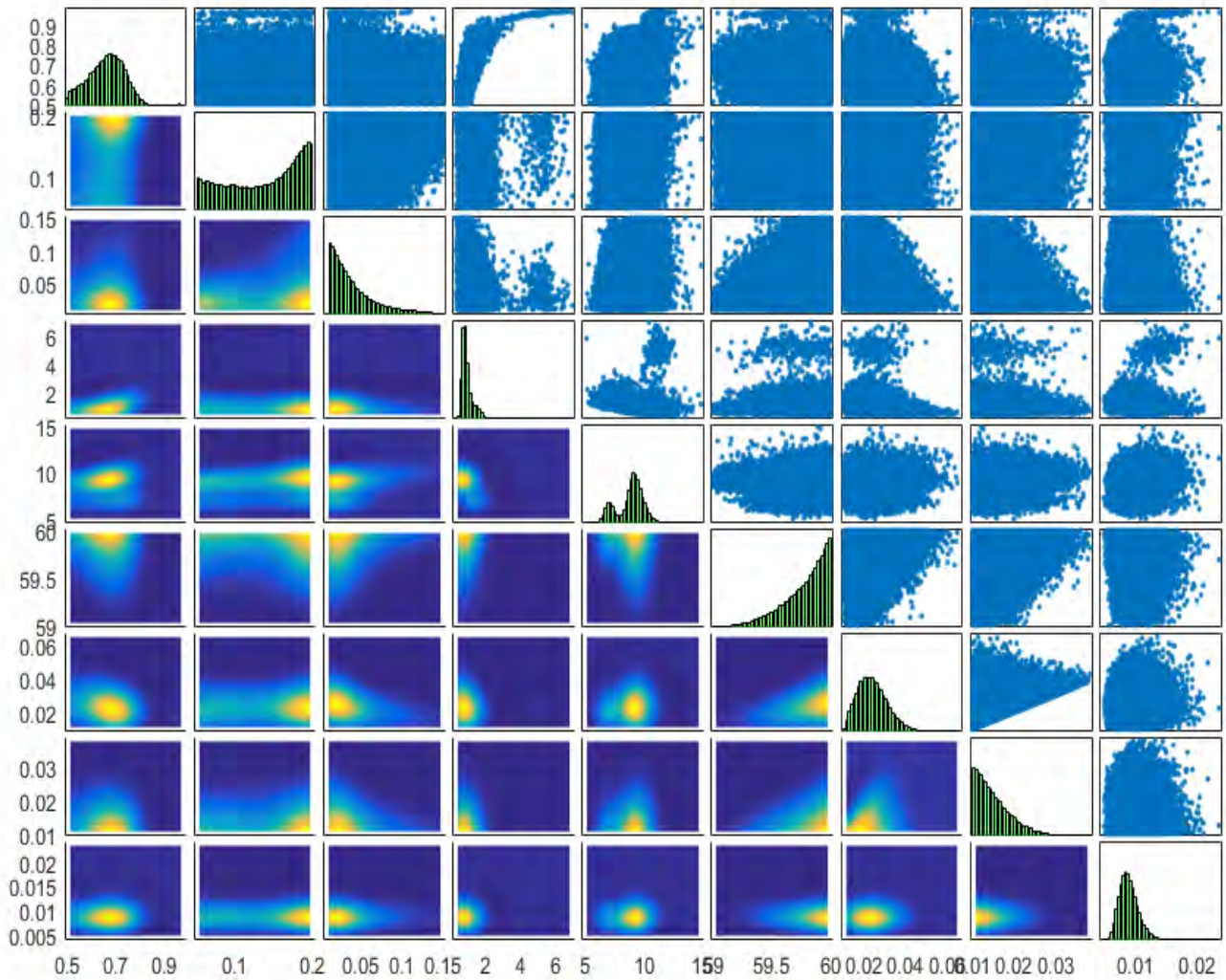
Figure 3.50: mTMCMC results for the parameter set θ=[VOLF Eopt P1 T1 T2 THETA GF GM]
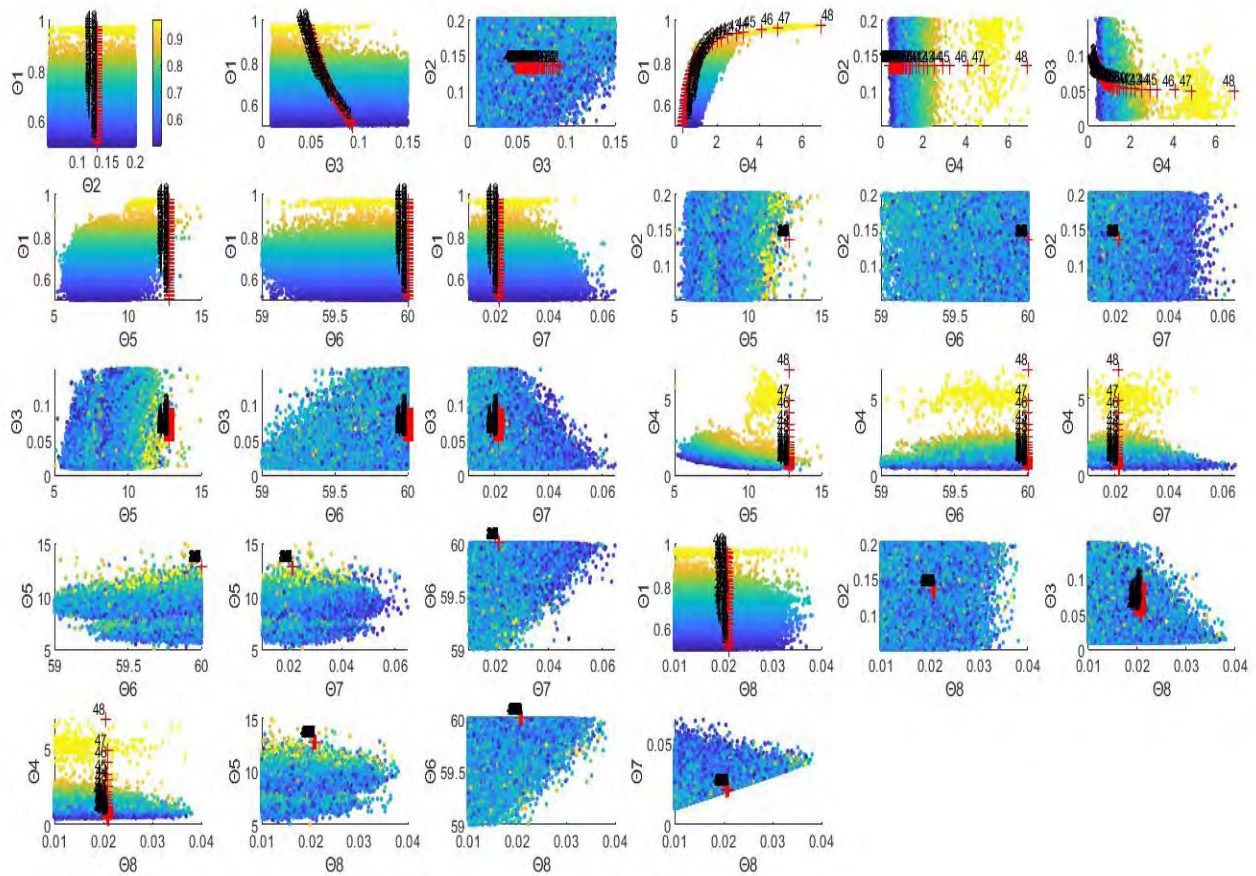
Figure 3.51: Colored mTMCMC samples and CMA points
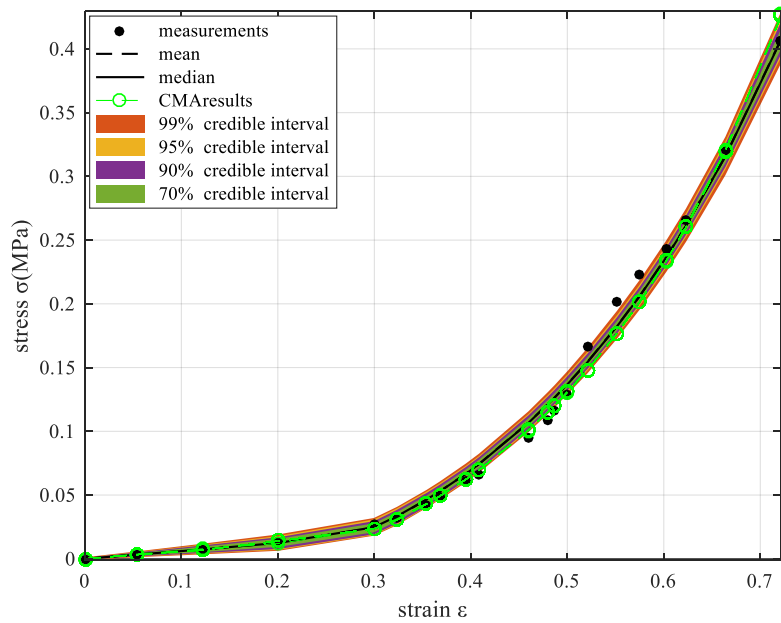

Figure 3.52: Model uncertainty propagation using mTMCMC and CMA results

66

3.2.5 Fifth experiment

In the next paragraphs, we exhibit the same result for the fifth experiment from [2].

3.2.5.1 Optimization analysis

In the next figures we present the results from the automated multiple executions of the CMA-ES framework. In the first figure, we prove that we get only the global optimal parameter values that give the optimal model propagation.
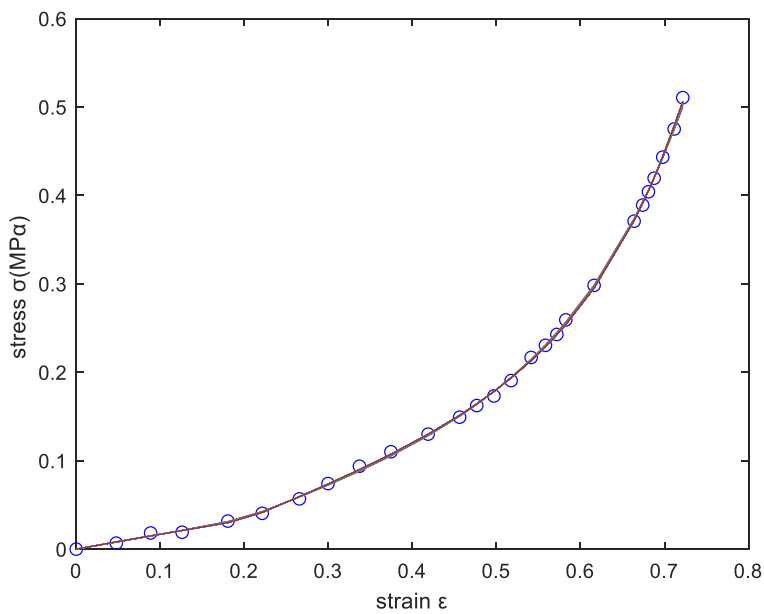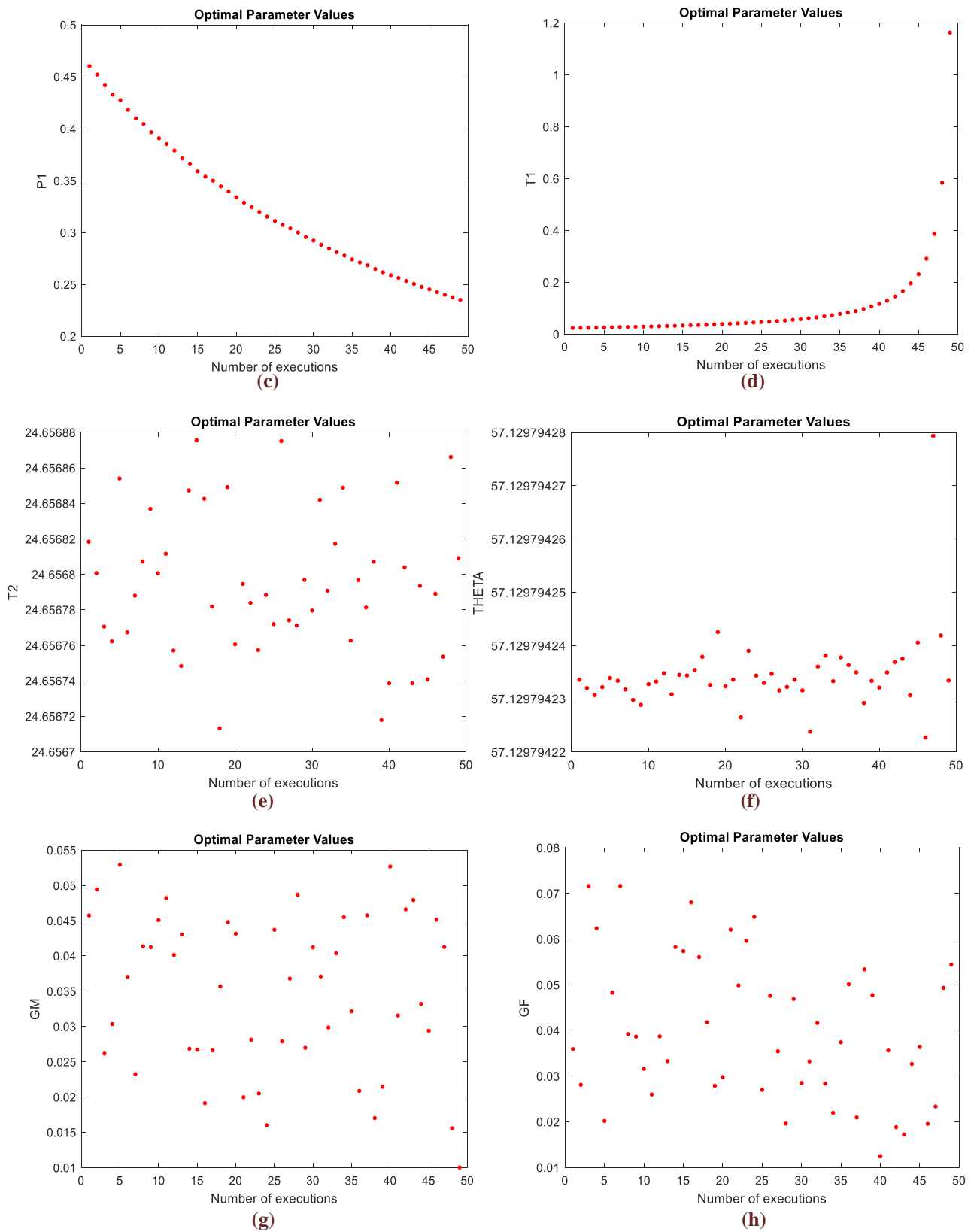

Figure 3.53: Global model approximation of the 5ᵗʰ experiment

The multiple solutions are illustrated in a clear way in Figures 3.54.

(a)   (b)

67
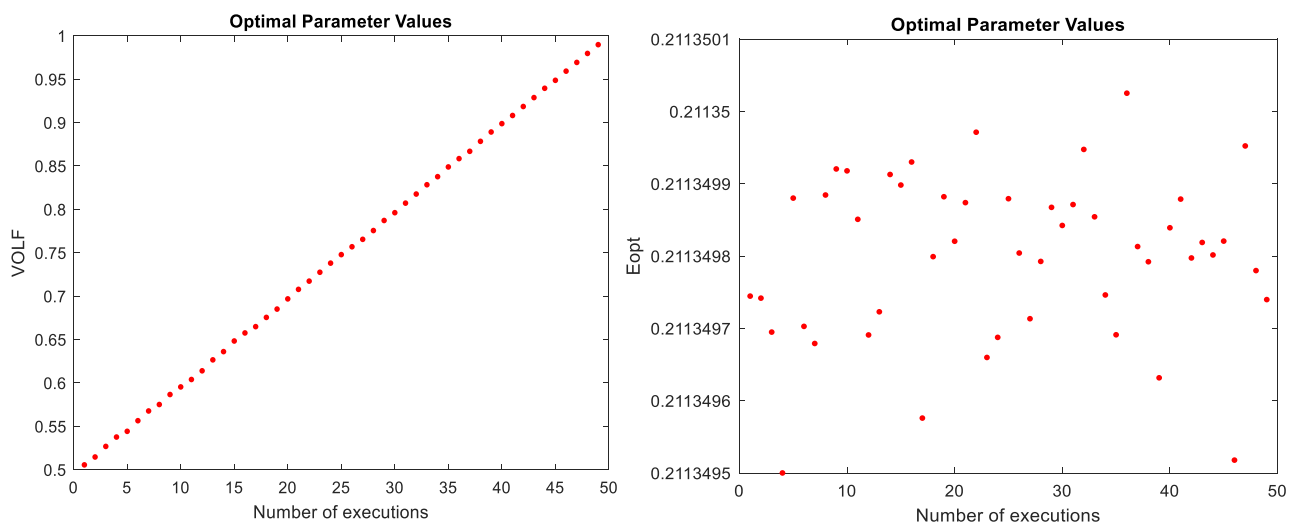
Figure 3.54: Variability of the optimized parameter values for the fifth experiment, (a)VOLF: fiber volume fraction, (b)Eopt: optimal fiber strain, (c)P1: fiber elastic modulus, (d),(e)T1,T2: mathematical parameters related to the CME's response, (f)THETA: angle between collagenous fibrils and myofibrils, (g),(h)GF,GM: fiber and connective tissue shear modulus

3.2.5.2 Bayesian framework

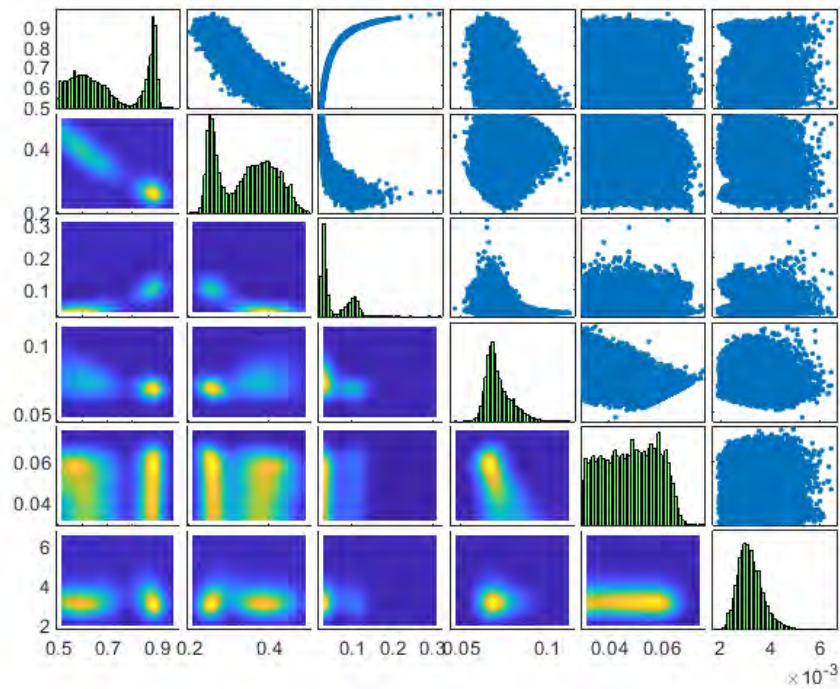We run the mTMCMC framework for the parameter set θ=[VOLF P1 T1 GF GM].

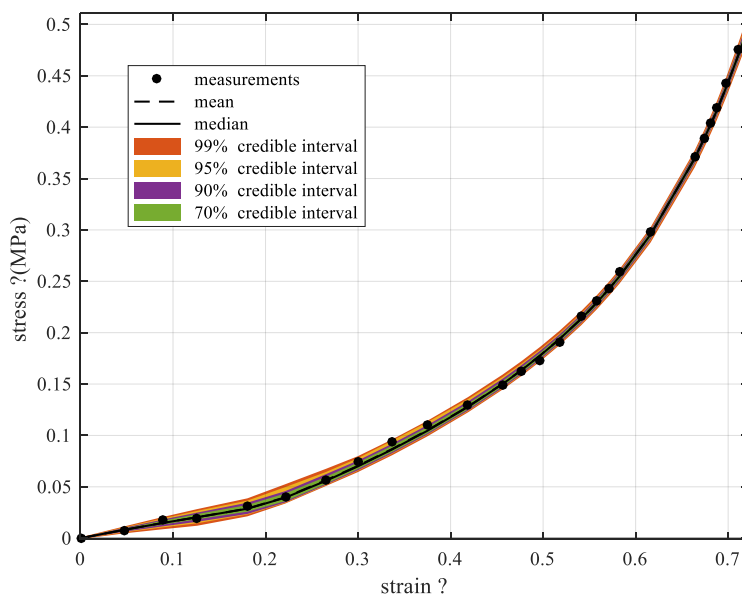**Figure 3.55: mTMCMC results for the 5th experiment, θ = [VOLF P1 T1 GF GM]**

**Figure 3.56: Model uncertainty propagation using mTMCMC**

Table 3.12: Probable parameter values

PARAMETERS	MPV
VOLF	Multiple (User's choice)
P1	Correlation
T1	Strict correlation
GF	~ 0.06
GM	~0.04

Examining the results, the VOLF takes a leading role about the parameter estimation by affecting the other optimal parameters' values. In this case of experiment, optimization results and mTMCMC samples have discover another possible correlation between VOLF and P1. Although this correlation is also shown up in other experiments in the CMA results, in this specific case the mTMCMC samples are also similarly distributed. As we can see the mTMCMC samples for the other experiments are uniformly distributed in the whole domain. This correlation is clearly illustrated in the next figures. Subsequently, there are correlations between VOLF and T1 and T1 and P1, respectively.


(a)

(b)

(c)
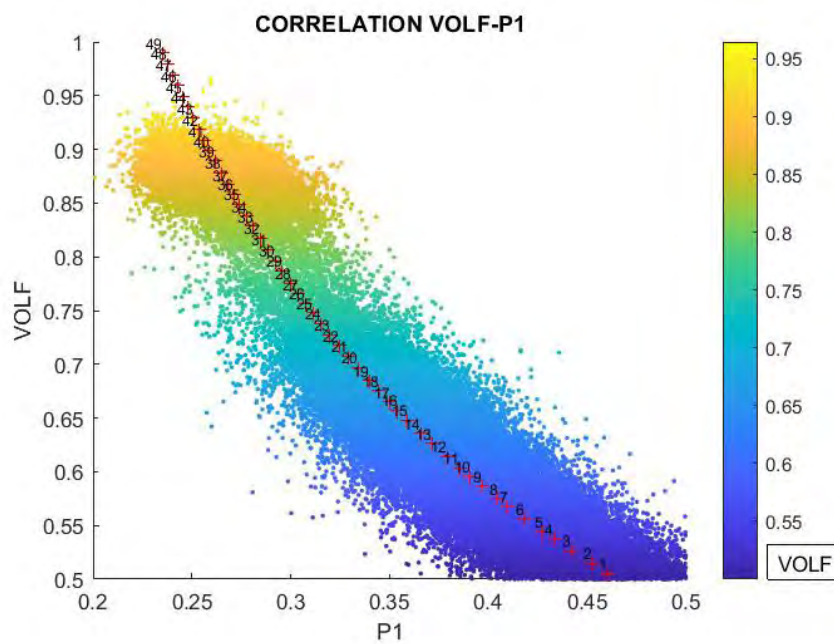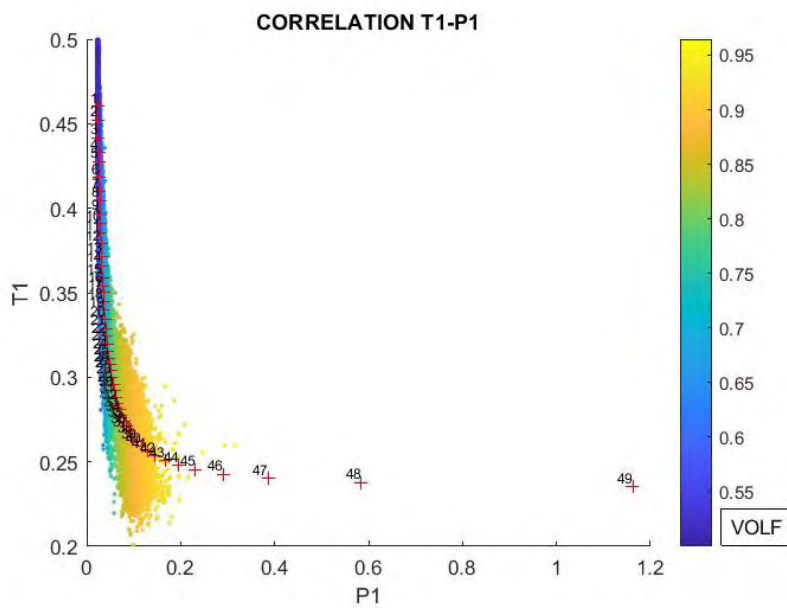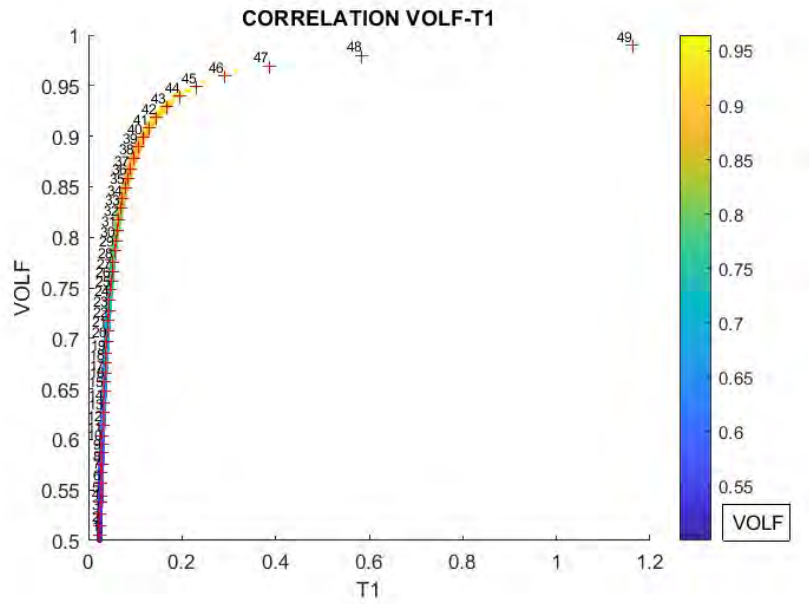
Figure 3.57: Several correlations among the parameters, (a) VOLF-P1, (b) VOLF-T1, (c) T1-P1

The CMA points are included in the mTMCMC samples. That proves the accuracy of the analyses. However, it is also noticeable that the sampling method was unable to give sample for the VOLF's values upper than 0.95, affecting the samples from the other parameters.

Let's concentrate to the whole parameter set which is θ=[VOLF Eopt P1 T1 T2 THETA GF GM].
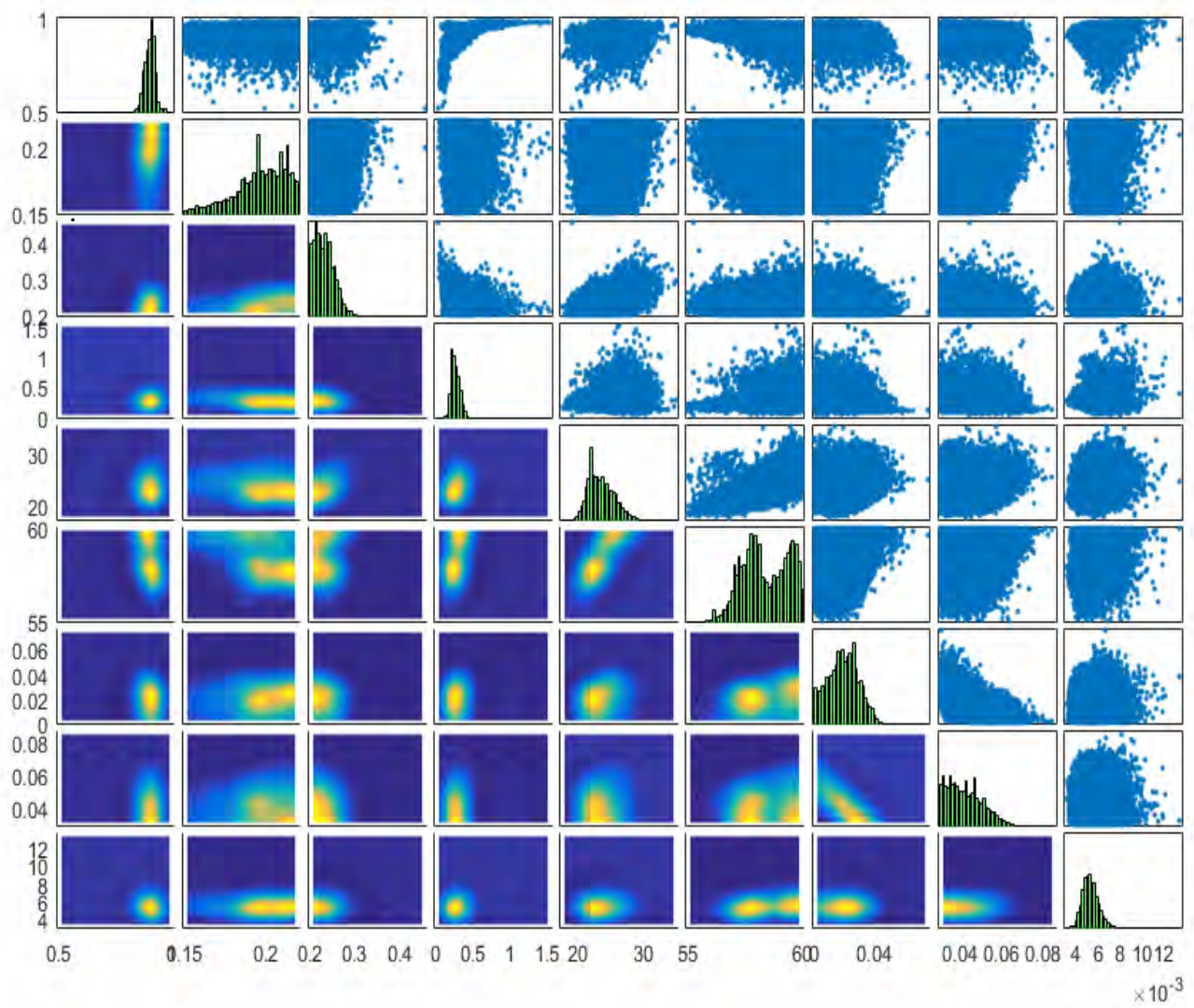
Figure 3.58: mTMCMC results for the parameter set θ=[VOLF Eopt P1 T1 T2 THETA GF GM]
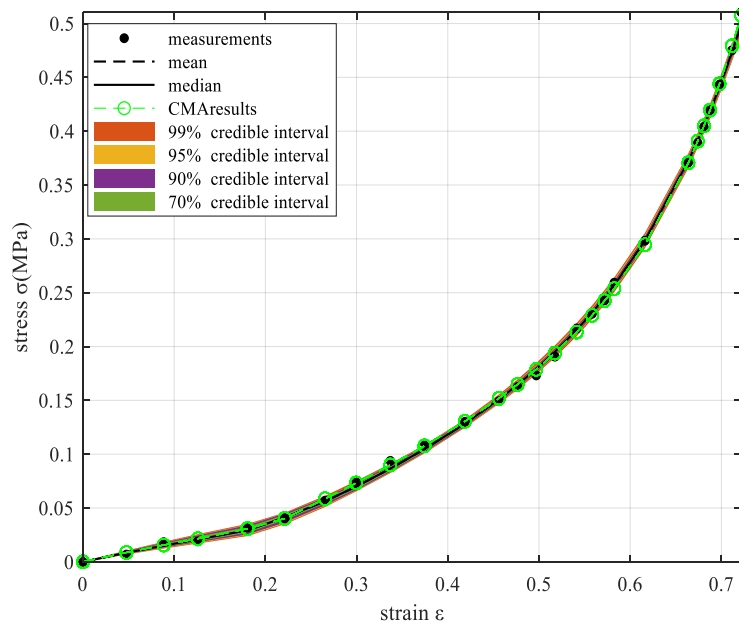
Figure 3.59: Model uncertainty propagation using mTMCMC and CMA results

Examining the results, we can say that the Eopt's most probable value is around 0.21 while the T2's is around 24, as the results from mTMCMC and CMA agree. The GF and GM can take values around 0.04. Any small discrepancy around this value cannot influence the mechanical response as it is proved through the Sobol analysis. According the mTMCMC, the angle (THETA) can take two possible values such that can give good approximation of the fifth Calvo's experiment. This is a unique characteristic of this specific marginal distribution. Implementing the optimization process limiting the THETA inside the range [59-60], there are also acceptable solutions, with a little larger error between model and experiment. Another characteristic of this case that is noticeable specifically in the results for θ=[VOLF P1 T1 GF GM] is the correlations between some parameters ,as it is also shown previously.

However, it is also clear the barrier existed in the sampling procedure. This is why we run once more. The results are exhibited below.
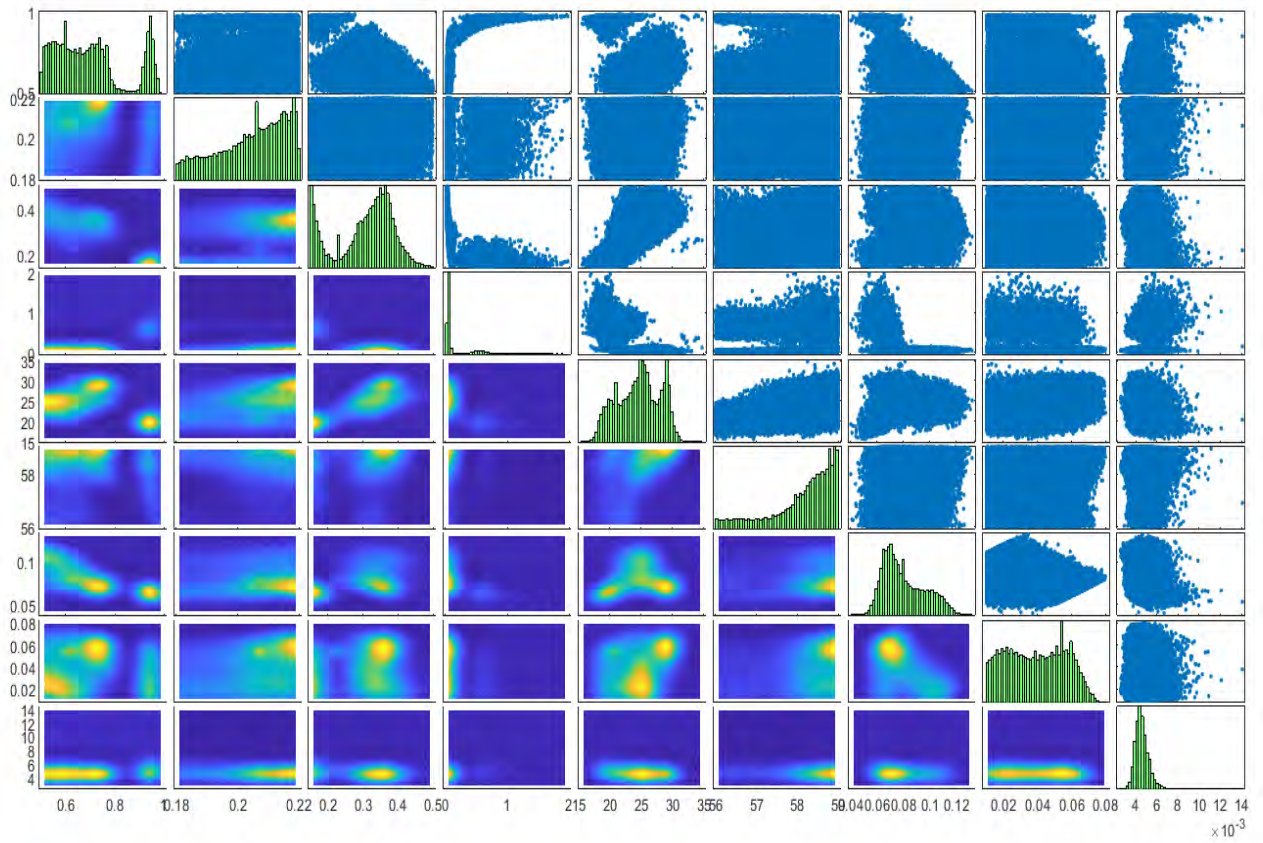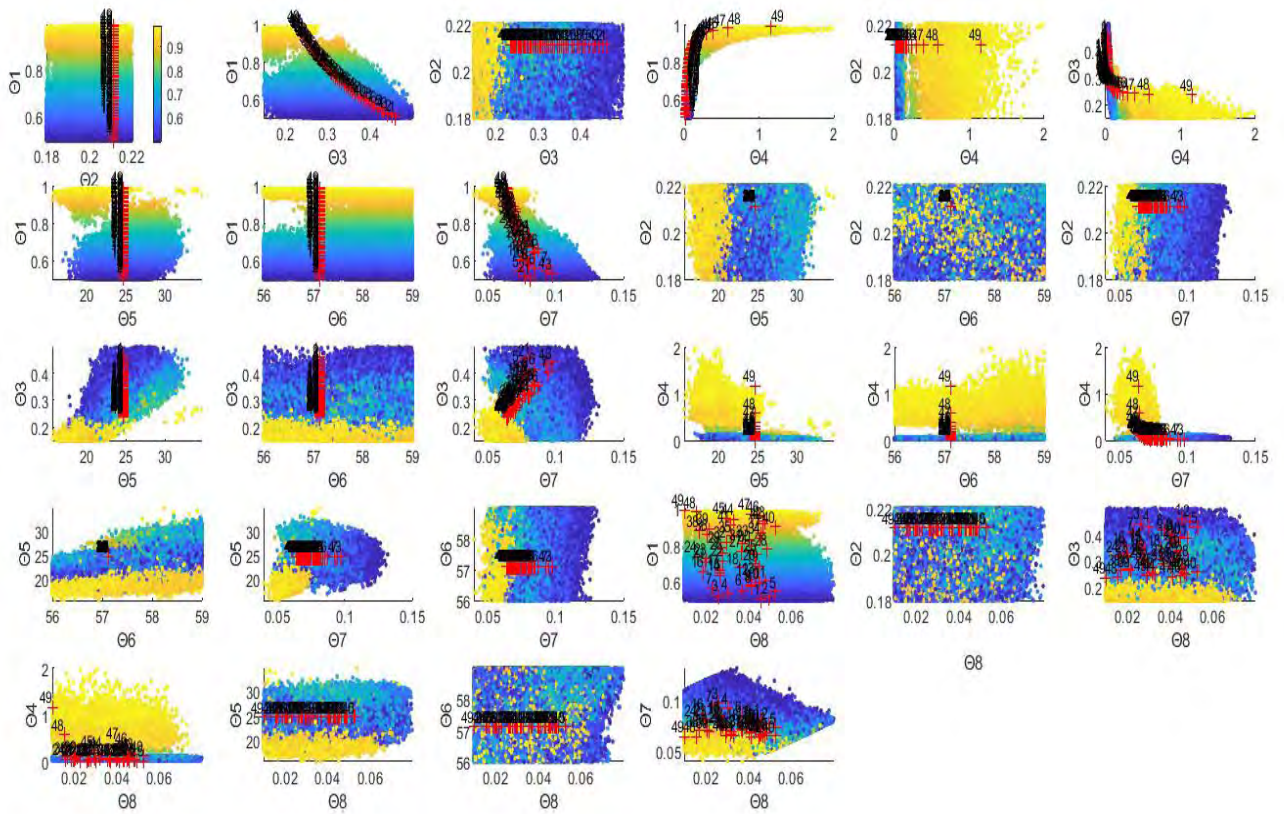
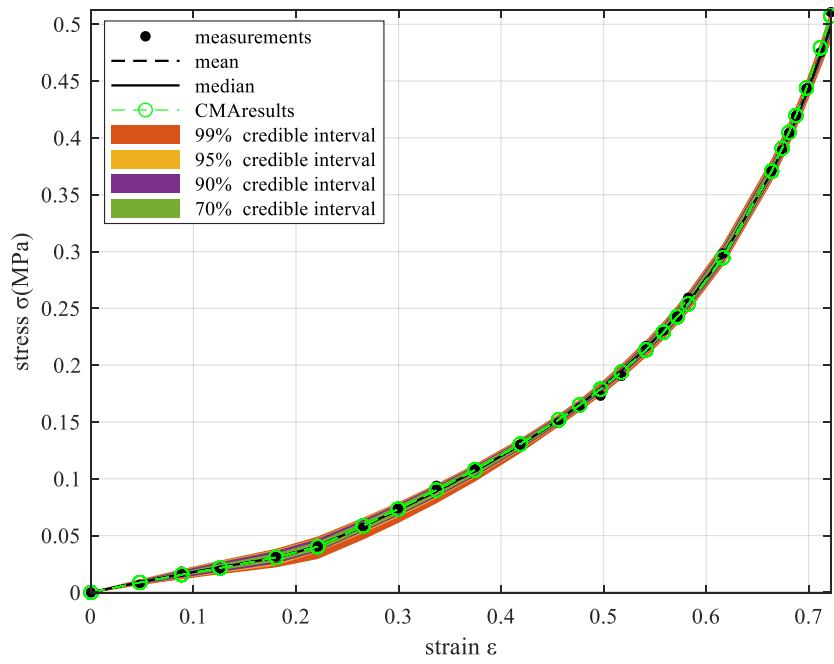**Figure 3.60: mTMCMC results**


Figure 3.61: Colored samples respect to VOLF

**Figure 3.62: Model uncertainty propagation using mTMCMC and CMA results**

3.3 Specimens' variability

Examining the results of the analyses that have been run for all the experiments, we notice that there is a large variance in the values of the parameters among the specimens. Seeing their different mechanical behavior, it is proved that the microstructure of the skeletal muscle has a great impact on the response of it. Thus, the variance of the mechanical behavior is caused by the differences in biological characteristics such as weight, gender or age or other microstructural properties. In this section we will give some emphasis in this attribute.

3.3.1 Comparison among the experiments from Calvo et al. [2] using CMA results

As we have mentioned, it would be very useful to compare the results from the experiments from [2], as these rats have been grown up in the same conditions and treatment and they have been objected to the same experiment by the same equipment. Let's direct our attention to each different parameter. The fiber volume fraction takes values inside the range [0.5-0.99] in each different case of experiment. Regarding the other parameters, they are characterized by a variance, as it is illustrated in the next figures.

(a) (b)
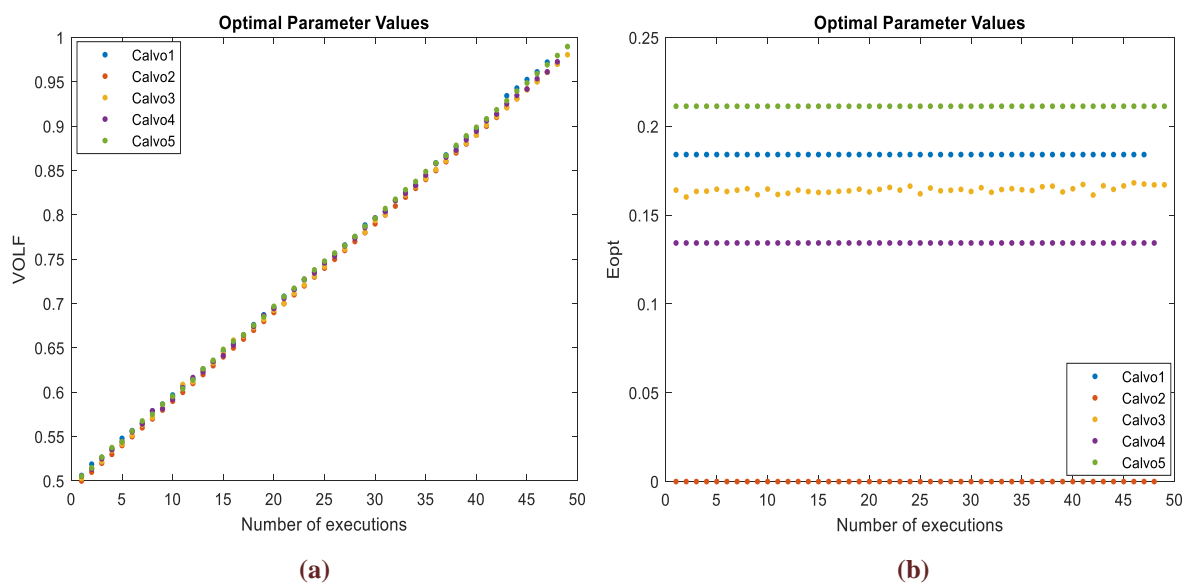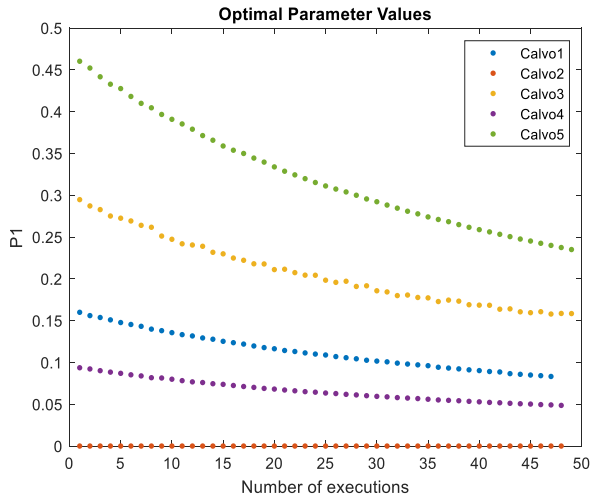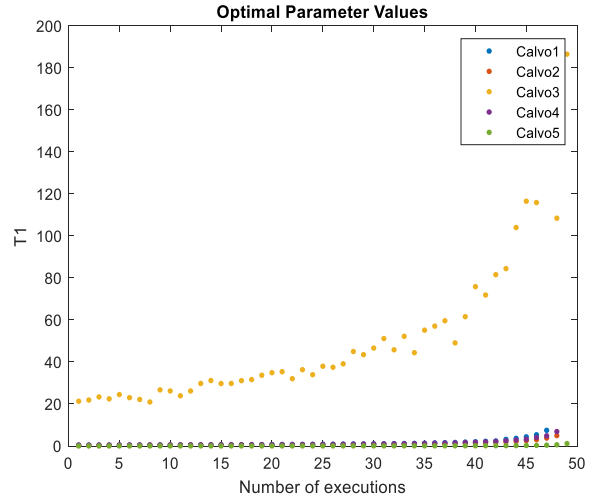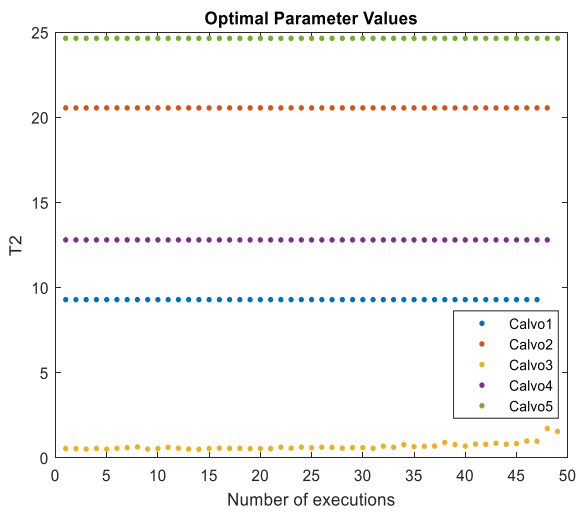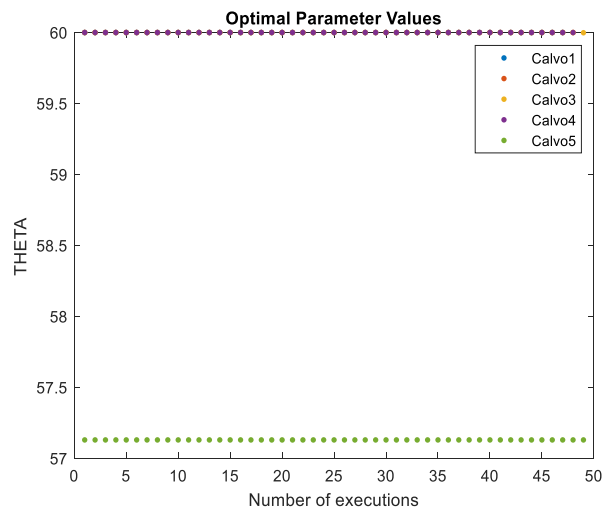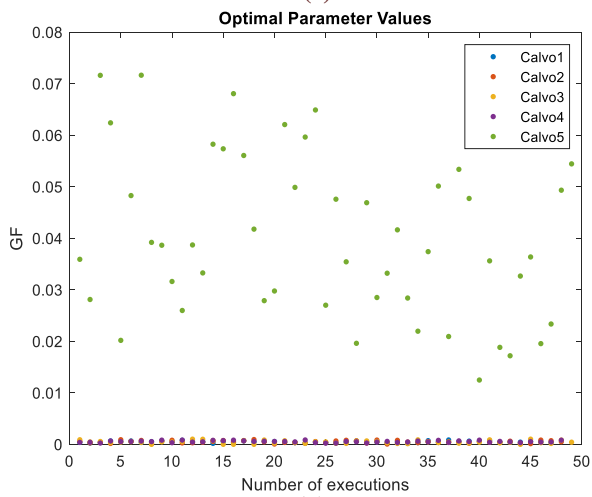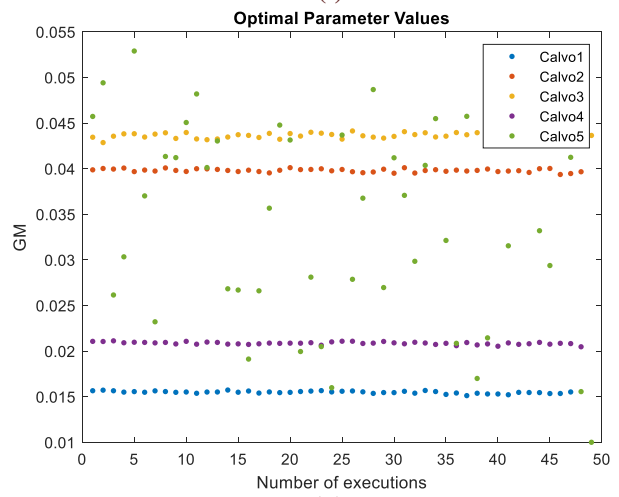
Figure 3.60: CMA points among the specimens from [2], (a)VOLF: fiber volume fraction, (b)Eopt: optimal fiber strain, (c)P1: fiber elastic modulus, (d),(e)T1,T2: mathematical parameters related to the CME's response, (f)THETA: angle between collagenous fibrils and myofibrils, (g),(h)GF,GM: fiber and connective tissue shear modulus

Examining these figures, we can notice that the CMA results differ from each other. In some figure (b, c, d, e, f), the parameters are changed in a same way. However, the GF and GM of the fifth experiment take values that are chaotically distributed in their considered range. Regarding these characteristics, we can conclude that the different mechanical responses of the skeletal muscle of the specimens are caused by differences in their microstructure and their characteristics. We develop analyses that can be implemented for each different experiment. These analyses can give us vital information about the microstructure of an organism but cannot take into consideration this species variability. For this reason, we cannot make any general conclusion about these 5 specimens. It seems that these properties are characterized by individuality.

We are also interested in the correlation between VOLF and T1 and the comparison of them among the experiments from [2].
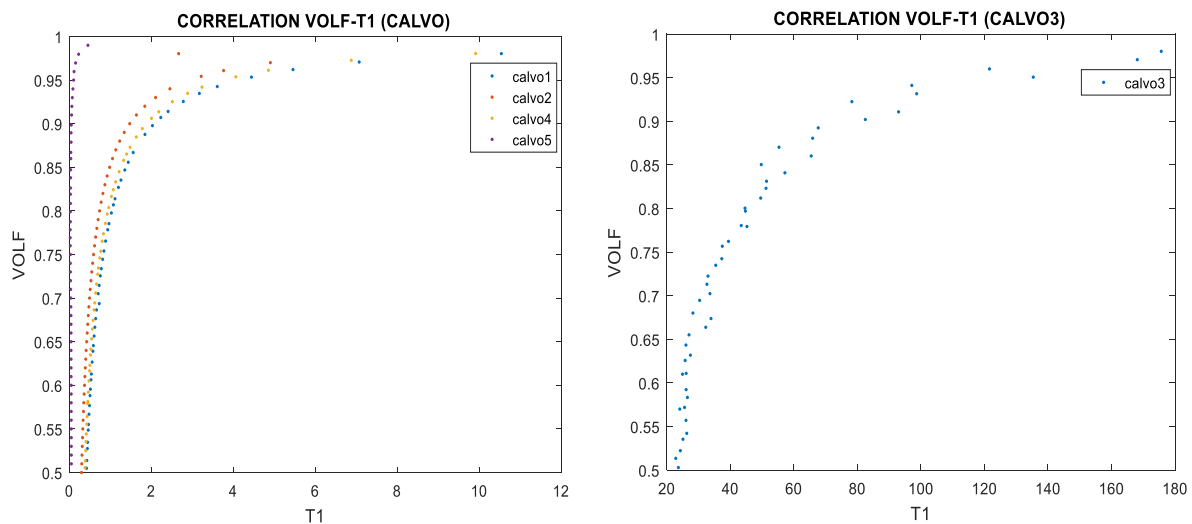

Figure 3.61: Correlation VOLF-T1 among the experiments

As it seems there is a large divergence between these correlations. This fact is related to the variety of mechanical behaviors that took from the experiments. This variability is depended in the species and their biological differences. Someone can say that the third and the fifth experiment from [2] have given the most divergent correlations VOLF-T1, as it is shown. The T1 is described as a mathematical variable related to the connective tissue's response and consequently it doesn't have a direct physical meaning. For this reason, we cannot explain this large variability as it does not have a reasonable impact on the microstuctural characteristics of the skeletal muscle. However, there is no doubt that its different value of T1 and the other parameters related to it, such as T2 and THETA have an impact on the final mechanical behavior. Moreover, it is a great proof that there is the same form of relationship between these two parameters regardless the experiment.

It is also worth to be noted that examining the CMA results for the third experiment, the correlation is not a strict line but it seems to be a surface.

3.3.2 Model prediction of a Fusiform type of skeletal muscle based on the specimens' variability

There are several types of skeletal muscle that response in a different way in loading conditions. In this paragraph we direct our attention to the Fusiform type of muscle. Fusiform muscles consist of the muscle and the tendon and have fibers that run parallel to one another following the direction of the tendon (Figure 3.62). These muscles are built to provide large ranges and a great variety of motion. We use the finite element model proposed in [22], as it is shown in Figure 3.63. It is an axisymmetric geometry in which every finite element follows the formulation that is described in the Chapter 1. More details are exhibited in the considered paper.
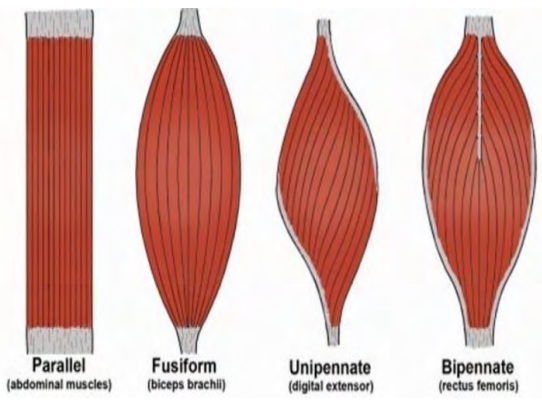
Figure 3.62: Types of skeletal muscle
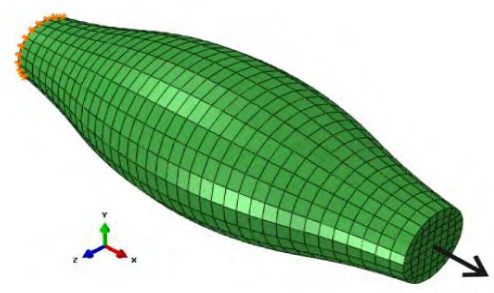
Figure 3.63: Finite element model

Firstly, we want to ensure that the model prediction of the model described in the Chapter 1 for larger strain than the experimental strain will be accurate, characterized by a small discrepancy.
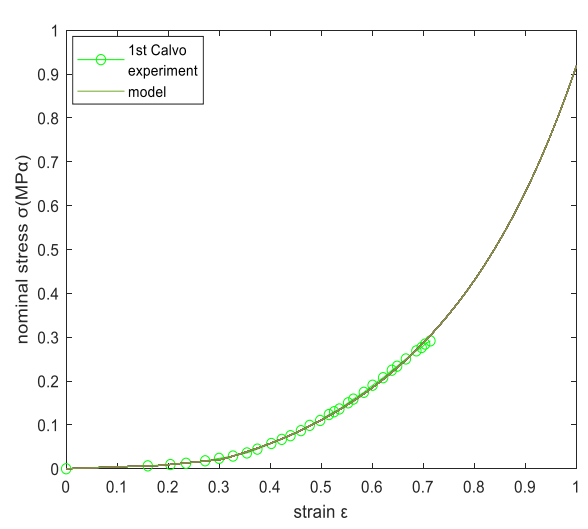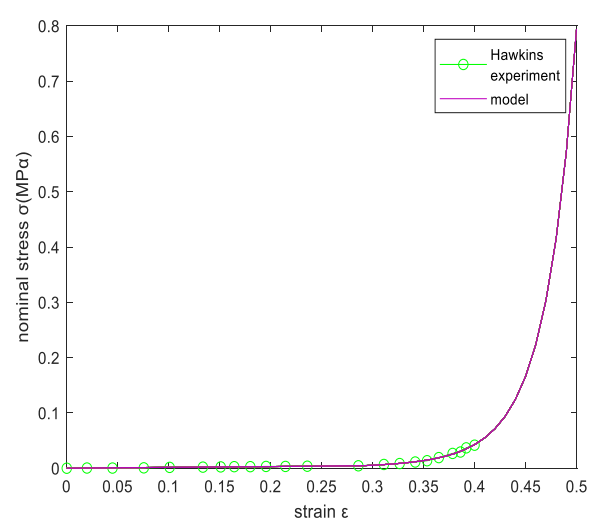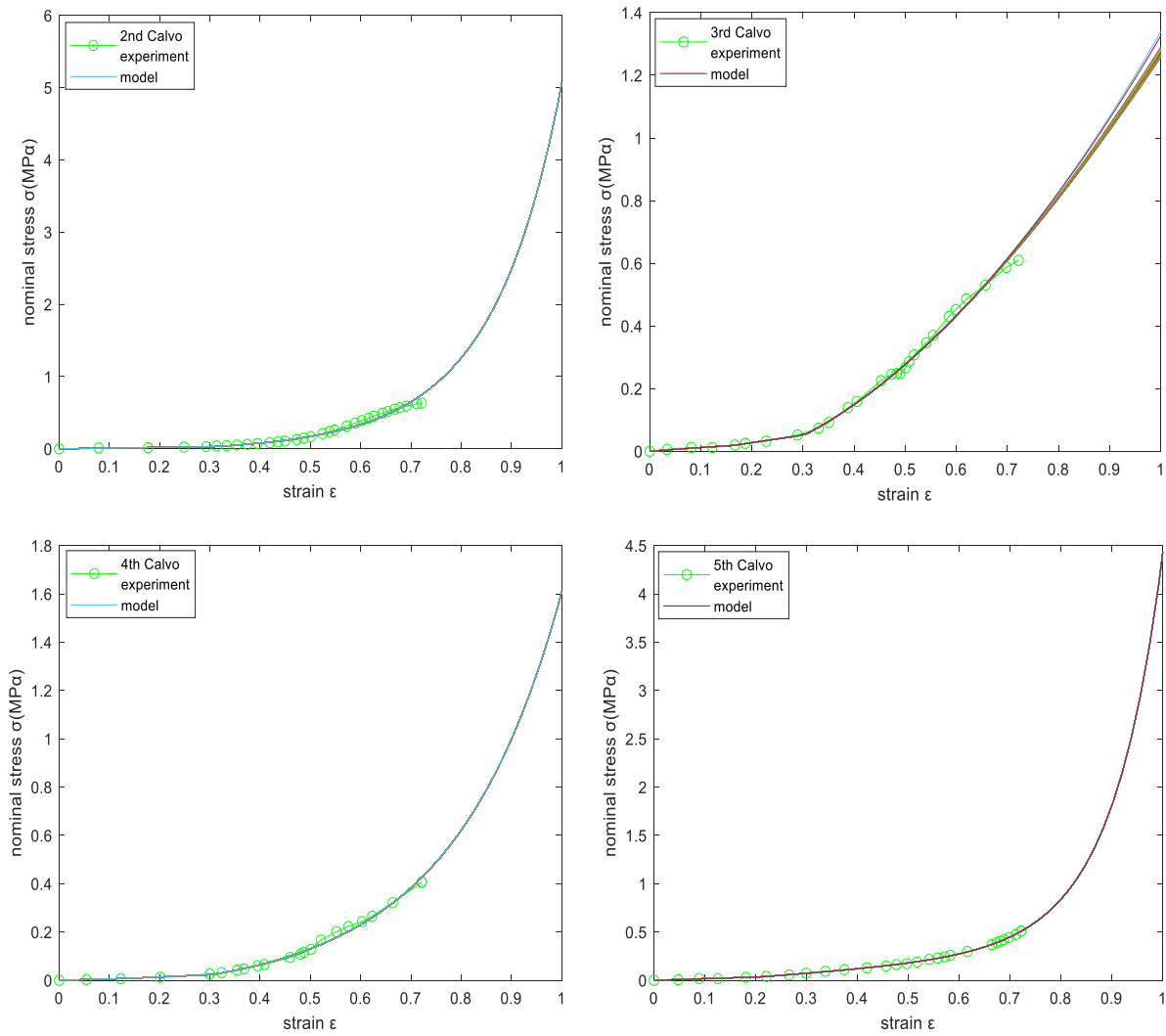
Figure 3.64: Model prediction for strains larger than the experimental using CMA points

As we can notice, the stresses, calculated for the large strains, are characterized by a small divergence that is not noticeable in Figures 3.64. This is why the stress-strain curves are seemed to coincide. This attribute is related to the fact that we optimized only till the maximum strain of the experimental data. Thus any discrepancy for larger strains is reasonable. In our case, it does not play any significant role for the model prediction, except for the 3rd experiment from [2] in which it is distinguishable.

In the next step, we focus on the Fusiform skeletal muscle. The optimal parameter sets are used to determine the properties of each different finite element. In the next figure, the model prediction of this model is illustrated. In this case we present only the result originated by using the CMA points of the experiment from [1]. Let's take into consideration that this framework propose several different optimal sets. These optimal parameter sets were originated so that they can give the same model propagation that minimizes globally the error between model and experimental data. As it is shown, the structure of the Fusiform muscle has the same model prediction, regardless which optimal parameter set we use. This is reasonable as we have proved that all these sets give the same global approximation of the experiment (Figure 3.2)
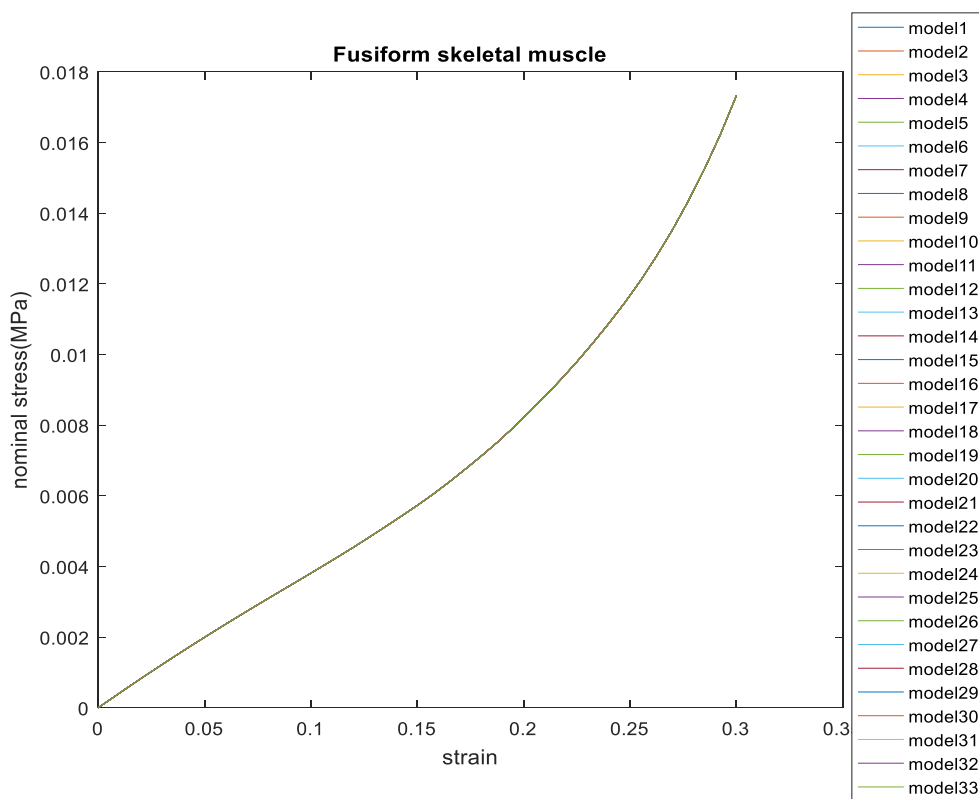
Figure 3.65: Model prediction of the Fusiform skeletal muscle using CMA points of experiment from [1]

As it seems, the curves coincide with each other. This is useful while we can focus on the model predictions of this muscle for different specimens using only one optimal parameter set without losing accuracy. The previous steps were necessary to prove the accuracy of the results generated for the purpose of this study, so that someone based on it can make an efficient model prediction. Moreover, according to the last result, we also manage to find a valid way for the model prediction of a macroscale structure of skeletal muscle, while reducing effectively the computational cost of this task. Regarding this, we continue with implementing model prediction for each different

specimen of rats. In this way we investigate the species variability and its influence in the total mechanical response of a structure of a muscle in the macroscale.
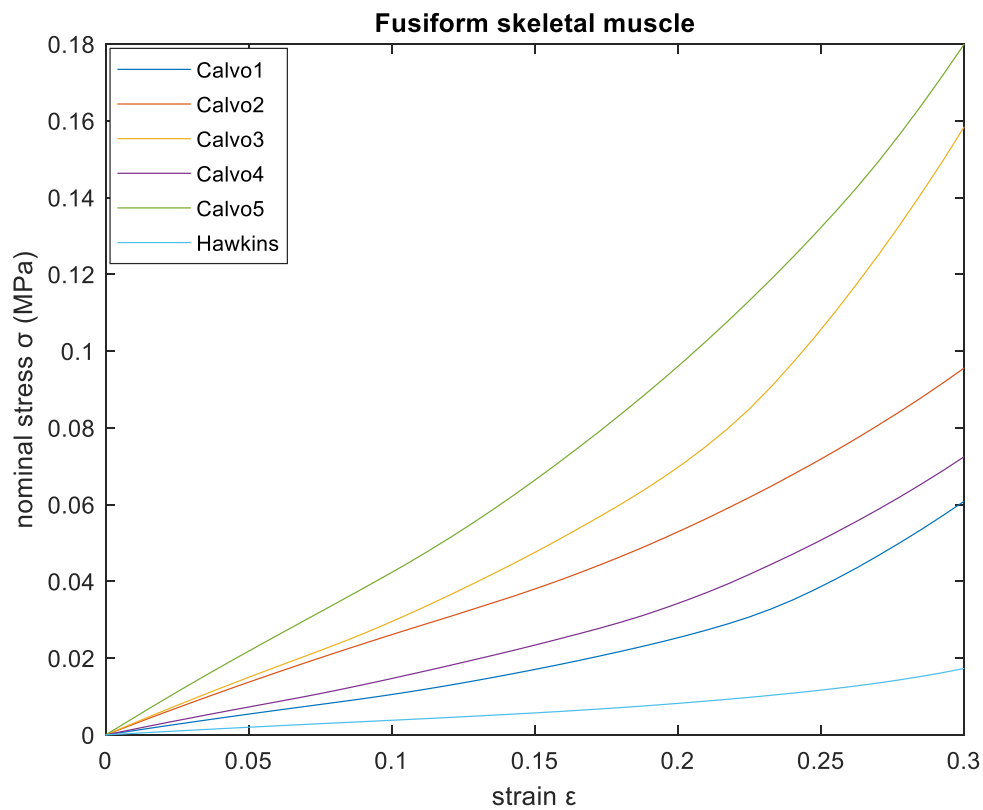
Figure 3.66: Model prediction of Fusiform skeletal muscle for each different experiment

Seeing the Figure 3.66, we can say that the macroscaled mechanical response of a specimen is strongly bonded with its unique microstructural characteristics. This attribute of the uniqueness of each living organism should be also investigated.

CHAPTER 4

Conclusions and future work

In this thesis Bayesian analysis is used to make parameters estimation and uncertainty quantification of a skeletal muscle model. We were confronted with a three dimensional constitutive model that is proposed by [15] and it is characterized by a large dimensional unknown parameter space. Particularly, the unknown parameters are eight, included biological, mechanical properties and mathematical parameters (constants). Estimating them is vital about understanding how the microstructure has an impact on the macroscaled mechanical behavior of the muscle. However, the lack of previous knowledge and a few experimental data stand as an obstacle through our mission. The model can be characterized as unidentifiable while the uncertainties cannot be dealt with, using only one set of experimental data at the time which are stress-strain relationship. The information that is included in the experiments is not capable of uniquely inferring the values of the eight unknown model parameters using the Bayesian framework.

Seeing this, we seek alternative ways to estimate them, by combining several different approaches to identify this model. Thus, we implement not only Bayesian approach, but also optimization process and Sobol analysis so that we are capable of examine our results and evaluate them. In this way, we take advantage of each different analysis that provides also different types of information and results which are finally combined so as to result in an accurate conclusion.

The current research has given to us the opportunity to make a step closer to parameter estimation, leading us to broaden our knowledge and perspective not only about this model but also about uncertainty quantification and its capabilities. In this regard, there are many topics that may enable the expansion of this thesis. It would gain a lot of interest to implement hierarchical Bayesian analysis by assuming that the prior follows a Gaussian distribution with the mean and the covariance matrix to constitute the hyperparameters to be estimated. In this way, someone increase his previous information about the model and this may be useful to better quantify the variability in the values of the model parameters. However, this task demands high knowledge of the structure of skeletal muscle and experimental at different hierarchical modeling levels, something that we did not have access.

Future work should concentrate on using in the analysis other experimental data focused on subsystems of the skeletal muscles. For instance, mechanical experiments were recently carried out on a wide variety of scales, from the myofibrils, fibres and tissue. One could take advantage of these experimental data and use the Bayesian framework for the different components of the tissue to learn the values and the uncertainties in the model parameters so that they are consistent with the experimental

data obtained from different components. It is expected that the additional experiments at the component level will also significantly reduce the uncertainty in the model parameters of the skeletal muscle system.

Another interesting step of a future research should be the Hierarchical Bayesian implementation applied on experimental data available from different components of the tissue. Developing this analysis, we take into consideration several different experimental data characterizing the different mechanical response among the species. As it is proved through this research the properties characterize individually each different organism. This variability, based on the species' uniqueness, should be investigated. The Hierarchical Bayesian approach is capable to accomplish that. Let's keep in mind that implementing the classical Bayesian analysis, we managed to make an accurate parameter investigation about each different organism.

To sum up, this model combines the microstuctural characteristics of the skeletal muscle with the macroscale mechanical behavior. This attribute renders its parameters essential to be inferred, while it has a fundamental meaning for the skeletal muscle's response. We made the some steps to this direction by fulfilling the task of this thesis and we can continue our exploration by developing more strategies.

Literature

1. Hawkins, D. and M. Bey, *A comprehensive approach for studying muscle-tendon mechanics.* Journal of biomechanical engineering, 1994. **116**(1): p. 51-55.
2. Calvo, B., et al., *Passive nonlinear elastic behaviour of skeletal muscle: experimental results and model formulation.* Journal of biomechanics, 2010. **43**(2): p. 318-325.
3. Morrow, D.A., et al., *Transversely isotropic tensile material properties of skeletal muscle tissue.* Journal of the mechanical behavior of biomedical materials, 2010. **3**(1): p. 124-129.
4. Gras, L.-L., et al., *Hyper-elastic properties of the human sternocleidomastoideus muscle in tension.* Journal of the mechanical behavior of biomedical materials, 2012. **15**: p. 131-140.
5. Holzapfel, G.A., et al., *Determination of layer-specific mechanical properties of human coronary arteries with nonatherosclerotic intimal thickening and related constitutive modeling.* American Journal of Physiology-Heart and Circulatory Physiology, 2005. **289**(5): p. H2048-H2058.
6. Lieber, R.L., et al., *Inferior mechanical properties of spastic muscle bundles due to hypertrophic but compromised extracellular matrix material.* Muscle & Nerve: Official Journal of the American Association of Electrodiagnostic Medicine, 2003. **28**(4): p. 464-471.
7. Purslow, P.P. and J.A. Trotter, *The morphology and mechanical properties of endomysium in series-fibred muscles: variations with muscle length.* Journal of Muscle Research & Cell Motility, 1994. **15**(3): p. 299-308.
8. Hansen, N., S.D. Müller, and P. Koumoutsakos, *Reducing the time complexity of the derandomized evolution strategy with covariance matrix adaptation (CMA-ES).* Evolutionary computation, 2003. **11**(1): p. 1-18.
9. Christley, S., et al., *Bayesian inference of the lung alveolar spatial model for the identification of alveolar mechanics associated with acute respiratory distress syndrome.* Physical biology, 2013. **10**(3): p. 036008.
10. Wang, S., et al., *Bayesian inference-based estimation of normal aortic, aneurysmal and atherosclerotic tissue mechanical properties: from material testing, modelling and histology.* IEEE Transactions on Biomedical Engineering, 2019.
11. Madireddy, S., B. Sista, and K. Vemaganti, *Bayesian calibration of hyperelastic constitutive models of soft tissue.* Journal of the mechanical behavior of biomedical materials, 2016. **59**: p. 108-127.
12. Doraiswamy, S., J.C. Criscione, and A.R. Srinivasa, *A technique for the classification of tissues by combining mechanics based models with Bayesian inference.* International Journal of Engineering Science, 2016. **106**: p. 95-109.
13. Karathanasopoulos, N., et al., *Bayesian identification of the tendon fascicle's structural composition using finite element models for helical geometries.* Computer Methods in Applied Mechanics and Engineering, 2017. **313**: p. 744-758.
14. Franck, I.M. and P.-S. Koutsourelakis, *Multimodal, high-dimensional, model-based, Bayesian inverse problems with applications in biomechanics.* Journal of Computational Physics, 2017. **329**: p. 91-125.
15. Spyrou, L.A., M. Agoras, and K. Danas, *A homogenization model of the Voigt type for skeletal muscle.* Journal of theoretical biology, 2017. **414**: p. 50-61.
16. Bishop, C.M., *Pattern recognition and machine learning*. 2006: springer.
17. Arampatzis, G., et al., *Langevin Diffusion for Population Based Sampling with an Application in Bayesian Inference for Pharmacodynamics.* SIAM Journal on Scientific Computing, 2018. **40**(3): p. B788-B811.

18.   Cannavó, F., *Sensitivity analysis for volcanic source modeling quality assessment and model selection.* Computers & geosciences, 2012. **44**: p. 52-59.
19.   Bonet, J. and R.D. Wood, *Nonlinear continuum mechanics for finite element analysis*. 1997: Cambridge university press.
20.   Thacker, B.E., et al., *Passive mechanical properties and related proteins change with botulinum neurotoxin A injection of normal skeletal muscle.* Journal of orthopaedic research, 2012. **30**(3): p. 497-502.
21.   Gill, J., *Bayesian methods: A social and behavioral sciences approach*. 2002: Chapman and Hall/CRC.
22.   Spyrou, L.A. and N. Aravas, *Muscle and tendon tissues: constitutive modeling and computational issues.* Journal of Applied Mechanics, 2011. **78**(4): p. 041015.

APPENDIX

Appendix A

The measured data that we use are collected by previous experimental studies. In this section, a table of them is presented so that it can be clear what data we use in every presented result in the next sections. There is also a table about the characteristics of each experiment.

TENSION

PAPERS	CODE	SPECIES	NUMBER OF DATA
Hawkins and Bey [1] (1994)	A	Rat	1
Calvo [2](2010)	B	Rat	5
			6

CHARACTERISTICS

CODE	TYPE OF MUSCLE	TYPE OF EXPERIMENT	STRAIN RATE	TIMELINE
A	Tibialis anterior	In vitro	-	-
B	Tibialis anterior	In vitro (In vivo)	$0.022\% \sec^{-1}$	Fresh

Appendix B

<u>Cubic spline interpolation:</u>

Given a set of n data (x_i, y_i) , where i=1,2,…n. We are interested in finding a function that satisfies $S(x_i)=y_i$. The cubic spline $S(x_i)$ is determined by:

$S(x_i)=C_i(x),\ x_{i-1} < x < x_i$

where $C_i = a_i + b_i x + c_i x^2 + d_i x^3$

In our case, we seek a group of functions that satisfy $S(Eopt_i)=VOLF_i$

 The next table illustrates the optimal values of the constants respect to the ranges of the Eopt

Hawkins experiment				
Ranges Eopt	a_i	b_i	c_i	d_i
0.0078-0.0081	-2645790,8564	-2767,57819	61,0517	0,5099
0.0081-0.0084	-2645790,8564	-5212,2846	58,5939	0,5285
0.0084-0.0089	2296860,4511	-7886,78275	54,18015	0,54751
0.0089-0.0093	-1598943,9183	-4533,01917	48,1352	0,57228
0.0093-0.0097	2562251,6615	-6232,34317	44,3215	0,58869
0.0097-0.0104	-475146,5874	-3159,82406	40,5673	0,60557
0.0104-0.0106	2515482,5027	-4227,72917	35,03271	0,63399
0.0106-0.0115	-93356,09326	-2574,91841	33,5428	0,64149
0.0115-0.0124	447844,1794	-2821,67153	28,78816	0,66898
0.0124-0.0131	-133682,1704	-1644,78472	24,8757	0,69233
0.0131-0.0144	203761,3134	-1934,7185	22,2879	0,70940
0.0144-0.152	1241,5356	-1123,2183	18,2284	0,73606
0.152-0.0168	68235,0465	-1120,5185	16,602	0,74868
0.0168-0.0187	37649,51105	-784,59984	13,4757	0,77321
0.0187-0.0197	21462,1484	-565,8362	10,8602	0,79664

0.0197-0.0221	22235,8614	-502,416	9,80794	0,80681
0.0221-0.0258	11334,68865	-343,079	7,7884	0,82767
0.0258-0.0302	6444,5951	-218,7334	5,73398	0,85212
0.0302-0.0355	3150,8894	-133,0486	4,17492	0,8738
0.0355-0.04	1380,8118	-83,10816	3,03292	0,892607
0.04-0.0404	10435,9908	-64,3576	2,36543	0,904761
0.0404-0.0448	763,92581	-52,45474	2,32101	0,905651
0.0448-0.052	727,6683	-42,35786	1,9033	0,914924
0.0520-0.0575	479,2253	-26,6251	1,40614	0,926713
0.0575-0.0585	-184,3744	-18,7244	1,1569	0,933716
0.0585-0.0696	251,2772	-19,27426	1,11915	0,934848
0.0696-0.0759	152,9245	-10,9301	0,7848	0,945215
0.0756-0.1082	55,7633	-8,00795	0,66419	0,94981
0.1082-0.1317	12,7689	-2,60295	0,3214	0,964791
0.1317-0.1594	10,9781	-1,7035	0,2202	0,971067
0.1594-0.2523	2,00252	-0,7936	0,15126	0,976083
0.2523-0.31	2,00252	-0,2353	0,05564	0,984893